AD-A142 589 J-INTEGRAL TEARING INSTABILITY ANALYSIS FO 8-INCH DIAMETER ASTM A106 STE..(U) DAVID W TAYLOR NAVAL SHIP RESEARCH AND DEVELOPMENT CENTER ANN..

1/2

UNCLASSIFIED M G YASSILAROS ET AL. MAY 84 F/G 11/6 NL

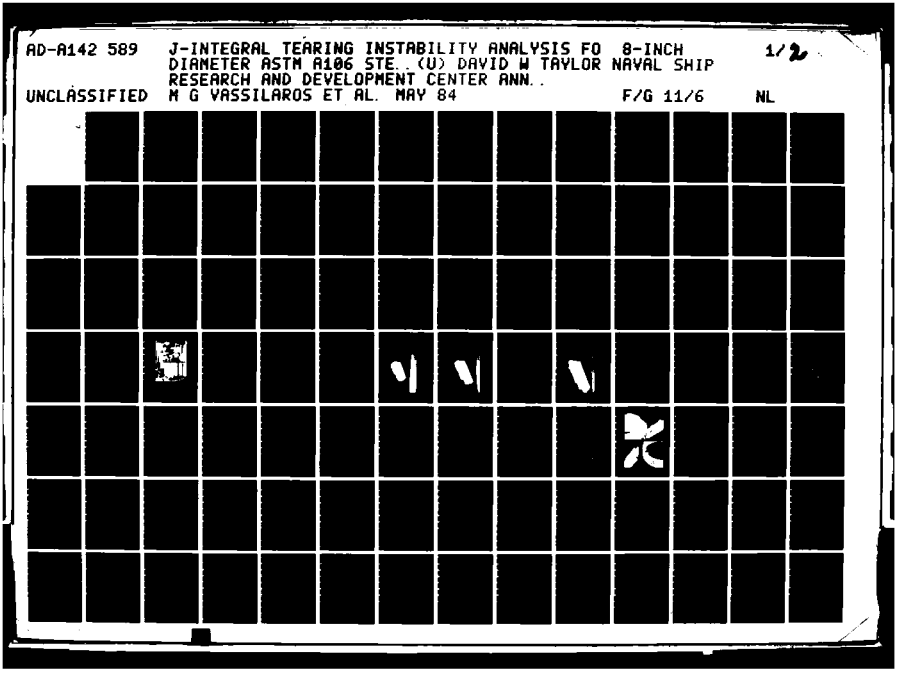

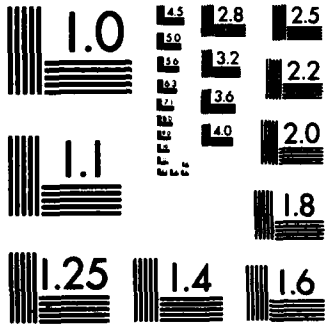

MICROCOPY RESOLUTION TEST CHART
NATIONAL BUREAU OF STANDARDS-1963-A

(12)

DAVID W. TAYLOR NAVAL SHIP RESEARCH AND DEVELOPMENT CENTER

Bethesda, Maryland 20084

J-INTEGRAL TEARING INSTABILITY ANALYSIS FOR 8-INCH DIAMETER ASTM A106 STEEL PIPE

by

M.G. Vassilaros, R.A. Hays,
J.P. Gudas, and J.A. Joyce

APPROVED FOR PUBLIC RELEASE; DISTRIBUTION UNLIMITED

SHIP MATERIALS ENGINEERING DEPARTMENT

RESEARCH AND DEVELOPMENT REPORT

May 1984

DTNSRDC/SME-83-104

J-INTEGRAL TEARING INSTABILITY ANALYSIS FOR 8-INCH DIAMETER ASTM A-106 STEEL PIPE DTNSRDC/SME-83-104

MAJOR DTNSRDC ORGANIZATIONAL COMPONENTS

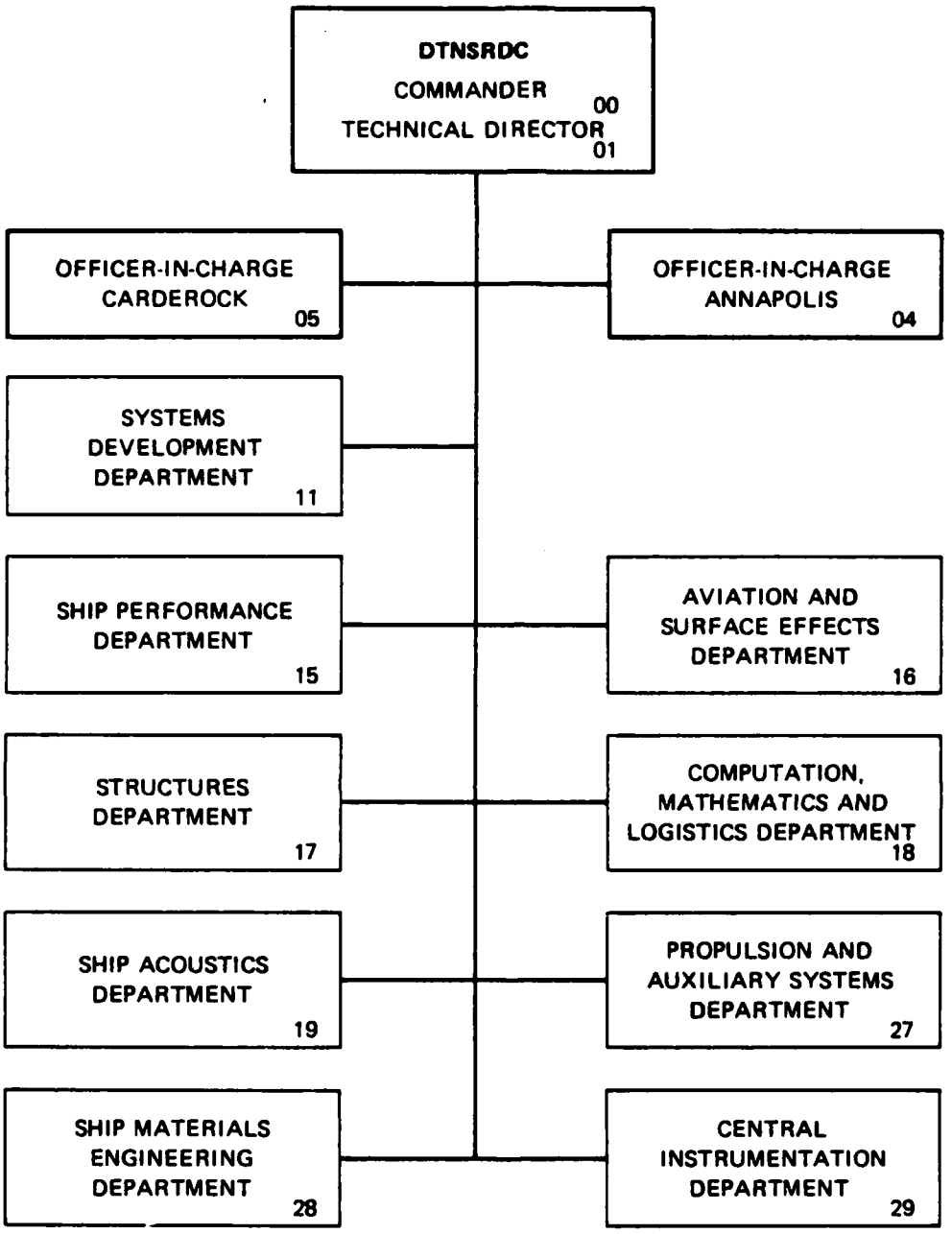

UNCLASSIFIED

SECURITY CLASSIFICATION OF THIS PAGE (When Data Entered)

REPORT DOCUMENTATION PAGE	READ INSTRUCTIONS BEFORE COMPLETING FORM
1. REPORT NUMBER DTNSRDC/SME-83-104	2. GOVT ACCESSION NO. AD-A142 589
3. RECIPIENT'S CATALOG NUMBER	
4. TITLE (and Subtitle) J-INTEGRAL TEARING INSTABILITY ANALYSIS FOR 8-INCH DIAMETER ASTM A106 STEEL PIPE	5. TYPE OF REPORT & PERIOD COVERED Research and Development
	6. PERFORMING ORG. REPORT NUMBER
7. AUTHOR(s) M.G. Vassilaros, R.A. Hays, J.P. Gudas, and J.A. Joyce	8. CONTRACT OR GRANT NUMBER(s)
9. PERFORMING ORGANIZATION NAME AND ADDRESS David W. Taylor Naval Ship R&D Center Annapolis, Maryland 21402	10. PROGRAM ELEMENT, PROJECT, TASK AREA & WORK UNIT NUMBERS Interagency Agreement RES-78-104
11. CONTROLLING OFFICE NAME AND ADDRESS U.S. Nuclear Regulatory Commission Washington, D.C.	12. REPORT DATE May 1984
	13. NUMBER OF PAGES 89
14. MONITORING AGENCY NAME & ADDRESS(if different from Controlling Office)	15. SECURITY CLASS. (of this report) UNCLASSIFIED
	15a. DECLASSIFICATION/DOWNGRADING SCHEDULE

16. DISTRIBUTION STATEMENT (of this Report)

APPROVED FOR PUBLIC RELEASE; DISTRIBUTION UNLIMITED.

17. DISTRIBUTION STATEMENT (of the abstract entered in Block 20, if different from Report)

18. SUPPLEMENTARY NOTES

19. KEY WORDS (Continue on reverse side if necessary and identify by block number)

Structural materials
Structural integrity
Elastic-plastic fracture mechanics
Tearing instability

20. ABSTRACT (Continue on reverse side if necessary and identify by block number)

An experimental investigation was performed to evaluate the applicability of using J-Integral tearing instability analysis to describe the fracture behavior of 8-inch (203 mm) diameter, nuclear grade, ASTM A106 steel pipe. Pipe sections measuring 48-inches (1219 mm) in length and 8.60 inches (219 mm) in diameter with circumferential fatigue precracks were loaded in four point bending using a variable compliance test arrangement.

(Continued on Reverse Side)

DD FORM 1 JAN 73 1473 EDITION OF 1 NOV 65 IS OBSOLETE
S/N 0102-014-6601

UNCLASSIFIED

SECURITY CLASSIFICATION OF THIS PAGE (When Data Entered)

(Block 20 Continued)

Variations in crack length, moment arm length, and machine stiffness were used to control the ductile fracture behavior of the pipes resulting in either stable or unstable crack extension. J-Integral tests were performed on 1/2 T, 1 T, and 2 T plan compact specimens machined from the pipe. These J-Integral resistance curves (J_I-R curves) were compared to the J_I-R curves from the pipe bend tests. Two different J-Integral analyses were used to describe fracture behavior. In one analysis, the material was modelled by assuming elastic-perfectly plastic behavior, while a second analysis utilized measurements of mechanical response of the loaded structure including hardening of the steel. A series of nine fracture tests were performed on the 8-inch diameter pipes with computerized data acquisition of load, deflection and crack length. The crack lengths were measured using elastic compliance, and direct current potential drop techniques simultaneously. These experimental and analytical techniques were used to generate J_I-R curves and T-applied values for all of the tests. The evaluation of the J-Integral tearing instability analysis was performed using J versus T plots of each test. The results of the investigation indicate that compact specimen J_I-R curve test results appear to agree with the J_I-R curves from full size pipe bend tests. Further, J-Integral tearing instability analysis can accurately describe the ductile tearing behavior of 8-inch ASTM A106 steel pipe provided the actual load, displacement, crack length and hardening behavior is available. Additionally, the results indicated that such an analysis with assumed elastic fully plastic behavior appears to produce conservative results.

TABLE OF CONTENTS

LIST OF FIGURES

LIST OF FIGURES (Continued)

LIST OF FIGURES (Continued)

LIST OF TABLES

LIST OF ABBREVIATIONS

ASME	American Society of Mechanical Engineers
ASTM	American Society for Testing and Materials
°C	Degrees Celsius
DCPD	Direct Current Potential Drop
°F	Degrees Fahrenheit
ft-lb	foot pound
in.-lb	inch pound
in.-lb/in.^{2}	inch-pound per square inch
in./in./min	inch per inch per minute
kJ	kilojoule
kN/m	kilonewton per meter
ksi $\sqrt{in.}$	thousand pounds per square inch - square root inch
lb/in.	pound per inch
MPa $\sqrt{m}$	megapascals - square root meter
mm	milimeter
N/mm	Newton per milimeter
UTS	Ultimate tensile strength
YS	Yield strength

ABSTRACT

An experimental investigation was performed to evaluate the applicability of using J-Integral tearing instability analysis to describe the fracture behavior of 8-inch (203 mm) diameter, nuclear grade, ASTM A106 steel pipe. Pipe sections measuring 48-inches (1219 mm) in length and 8.60 inches (219 mm) in diameter with circumferential fatigue precracks were loaded in four point bending using a variable compliance test arrangement. Variations in crack length, moment arm length, and machine stiffness were used to control the ductile fracture behavior of the pipes resulting in either stable or unstable crack extension. J-Integral tests were performed on 1/2 T, 1 T, and 2 T plan compact specimens machined from the pipe. These J-Integral resistance curves (J_I-R curves) were compared to the J_I-R curves from the pipe bend tests. Two different J-Integral analyses were used to describe fracture behavior. In one analysis, the material was modelled by assuming elastic-perfectly plastic behavior, while a second analysis utilized measurements of mechanical response of the loaded structure including hardening of the steel. A series of nine fracture tests were performed on the 8-inch diameter pipes with computerized data acquisition of load, deflection and crack length. The crack lengths were measured using elastic compliance, and direct current potential drop techniques simultaneously. These experimental and analytical techniques were used to generate J_I-R curves and T-applied values for all of the tests. The evaluation of the J-Integral tearing instability analysis was performed using J versus T plots of each test. The results of the investigation indicate that compact specimen J_I-R curve test results appear to agree with the J_I-R curves from full size pipe bend tests. Further, J-Integral tearing instability analysis can accurately describe the ductile tearing behavior of 8-inch ASTM A106 steel pipe provided the actual load, displacement, crack length and hardening behavior is available. Additionally, the results indicated that such an analysis with assumed elastic fully plastic behavior appears to produce conservative results.

ADMINISTRATIVE INFORMATION

This study was sponsored by the U.S. nuclear Regulatory Commission and was performed under Interagency Agreement RES-78-104. The program manager was Mr. Milton Vagins. Mr. Jack Strosnider has been the NRC's Program Manager since 1 October 1982. Mr. Vagins and Mr. Strosnider are both members of the Materials Engineering Branch of the Office of Nuclear Regulatory Research.

INTRODUCTION

Since its introduction by Paris and co-workers in 1979[1], the tearing instability concept has gained increasing analytical and experimental interest. Tearing instability theory states that a flawed member of ductile material will tear in a stable manner when loaded beyond J_{Ic} at limit load, where $T_{applied}$ is less than $T_{material}$, and crack instability will occur when $T_{applied}$ equals or exceeds the material tearing modulus. A substantial amount of experimental and analytical effort has been devoted to the validation of this theory, and relating it to realistic structural safety analyses. The objective of this investigation was to evaluate the applicability of using J-Integral tearing instability analysis to describe the behavior of nuclear grade piping. The approach included a three phase effort. The first phase addressed the effect of compact test specimen geometry on the J-Integral-resistance curve (J_I-R curve) behavior of ASTM A106 steel. This was accomplished by performing J-Integral fracture toughness tests on 8-inch diameter circumferentially fatigue precracked pipes subjected to four point bending, and compact specimens machined from the same steel pipes. The second phase of the study investigated the tearing instability behavior of circumferentially precracked pipes. The occurrence of tearing instability was controlled by varying the initial crack length, and the stiffness of the test machine and loading fixture. The stiffness was varied by installing Bellville springs between the pipe test fixture and the machine test bed. The third phase of the program focused on analyses to assess the ability of J-Integral fracture mechanics to accurately describe tearing instability events in large pipes using the compact specimen data, and output from tests of actual pipe specimens.

BACKGROUND

The concept of tearing instability was first introduced by Paris and co-workers.[1] In this theory, the slope of the J-Integral R-curve was originally considered to be constant beyond the point of crack initiation, and is normalized by the elastic modulus and flow stress of a material such that the tearing modulus is defined as:

$$T = \frac{dJ}{da} \times \frac{E}{\sigma_f 2} \qquad (1)$$

where: T = Tearing Modulus

dJ/da = Slope of the J_I-R-curve

E = Elastic Modulus

σ_f = Flow Stress = $\frac{\sigma_{ys} + \sigma_{uts}}{2}$

For the case of plane strain, assuming elastic-perfectly plastic behavior, criteria for instability of common test specimens were developed by comparing conditions of elastic deformation and crack extension. In this development by Paris, conditions for stable tearing were defined where the material property related to the J_I-R curve ($T_{material}$), is less than the driving force for fracture ($T_{applied}$). Hutchinson and and Paris[2] developed a theoretical justification for use of deformation-theory J in the analysis of crack growth, and an analysis of the influence of strain hardening and system compliance in the stability of the deeply cracked bend specimen. It was shown that the $T_{applied}$ parameter increases with increasing compliance.

The first experimental validation of the tearing instability theory was provided by Paris and co-workers.[3] In this experiment, three point bend tests were performed with ASTM A471 Ni-Cr-Mo-V rotor steel in an arrangement where the effective elastic span of the specimen was varied by use of a spring bar with adjustable span. Results showed that within 5 percent, the tearing instability theory was obeyed, and where $T_{material}$ was less than $T_{applied}$, unstable crack extension occurred. Similarly where $T_{material}$ exceeded $T_{applied}$, stable crack extension was observed. Further, these results showed cases where unstable crack extension was related to a relatively small change in crack length.

Joyce and Vassilaros[4] performed an extensive series of experiments to validate tearing instability theory using the compact specimen. They constructed a test arrangement with a mechanical spring in series with the load train and evaluated the fracture performance of steels, aluminum and titanium alloys. In this investigation, $T_{material}$ values ranged up to 30. The results again showed that unstable crack extension was assured where $T_{applied}$ exceeded $T_{material}$. A zone of limited instabilities was observed near the line of theoretical prediction, and this was attributed to local variation in the J-Integral R-curve.

Vassilaros and coworkers[5] broadened the scope of tearing instability theory validation with the compact specimen to include ASTM A106, ASTM A516 Grade 70, ASTM A533B and other structural steels with $T_{material}$ values in the range 12 to 170. Three formulations of $T_{applied}$ were evaluated, two of which assumed elastic fully plastic material behavior, and another which utilized the actual load-displacement data. Again, the theory was verified for materials with these high tearing moduli, and the region of limited instability appeared to be reduced or eliminated. For cases where the J-Integral R-curves were highly curved, the average $T_{material}$ from a linear extrapolation was not an accurate predictor of instability, and the instantaneous value of $T_{material}$ at instability was required. Finally, it was shown that the generalized limit load analysis applied to the compact specimen and evaluated at maximum load was most consistent in predicting instability.

Wilkowski and coworkers[6] evaluated the fracture performance of Type 304 stainless steel pipe loaded in bending. J_I-R curves were evaluated from center cracked tension, and three point bend specimens as well as two 4-inch diameter schedule 80 pipe specimens with through wall circumferential cracks. This single instability experiment was performed with a through wall crack length of 104 mm, and a spring in series with the load train to induce instability after some stable crack growth in a displacement controlled test arrangement. Direct current electric potential (DCPD) measurements were utilized to monitor crack growth during loading, and both cross head and crack-tip displacements were monitored. The instability occurred at a point past maximum load at an equivalent length of unsupported pipe of 29-feet. These results confirmed the J-Integral tearing modulus approach, but identified limitations related to using small specimen R-curve measurements to predict pipe behavior.

The results of these tearing instability validation experiments show a positive correlation between specimen crack extension behavior, the J_I-R curve and the calculations of $T_{applied}$. For the cases of bend specimens, the ability to utilize laboratory specimen data to predict tearing instability was rigorously demonstrated. However, the translation to more complex specimen geometries pointed out discrepencies in using laboratory information to predict crack stability. This lack of correlation of laboratory and full scale specimen tests formed the focus of this experimental and analytical program.

EXPERIMENTAL PROCEDURE

The experimental tasks in this program first involved a characterization of the mechanical and impact properties of the ASTM A106 Grade B steel supplied in the form of 8-inch diameter pipe. This was followed by J_I-R curve tests of compact specimen removed from the pipe. Subsequently, J_I-R curve and tearing instability tests of the pipe were performed and results were compared using published analyses for $T_{applied}$. Each of these experimental tasks is described below.

Materials

The alloy used in this investigation was ASTM A106 Grade B steel. This was supplied in the form of 8.625-inch (219 mm) outside diameter schedule 80 pipe, with a typical wall thickness of 0.54-inch (14 mm). The pipe was manufactured by the United States Steel Corporation, and conformed to the requirements of ASME Section III Sub Article NCA 3800. The chemical composition of the steel is shown in Table 1.

Twelve tensile tests were performed with three specimens from each of the four 20-ft pipe lengths which comprised the total stock of pipe. The specimens were machined with the longitudinal axis of the specimen parallel with the longitudinal axis of the pipe which corresponds to the direction of the tensile properties governing crack extension in the pipe tests. The 0.357-inch (9.1 mm) diameter specimens with 1.40-inch (35.6 mm) gage length were tested in accordance with ASTM E8-69. The tests were conducted with a strain rate of 0.003 in./in./min until yielding. The results of these tests are shown in Table 1.

Charpy V-notch specimens were machined from several pipe sections and orientated with the plane of the notch perpendicular to the longitudinal axis of the pipe and crack growth occurring in the circumferential direction as shown in Figure 1. This orientation (LC) was the same as that used for the compact specimens and the full scale pipe tests. ASTM E-23 was followed when testing the Charpy specimens and the results are presented in Figure 2. The figure shows the upper shelf value on the order of 110 ft-lb (149 joules) was attained above room temperature, at approximately 100°F (38°C).

Compact Specimen J_I-R-Curve Testing

Three geometries of compact specimen were produced from the pipe, including 1/2 T, 1 T, and 2 T plan geometry as shown in Figure 3 and 4. All compact specimens were

TABLE 1 - CHEMICAL COMPOSTION AND ROOM TEMPERATURE MECHANICAL PROPERTIES OF ASTM A106 GrB STEEL PIPE

Chemical Composition
(weight percent)

C	Mn	P	S	Si	Fe
0.23	0.81	0.0062	0.013	0.164	REM

Mechanical Properties

Spec #	Yield Strength ksi (MPa)	Ultimate Tensile Strength ksi (MPa)	Elongation % in 2-inches	Reduction in Area % (L = 4D)
1	41.5 (286)	71.2 (491)	40	65
2	41.7 (287)	72.2 (498)	37	65
3	41.5 (286)	71.1 (490)	37	64
4	41.6 (287)	70.7 (487)	33	64
5	42.0 (289)	70.7 (487)	39	64
6	41.5 (286)	72.7 (501)	41	65
7	38.4 (264)	71.3 (491)	38	64
8	38.0 (262)	70.4 (485)	46	64
9	39.6 (273)	72.0 (496)	42	64
10	42.9 (296)	72.9 (503)	34	65
11	43.0 (296)	73.0 (403)	37	65
12	42.1 (290)	72.3 (498)	33	65
Average	41.1 (287)	71.7 (495)	38	64.5

0.4-inch (10 mm) thick. The 1/2 T and 1 T specimens were machined directly from blanks cut from the pipe. The 2 T specimens blanks cut from the pipe wall were pressed flat before machining. This flattening procedure produced a prestrain of +3 percent to -3 percent across the specimen thickness. All specimens were produced such that the plane of the notch was oriented perpendicular to the longitudinal axis of the pipe, and the crack growth was in the circumferential direction (L-C).

J-Integral fracture toughness tests performed on the compact specimen utilized two separate techniques for measuring crack extension. The first used on all three geometries of compact specimens, was the elastic compliance technique described by Joyce and Gudas[7]. The second method utilized the Direct Current Potential Drop technique (DCPD) to measure the crack extension during the J-Integral fracture toughness tests. This method as described by Vassilaros and Hackett[8] monitored the IR drop across the notch face of the compact specimen subjected to a constant D.C. current. The technique partitions the changes in electrical resistance into components resulting from plasticity and crack blunting, and that resulting from a a change in crack length. DCPD was only used on the 1/2-inch thick 2 T plan specimens, and measurements were gathered concurrently with the elastic compliance data.

The J-Integral values calculated for the compact specimen test results utilized the crack growth correction expression by Ernst, Paris, and Landes[9]. The expression is as follows:

$$J(i+1) = \left[J_i + \frac{\eta}{b_i} \times \frac{A_{i,\,(i+1)}}{B_N} \right] \times \left[1 - \frac{\gamma}{b_i} \left(a_{(i+1)} - a_i \right) \right] \qquad (2)$$

where: η = 2 + (0.522) b/W for compact specimen;

W = Specimen width;

γ = 1 + (0.76)b/W;

b_i = Instantaneous length of remaining ligament;

B_N = Minimum specimen thickness;

a_i = Instantaneous crack length;

$A_{i,\,(i+1)}$ = Area under the load versus load-line displacement record between lines of constant displacement at points i and (i+1).

All specimen preparation and measurement procedures detailed in ASTM E813-81 were followed in this phase of the testing. Fatigue precracks were grown to 0.65 a/W in all compact specimen geometries where a is the crack length.

$J_{initiation}$ was calculated using a modification of ASTM Method E813. A least squares linear regression analysis was performed on the first four valid points closest to the blunting line and then again after the addition of each qualified point representing the next increment through the ASTM E813 prescribed region of crack growth. The specific $J_{initiation}$ value selected for each test was the point of intersection between the blunting line and the fit line from the set of data corresponding with the first peak in correlation of the least squares fit as a function of crack length. The slope of data in this range was used to calculate the tearing modulus for each specimen test.

The compact specimens tested had thicknesses ranging from 0.4 to 0.5-inch (10 to 13 mm). This range of thickness imposes an upper bound valid J-Integral value on the order of 900 in.-lb/in.^{2} (155 kJ/mm^2) in order to maintain plane strain condition, according to ASTM E813. These conditions and the extensive shear apparent on the fracture surface (to be described later) indicate that all of the fracture occurred under plane stress conditions.

J_I-R-Curve Testing of Pipe Specimens

The J-Integral tests were performed with the ASTM A106 Grade B Steel pipe configured in four-point bending. The pipe specimen had an overall length of 48-inches (1219 mm). Figure 5 presents a schematic view of the arrangement of the test fixture, as well as points of measurement included in the test. For all tests, the center span length was 12-inches (305 mm), and the moment arm length was either 15- or 18-inches (381 or 457 mm). Machined notches were used to initiate fatigue precracks in this series. The initial total crack lengths (2a) measured on the mean circumference of the pipe ranged from 5.3 to 8.3-inches (135 to 211 mm), or 21 to 33% of the total circumference. Measurements taken during the tests included crack mouth opening deflection (δ_1), deflection of neutral axis of the pipe (δ_2), total system deflection (δ_3) and load (see Figure 5). DCPD crack length measurement current inputs were located at the extreme ends of the pipe, and the potential output leads were located 2 inches (51 mm) apart, and centered about the crack plane at the crack mouth. To avoid any grounding problem, the pipes were electrically insulated at the loading saddle blocks.

All tests were performed in a 300,000 lb. servo-hydraulic test machine in the deflection-controlled mode. The test machine was also used to precrack the pipe specimens. Fatigue precracks were grown a minimum of 0.2-inch (5 mm) from the tip of each machined notch, and maximum ΔK applied during the final stages of precracking was 30 ksi $\sqrt{in.}$ (33 MPa $\sqrt{m}$). The test temperature for all tests was maintained in the range 125 to 150°F (52 to 65°C) in the center test span using strip heaters. This temperature guaranteed upper shelf behavior as measured in the Charpy impact toughness tests, Figure 2.

Total system compliance was varied by the insertion of Bellville springs between the specimen bend fixture and the machine test bed. Eight columns of springs were employed, and the system stiffness was varied from 36,200 lb/in. (6.34 kN/m) to 500,000 lb/in. (87.5 kN/m). Figure (6) is a photograph of a pipe specimen during a tearing instability test showing the overall arrangement.

The J-Integral tests performed with the 8-inch diameter schedule 80 pipe utilized both the elastic compliance and the DCPD techniques to measure the crack extension. The elastic compliance technique utilized the slope of the crack mouth opening displacement measurements (Figure 5) obtained during small unloadings (15 to 20%) performed during the J-Integral tests. The compliance expression experimentally determined by Joyce[10] using 4-inch diameter Aluminum-6061 pipe was modified for these tests using the elastic compliance measurements of initial fatigue cracks which were optically measured after test. The DCPD technique for crack length measurement was similar to the compact specimen technique described by Vassilaros and Hackett.[8] However, the relationship between crack length and potential drop used for the pipe was obtained by fitting an exponential equation to the data published by Wilkowski and Maxey.[11]

The J-Integral values for these pipe tests were evaluated using two different expressions. The first expression was published by Tada, Paris and Gamble[12] and used the pipe bend angle and the material flow stress to evaluate J_I. The expression for J(Tada) is as follows:

$$J = \sigma_f R [\sin (\Theta/2) + \cos \Theta] \Phi + K^2/E \qquad (3)$$

σ_f = flow stress

R = mean radius

Θ = 1/2 total crack angle

Φ = total bend angle

K = applied stress intensity (elastically calculated)

E = elastic modulus

The bend angle was calculated using the measured load line deflection taken near the neutral axis divided by the span of the moment arm (δ_2/S in Figure 5). This expression is an approximation to the actual J-Integral utilizing bend angle and average flow stress without any crack growth correction.

The second J-Integral expression was published by Zahoor and Kanninen.[13] This expression utilizes the actual bending moment and load line deflection, rather than an assumed flow stress, and has a crack growth correction component. The expression for J(ZAHOOR) is as follows:

$$J = K^2/E + \beta \int_{\delta_o}^{\delta} (2P)\, d\delta + \int_{\phi_o}^{\phi} \gamma\, J\, d\phi \qquad (4)$$

where:

K = stress intensity factor;

E = elastic modulus;

$\beta = -h'(\phi)/Rt\, h(\phi)$

2P = Total Bending Load

δ = plastic load line deflection

$\gamma = h''(\phi)/h'(\phi)$

R = radius

t = thickness

ϕ = total crack angle

$h(\phi) = [\cos(\phi/4) - 1/2 \sin(\phi/2)]$

The J-Integral crack initiation values for the pipe bend tests could not be calculated using ASTM E813 due to the insufficient number of data points in the required range. The crack initiation values reported for this study were obtained by calculating the J-Integral value at the intersection of the blunting line ($J_I = 2\, \Delta\, a\, \sigma_f$) and a power law approximation to the J_I-R curve data beyond the blunting line.

Tearing Instability Analysis

The tearing instability analysis performed on the results of the ASTM A106 steel pipe tests utilized two approaches to calculate the $T_{applied}$ values generated

during the tests. The first analysis was that published by Tada, Paris and Gamble[12] which employs the pipe bend angle, pipe geometry, crack length, material flow stress, and the structural stiffness. Structural stiffness included the machine stiffness, fixture stiffness and the spring stiffness. This analysis assumes elastic-perfectly plastic material behavior and thus does not require actual load displacement data in order to predict the value of $T_{applied}$. The expression for $T_{applied}$ by Tada for pure bending is as follows:

$$T_{applied}\ (Tada) = F_1 \frac{L_{eff}}{R} + F_2 \frac{JE}{\sigma_f^{\,2} R} \tag{5}$$

$$F_1 = \frac{1}{\pi} F_J^{\,2}$$

$$F_2 = \frac{1}{2\ F_J} [\cos\ (\ \Theta\ /2) - 2 \sin\ \ \Theta]$$

$$F_j = \sin\ (\Theta/2) + \cos\ \Theta$$

Θ = 1/2 total crack angle

R = mean radius

J = J Integral

E = elastic modulus

σ_f = flow stress

L_{eff} = total effective pipe length including contribution from machine and spring stiffness

This expression restated for 4 point bending with a spring in series is as follows:

$$T_{applied}\ (Tada) = \frac{8}{\pi R}\left[\frac{L}{4} - \frac{8}{3} + \frac{8R^2tE}{s^2Km}\right] F_j^2 + \frac{EJ}{\sigma_f{}^2 R} \quad (F_2) \qquad (6)$$

R = mean radius

F_j = sin (θ/2) + cos Θ

$$F_2 = \frac{1}{2\ F_J}\ [\cos\ (\ \Theta\ /2) - 2\ \sin\ \ \Theta]$$

θ = 1/2 total crack angle

J = J-Integral

E = elastic modulus

L = pipe length

s = moment arm length

t = pipe thickness

K_m = spring stiffness

The second expression used to evaluate $T_{applied}$ was that of Zahoor and Kanninen[13]. This formulation accounts for real material behavior and hardening. The expression for $T_{applied}$ from Zahoor and Kanninen is:

$$T_{applied}\ (Zahoor) = 4t\ (\beta P)^2\ \frac{2C_s + Ce}{1 + (2C_s + C_e)\ \frac{\partial P}{\partial \delta}_{\phi}}\ \frac{2\gamma J}{R}\ \frac{E}{c_f{}^2} \qquad (7)$$

t = pipe thickness

β = -h'(ϕ)/Rth (ϕ)

R = mean radius

C_s = compliance of springs, test machine and fixture

C_e = elastic compliance of uncracked pipe

γ = h" (ϕ)/h'(ϕ)

$h(\phi) = [\cos(\phi/4) - 1/2 \sin(\phi/2)]$

$(\partial P/\partial \delta)_\phi$ = strain hardening coefficient at constant crack length

E = elastic modulus

P = load (1/2 total load)

σ_f = flow stress

ϕ = total crack angle

If the $T_{applied}$ expression from Zahoor and Kanninen was evaluated with the assumption that the material behavior was elastic-perfectly plastic (P = limit load, $\partial P/\partial \delta = 0$), the result would be the same as that derived in the expression by Tada, Paris and Gamble.

The test series in this investigation included nine individual tests of pipe specimens under various test arrangement conditons. These are detailed in Table 2. For each specimen, a J-Integral R-Curve was developed from either elastic compliance or DCPD measurements, or both. The $J_{applied}$ and $T_{applied}$ analyses were than applied to individual sets of measurements. To accomplish this, all input signals were digitized and analyzed using a 16-bit data acquisition and analysis system. During the course of the testing, computer interactive measurements of crack length were used to control test parameters.

FRACTURE TOUGHNESS TEST RESULTS

Compact Specimen Tests

J-Integral resistance curves were produced using 1/2 T and 1 T plan specimens with a thickness of 0.4-inch (10 mm). The curves shown in Figures 7 and 8 were produced using the elastic compliance technique. The curves indicate that the A106 steel had a high initiation toughness (where the resistance curve departs from blunting behavior) ranging from 2073 to 3962 in.lb/in.^{2} (363 to 694 kJ/m^2) and high residual toughness beyond initiation as measured by the tearing modulus values of 222 to 396. The individual values are tabulated in Table 3. The large scatter in the $J_{initiation}$ and tearing modulus values was due partly to normal material scatter, and additionally to the difficulties in evaluating R-curves with high resistance curve slopes. The evaluation of such curves can produce large variations in toughness values from small changes in calculated J_I-R curve slope values. The variation can be minimized with lower slope values produced with side grooved

TABLE 2 - TEST MATRIX FOR 8 INCH DIAMETER ASTM A106 STEEL PIPES SUBJECTED TO FOUR-POINT BENDING

Pipe Test No.	Pipe Length in. (mm)	Mean Radius in. (mm)	Mean Thickness in. (mm)	Initial Crack Length(2a) inch (mm)	Moment arm length (span) inch (mm)	Total Machine Stiffness lb/in (N/mm)
3	48 (1219)	4.02 (102)	0.551 (14.0)	7.58 (192)	18 (457)	500,000 (87,550)
7	48 (1219)	4.03 (102)	0.540 (13.7)	8.30 (210)	18 (457)	500,000 (87,550)
8	48 (1219)	4.04 (103)	0.536 (13.6)	7.66 (194)	18 (457)	500,000 (87,550)
10	48 (1219)	4.04 (103)	0.538 (13.7)	6.66 (169)	18 (457)	39,000 (6,829)
11	42 (1067)	4.03 (102)	0.597 (15.2)	6.29 (160)	15 (381)	37,000 (6,479)
12	42 (1067)	4.03 (102)	0.546 (13.9)	5.87 (149)	15 (381)	37,000 (6,479)
13	42 (1067)	4.04 (103)	0.526 (13.4)	5.45 (138)	15 (381)	36,200 (6,339)
14	42 (1067)	4.06 (103)	0.573 (14.6)	4.90 (124)	15 (381)	37,000 (6,479)
15	42 (1067)	4.03 (103)	0.560 (14.2)	5.32 (135)	15 (381)	36,800 (6,443)

TABLE 3 - $J_{-INITIATION}$ AND TEARING MODULUS FROM 1/2 T AND 1 T COMPACT SPECIMEN TESTS USING THE ELASTIC COMPLIANCE TECHNIQUE

Specimen Number	0.5-in. (13 mm) Thick Compact Spec. Geometry	Test Temp.	J Initiation in-lb/in^2 (kJ/m^2)	Crack Extension Range for J Initiation Calc. inch (mm)	Tearing Modulus	Crack Extension		
						Predicted inch (mm)	Measured inch (mm)	% Error
202	1/2T	RT	2073 (363)	0.048 (1.22)	263	0.049 (1.24)	.066 (1.68)	-50
204	1/2T	RT	2684 (470)	0.051 (1.30)	285	0.093 (2.36)	.119 (3.02)	-28
300	1/2T	RT	3962 (694)	0.061 (1.55)	222	0.196 (4.90)	Not measured	--
301	1/2T	RT	3220 (660)	0.057 (1.45)	230	0.209 (5.31)	.272 (6.91)	-30
303	1/2T	RT	2623 (459)	0.058 (1.47)	260	0.152 (3.86)	.175 (4.45)	-15
100	1T Plan	RT	3606 (632)	0.074 (1.88)	355	0.152 (3.86)	.224 (5.69)	-47
102	1T Plan	RT	2543 (445)	0.075 (1.91)	396	0.096 (2.44)	.132 (3.35)	-37
103	1T Plan	RT	3149 (551)	0.078 (1.98)	352	0.163 (4.14)	.186 (4.72)	-12
104	1T Plan	RT	3299 (578)	0.071 (1.80)	340	0.149 (3.78)	.128 (3.25)	-14

RT = Room Temperature

compact specimens as shown in Figure 9. However, such R-curves would not be appropriate for evaluating the resistance curves of 1/2 inch wall thickness A106 steel pipe. Another favorable result of side grooving is the propensity of the specimen to resist crack tunneling and thus minimize the error between the predicted final crack length and the optically measured final crack length. For the plane-sided specimens tested in this investigation, the errors in measuring the crack extension were as great as 50 percent as shown in Table 3. Figures 10 and 11 are photographs of 1/2 T and 1 T plan compact specimen fracture surfaces showing the crack tunneling and shear lips. The similarity of these fracture specimens was also apparent in comparing the J-Integral resistance curves of the 1/2 T and 1 T plan compact specimens, shown in Figures 7 and 8.

J-Integral tests were also performed on plane-sided 2 T plan compact specimens with a thickness of 0.5 inch (13 mm). However, these specimens could not be machined directly from the pipe without first flattening the pipe which induced a residual plastic prestrain across the specimen thickness from -3 percent to +3 percent strain. The testing of the 2 T compact produced resistance curves with more crack extension than that possible in 1/2 T and 1 T specimens. In addition, these specimens were tested with the D.C. potential drop (DCPD) technique which would eliminate the errors in crack extension measurement. Therefore, all 2 T plan compact specimens were tested using elastic compliance and DCPD crack length measurement techniques simultaneously. Figure 12 shows the J-Integral resistance curves obtained from testing two 2 T plan compact specimens. The DCPD technique produced resistance curves with lower initiation values and lower tearing moduli as shown in Table 4a. The lower inititation values may be due to the higher sensitivity in measuring tunnelled crack length with DCPD. The lower tearing modulus was due to the resistance curve not underestimating the final crack length. The fracture surface of the 2 T plan specimen shown in Figure 13 appears similar to the 1/2 T and 1 T specimens shown in Figure 10 and 11. The calculated J values at crack initiation for the 2 T compacts specimens using elastic compliance are shown in Table 4b and are within the range of values calculated from the 1/2 T and 1 T specimen tests.

However, comparison of the full J-Integral R-curves of the 3 types of specimens indicates some differences in behavior. In Figure 14, the divergence of the 1 T- and 2 T-plan compact specimen J_I-R curves is apparent. This difference between the curves appears to begin at about 0.05 inch (1.3 mm) of crack extension. Below this point the 1 T and 2 T specimen J_I-R curves were very similar. The 1/2 T

and 1 T plan compact specimen J_I-R curves shown in Figure 15 were similar over the entire range. The lower resistance curve for the 2 T plan compact specimens in most probably due to the $\pm$ 3 percent prestrain introduced prior to specimen machining. Similar effects have been reported for mild steel[14] and HY-80 steel.[15] Therefore, the extended crack growth portions of the J_I-R curves from prestrained 2 T plan compact specimen are probably not representative of the pipe material behavior, but instead would under-estimate the ductile fracture properties.

All of the J-R curve results discussed above were from compact specimen tests performed at room temperature. However, the Charpy "V" notch results shown in Figure 2 indicate that upper shelf behavior begins at approximately 85°F (30°C). The J-Integral resistance curve behavior for this ASTM A106 steel at an upper shelf temperature of 125°F (52°C) was evaluated to compare to full scale pipe bend tests. Two tests were performed on 2 T plan compact specimens at this temperature. These results presented in Table 4b appear in Figure 16 along with results from room temperature tests. The test results appear indentical indicating that no change in ductile fracture toughness has resulted from the modest temperature increase of 50°F (28°C).

Pipe Specimen Tests

J-Integral tests were performed on nine ASTM A106 steel pipes in four point bend loading. These tests were performed using elastic compliance and DCPD techniques simultaneously. The results of these tests are shown in Figures 17 and 18 which are plots of J-Zahoor (equation 4) versus crack extension using elastic compliance and DCPD techniques respectively. Had the two figures been produced using J-Tada (equation 3), the plots would have appeared very similar, within 5 percent on the value of J. An example is shown in Figure 19 for pipe test number 7. The reasons for such good agreement are several. By examining equations 3 and 4, it is apparent that both equations share the same elastic term. The second term (plastic term) is different for the two equations. The crack growth term (γ) in equation 4 was small for these tests. This was due to the choice of initial crack lengths which ranged from 5.32- to 8.30-inch in total length (135 to 211 mm). These values convert to total crack angles of 75 to 118 degrees which correspond to modest γ values of -0.1 to -0.2 as shown in Figure 20 reproduced from Reference 13. The elastic-perfectly plastic analysis (equation 3) uses the flow stress and the limit load expression whereas equation 4 utilizes the actual load displacement data. The values obtained

TABLE 4a - $J_{INITIATION}$ AND TEARING MODULUS RESULTS FROM COMPACT SPECIMENS TEST USING D.C. POTENTIAL DROP TECHNIQUE

Specimen Number	0.5 in. Thick Compact Spec. Geometry	Test Temperature	J Initiation in.lb/in.^{2} (kJ/m^2)	Crack Extension Range for J Initiation Calc. inch (mm)	Tearing Modulus
1a-PD	2T Plan	RT	1590 (278)	0.072 (1.83)	291
2a-PD	2T Plan	RT	2197 (385)	0.086 (2.18)	234
7a-PD	2T Plan	125°F	2234 (391)	0.073 (1.85)	299
8a-PD	2T Plan	125°F	2860 (500)	0.078 (1.98)	257

RT = Room Temperature

TABLE 4b - $J_{INITIATION}$ AND TEARING MODULUS FROM 2T COMPACT SPECIMEN TESTS USING ELASTIC COMPLIANCE TECHNIQUE

Specimen Number	0.5 in. Thick Compact Specimen Geometry	Test Temp.	J Initiation in.lb/in.^{2} (kJ/m^2)	Crack Extension Range for J Initiation Calc. inch (mm)	Tearing Modulus	Crack Extension		
						Predicted inch (mm)	Measured inch (mm)	% Error
1a	2T Plan	RT	2428 (425)	0.073 (1.85)	349	0.526 (13.4)	0.563 (14.2)	-7
2a	2T Plan	RT	2777 (486)	0.061 (1.55)	273	0.482 (12.2)	0.568 (14.3)	-17
7a	2T Plan	125°F	3661 (641)	0.076 (1.93)	113	0.485 (12.3)	0.506 (12.9)	-4
8a	2T Plan	125°F	2316 (405)	0.056 (1.42)	290	0.476 (12.1)	0.478 (12.1)	-0.5

RT = Room Temperature

from the limit load expression[10] using the instantaneous crack length for pipe specimen 10 are plotted in Figure 21 as a function of load line displacement. Also shown on Figure 21, is the measured load versus load line displacement behavior. In the region of plastic deflection (beyond about 0.15-in. (3.8 mm)), the limit load and measured load are generally within 12 percent of each other and cross over at or close to the maximum load of the pipe test. Thus, the product of load times plastic deflection using either method is very close. It should be noted that the values continue to diverge beyond maximum load which would increase the error between the measured and predicted load with large crack extensions. Additionally, the limit load expression always under predicts the slope of the load versus deflection curve since there is no hardening component in this expression. It is of interest to note the good agreement between predicted maximum load and measured maximum load during the pipe tests. The load values, measured and predicted, are shown in Table 5. The largest error was 8 percent underprediction of measured load in tests 13 and 15. These results indicate that a failure analysis scheme based on the maximum load capacity of a cracked pipe is quite feasible with limit load analysis for ferritic piping materials.

Returning to Figures 17 and 18, it can be observed that the two sets of J_I-R curves follow the same trends with the D.C. potential drop curves displaying less scatter than the elastic compliance method. The reduced scatter of the DCPD curves is a result of using both the initial and final measured crack lengths to generate the crack extension data, whereas, the unloading compliance technique cannot correct for errors in crack length. The J-Integral values calculated by inspection of Figures 17 and 18 at crack initiation ranged from 2000 to 4000 in.-lbs/in.^{2} (350 to 700 KJ/m^2). Exact values for J_{Ic} in the pipes cannot be calculated due to the sparseness of the data in the ASTM E813 region. However, a better examination of the J_I-R curve behavior can be performed by fitting the data of each J_I-R curve (beyond blunting) with a power law curve in a method described in Reference 5. Using this technique, the data in Figure 17 and 18 become the J_I-R curves shown in Figure 22, and 23 respectively. The resultant $J_{initiation}$ values are listed in Table 6. These crack inition values ranging from 2042 to 4397 in.-lb/in.^{2} (358 to 770 KJ/m^2) confirm the apparent crack initiation values mentioned earlier. Although the values have a wide range, they do agree with $J_{initiation}$ values obtained from elastic compliance tests performed on smooth sided 1/2 T compact specimens. In fact, the average $J_{intiation}$ values of 3022 in.-lb/in.^{2} (529 KJ/m^2) for 1/2 T compact

TABLE 5 - MEASURED MAXIMUM LOAD AND LOAD PREDICTED FROM LIMIT LOAD ANALYSIS AT CRACK EXTENSION WHERE MAXIMUM LOAD OCCURRED FOR PIPE TESTS

Pipe Test Number	Maximum Load				% Diff
	Actual		Predicted		
	lb	(kN)	lb	(kN)	
3	106,293	(473)	102,234	(455)	-4
7	92,550	(412)	91,902	(409)	-1
8	88,938	(396)	95,361	(424)	7
10	117,570	(523)	115,139	(512)	-2
11	145,227	(646)	145,096	(645)	<-1
12	152,502	(678)	142,818	(635)	-6
13	158,868	(707)	146,156	(650)	-8
14	175,572	(781)	174,582	(776)	-1
15	162,792	(724)	149,707	(666)	-8

TABLE 6 - $J_{INITIATION}$ VALUES FROM PIPE TESTS

Pipe Test #	$J_{Initiation}$ in.lb/in.^{2} (kJ/m^2)		Final Crack Extension Measurements		
	Elastic Compliance (Figure 22)	DCPD (Figure 23)	Elastic Compliance in. (mm)	Optically Measured in. (mm)	% Error
3	2947 (516)	—	1.101 (28.0)	1.41 (35.8)	-28
7	4397 (770)	3197 (560)	0.576 (14.6)	0.757 (19.2)	-31
8	3985 (697)	2940 (515)	0.738 (18.7)	0.803 (20.4)	-9
10	—	2530 (443)	0.733 (18.6)	0.995 (25.3)	-35
11	2042 (357)	2349 (411)	1.120 (28.4)	1.017 (25.8)	+9
12	2550 (446)	—	1.150 (29.2)	1.427 (36.2)	-24
13	—	2873 (503)	—	+	-
14	3880 (679)	—	—	+	-
15	2496 (437)	4125 (722)	—	+	-
Average	3185 (557)	3002 (525)	—	—	-

+ - No optical measurement

specimens, and 3149 in.-lb/in.^{2} (551 KJ/m^2) for 1 T compact specimens agree very well with the average initiation value of 3185 in.-lb/in.^{2} (558 KJ/m^2) from the pipe tests.

In addition to the crack initiation values, the J_I-R curve behavior of 1/2 T and 1 T plan compact specimens appears to be similar to the J_I-R curves for the pipe bend tests. When examining J_I-R curves which display an underestimation of the crack extension, the real J_I-R curve behavior must be kept in mind by using the final optically measured crack extension point as a guide. Figure 24 shows the resistance curves which represent the range of pipe tests, and two J_I-R curves which represent the range of curves from 1/2 T compact specimen tests. Although the J_I-R curves from elastic compliance technique performed on smooth sided 1/2 T compact specimens may over predict the toughness of the ASTM A106 steel pipe, the final measured crack lengths indicate that the actual specimen behavior was similar to the behavior of the material in the pipe test. It must be noted that the accuracy of the J-R curves for the pipe test is also in error from +9 to -35 percent as shown in Table 6.

Figure 25 shows the J_I-R curve behavior of the 1/2 inch (12 mm) thick 1 T plan compact specimens. Here again, the fracture resistance behavior of the pipes and 1 T compacts appears similar. However, the extent of crack extension of the 1 T compact is too limited for a good comparison of the J_I-R curves. The J-R curves from the 2 T plan compact specimen test display over 0.50 in. (12.7 mm) of crack extension providing a greater basis for comparisons of resistance curves as shown in Figure 26. The J-R curves of the 2 T plan specimen do not appear to agree with the pipe test data. They appear to have a lower average initiation value and lower slope. The average initiation value of the four 2 T compacts was 2795 in.-lb/in.^{2} (489 KJ/m^2) which was 14 percent lower than the average pipe fracture toughness. The entire resistance curves of the 2 T compacts specimens fall below those or most of the pipes tested using elastic compliance. This difference was also seen when comparing test results from the DCPD technique, Figure 27. However, the actual fracture surfaces of the pipe tests and 2 T compact specimens were very similar as shown in Figure 28. These results indicate that there may be good agreement between the J_I-R curves from compact specimens and four point bend pipe tests with through wall circumferential flaws provided the material of both types of specimens has experienced the same strain history.

Tearing Instability Tests

As stated earlier, tearing instability behavior of the 8 inch diameter ASTM A106 steel pipe was studied by testing circumferentially precracked pipes which had various initial crack lengths subjected to four-point bending with different levels of machine stiffness as shown in Table 7. According to the J-Integral tearing instability theory proposed by Paris and coworkers[1], whenever the $T_{material}$ of a structure (measured from a J-R curve) is less than the $T_{applied}$ driving force (calculated from geometric, structural, and material properties), unstable crack extension will occur. This unstable crack extension is not cleavage but ductile crack extension, and is not necessarily dynamic or even fast. Unstable crack extension is defined as that which does not require any further increase in load, deflection, or energy to be applied to the structure in order to continue the crack growth (after crack initiation).

The tearing instability behavior of the pipe specimen test series was analyzed with the use of J versus T diagram as suggested by Paris in NUREG 0744[16]. The $J/T_{material}$ curves for the pipe tests calculated using elastic compliance and DCPD results are shown in Figures 29 and 30 respectively. Because of the complex test arrangement, only three tests resulted in successful measurements of J_I-R curves using both measurement techniques. All of the J_I values were calculated using the J(Zahoor) expression (equation 4). These curves were produced from the original J_I versus crack extension data through the use of a power law fitting analysis. The curves developed from the DCPD technique in Figure 30 fall within a tighter band of material behavior than the curves from the elastic compliance technique for crack length measurement shown in Figure 29. However, the two techniques appear to describe the same overall J/T-material behavior of the ASTM A106 steel pipe tested.

The $T_{applied}$ curves were calculated using the expression of Tada, Paris, and Gamble[12] (equation 6) and the expression from Zahoor and Kanninen (equation 7). Figures 31, 32, and 33 each show the two $J/T_{applied}$ curves which were evaluated for pipe tests number 3, 7, and 8 respectively. Both of these analyses predicted stable crack extension throughout all three tests, as indicated by the fact that the $J/T_{applied}$ curves did not intersect the material curve. For these tests, $T_{applied}$ values ranged from 0 to 20.

Also shown on Figures 32 and 33 are $J/T_{material}$ curves using the J-Zahoor expression evaluated from the crack length data calculated using both the unloading compliance and DCPD data. The $T_{applied}$ curves in pipe test number 10, as shown in Figure 34, did not show the show the same range, but rather the $T_{applied}$ (Tada)

TABLE 7 - TEST CONDITIONS AND RESULTANT MODE OF CRACK EXTENSION FOR 8-INCH DIAMETER ASTM A106 STEEL PIPES SUBJECTED TO FOUR-POINT BENDING

Pipe Test No.	Initial Crack Length(2a) inch (mm)	Moment arm length (span) inch (mm)	Total Machine Stiffness lb/in. (N/mm)	Maximum Load lb x 10^3 (N x 10^3)	Crack Extension Behavior After Maximum Load
3	7.58 (192)	18 (457)	500,000 (87,550)	107.9 (480)	stable
7	8.30 (210)	18 (457)	500,000 (87,550)	93.8 (417)	stable
8	7.66 (194)	18 (457)	500,000 (87,550)	91.2 (406)	stable
10	6.66 (169)	18 (457)	39,000 (6,829)	119.4 (531)	stable
11	6.29 (160)	15 (381)	37,000 (6,479)	150.0 (667)	stable
12	5.87 (149)	15 (381)	37,000 (6,479)	156.0 (694)	stable
13	5.45 (138)	15 (381)	36,200 (6,339)	163.7 (728)	unstable
14	4.90 (124)	15 (381)	37,000 (6,479)	181.0 (805)	unstable
15	5.32 (135)	15 (381)	36,800 (6,443)	168.6 (750)	unstable

values appeared much more sensitive to the change in applied spring stiffness. This divergence of the T-applied analyses was also observed for pipe test numbers 11 through 15 configured with low machine stiffness. The Tada analysis was always more conservative (higher $T_{applied}$ values) than that of Zahoor for this such configurations. Figure 35 shows the J/T behavior which resulted from test number 11. The $J/T_{applied}$ (Zahoor) did not intersect the $J/T_{material}$ curve from DCPD, indicating stable crack extension throughout the test. However, this result also indicated that had the test continued, unstable crack extension should have occurred. This result was also observed for test number 12, Figure 36. After this test, the pipe was reloaded without instrumentation to a deflection beyond that imposed during the test, and unstable crack extension did occur. This test result indicates the accuracy of the $T_{applied}$ (Zahoor) analysis. It can also be seen that the $T_{applied}$ (Tada) analysis was conservative, indicating an early point of instability.

During the tests numbers 13, 14 and 15 (Figures 37, 38 and 39 respectively) unstable crack extension was observed. In pipe tests 13 and 15, the $T_{applied}$ (Zahoor) appeared to accurately predict the onset of instability as shown in Figure 37 and 39. The $T_{applied}$ expression was again conservative. The results for pipe test number 14 do not appear to agree with pipes 13 and 15. However, this is likely due to error in crack extension measurements which produced an overly optimistic J-Integral resistance curve and $T_{material}$ values. This may account for the high J-R behavior of pipe 14 shown in Figure 22.

The divergence in $T_{applied}$ analyses (equation 7 and 8) observed in pipe tests number 10 through 15 is mainly due to the differences in treating the hardening behavior of the pipe material. Equation 7 (T-Tada) assumes elastic perfectly plastic behavior, whereas equation 8 (T-Zahoor) requires the strain hardening behavior at constant crack length $(\partial P/\partial \delta)_{\phi}$. This value was obtained by evaluating the normalized load versus deflection behavior of the pipe test results. The evaluation accounted for crack extension in a manner suggested by Ernst, Paris and Landes.[9] The results of this "key curve" type analysis are shown in Figure 40. An average linear best fit was obtained for the data beyond a normalized bend angle of 0.0005. This value was then used to calculate the actual strain hardening coefficient used in equation 8 at any crack extension. Using equation 8 with a strain hardening coefficient of zero to evaluate the assumption of perfectly plastic behavior would produce results comparable to equation 7. The results of such an exercise performed on the data for pipe test number 12 are shown in Figure 41. This figure shows that

the assumption of elastic-perfectly plastic behavior is mainly responsible for the conservative results for $T_{applied}$ (Tada). It can also be concluded that by accounting for the strain hardening behavior of the pipe material, a more accurate $T_{applied}$ Tada could be calculated in a "predictive" mode.

Three significant observations are supported by the results of these nine tests of pipes in bending. The first is that J-Integral tearing instability analysis can be an accurate tool to indicate the onset of unstable crack extension provided the actual physical properties of the material, and specific mechanical response of the loaded structure including load, deflections, crack extension and hardening performance are available.

The second observation is that the assumption of elastic-fully plastic material behavior in applying J-Integral tearing instability analysis to 8-inch (219 mm) diameter A106 steel pipes is conservative in predicting the onset of unstable crack extension. $T_{applied}$ values for the actual instabilities were on the order of 1.5 to 2.7 times higher than those from the Tada analysis at the onset of unstable crack extension.

The third observation is that the results of both analyses are similar for conditions which produced low $T_{applied}$ values (0 to 20). This is important for the application of tearing instability analysis to real piping systems since such analyses would be performed in order to avoid conditions of high $T_{applied}$ values, and the possibility of unstable crack extension. Therefore, using the assumption of elastic-fully plastic behavior for tearing-instability analysis is justified when low $T_{applied}$ values result. Such analysis could provide a relatively simple and cost effective method for calculating $T_{applied}$ values for piping systems without the need to generate actual test data for full size pipes.

Predictive Capability of J-Integral Tearing Instability Analysis

In order to use J/T diagrams to predict conditions necessary to assure stable crack extension, both $J/T_{applied}$ and $J/T_{material}$ information is needed. Compact Specimen test results appear to be a good candidates for predicting the material behavior for large pipes in bending as shown in Figure 42. This figure has two $J/T_{material}$ curves from 1 T compact specimen tests which had crack extensions of 0.160 and 0.180-inch (4.1 to 4.6 mm) respectively. Also shown in Figure 42 is the data band containing all of the $J/T_{material}$ curves from the pipe tests generated using DCPD. The compact specimen test results appear consistent with the pipe

results. However, the J/T curves are limited by the relatively small amount of crack extension (less than 0.2-inch (5 mm)) produced in a 1 T compact specimen. The reasons for the good agreement between the two different types of specimens are that both had approximately the same thickness and very similar fracture surfaces. Thus both the compact and the pipe specimen experienced and displayed the same level of plane stress, shear lips and crack tunneling as shown in Figures 10, 11 and 28. Had the compact specimens been side grooved in order to supress tunneling, the resultant J/T curve would have been lower, flatter and more conservative.

The J versus T curves for the 1/2-inch (13 mm) thick 2 T compacts specimens machined from blanks which had experienced prestrain are shown in Figure 43. These curves are more conservative than the actual pipe data. In order to use these compact specimen $J/T_{material}$ curves which had only limited crack extension in a region beyond the test results, a linear extrapolation can be drawn from the end of the $J/T_{material}$ curve. Such an assumption of the $J/T_{material}$ behavior should be conservative since all $J/T_{material}$ behavior is curved upward with decreasing T values, and a linear extrapolation at any point along this curve should describe J/T values below the actual curve.

SUMMARY AND CONCLUSIONS

The purpose of this research was to investigate the applicablity of using J-Integral tearing instability analysis to describe the fracture behavior of 8-inch (219 mm) ASTM A106 steel pipe. The following conclusions have been drawn from the results of this investigaton:

- o J-Integral resistance curves from 1 T and 2 T plan compact specimens can predict the J_I-R curve behavior of 8-inch (219 mm) diameter ASTM A106 steel pipe in bending, but not to the same extent of crack extension;
- o J-Integral tearing instability analyses can accurately describe the ductile ductile tearing instability behavior of 8-inch ASTM A106 steel pipe provided the actual load, displacement, crack length and hardenability is available;
- o J-Integral Tearing Instability Analysis of 8-inch (203 mm) ASTM A106 pipe assuming fully plastic material behavior appears conservative, resulting from an apparent overestimation of $T_{applied}$;
- o Assuming elastic-fully plastic behavior and that the material remains ductile, the combination of J-Integral resistance curves and tearing instability analysis can be used to conservatively identify flawed structures which will experience stable crack extension after crack initiation.

ACKNOWLEDGMENTS

The authors wish to acknowledge the support of Messrs. Milton Vagins and Jack Strosnider of the U.S. Nuclear Regulatory Commission. Additionally the authors wish to thank those at the David Taylor Naval Ship R&D Center who have contributed to the many experimental phases of the program particularly David Anderson, Dan Davis, and Mark Kirk. Finally, the advice and guidance of Dr. Hugo Ernst, Mr. Gery Wilkowski, Prof. Paul Paris and Dr. Akram Zahoor is greatfully acknowledged.

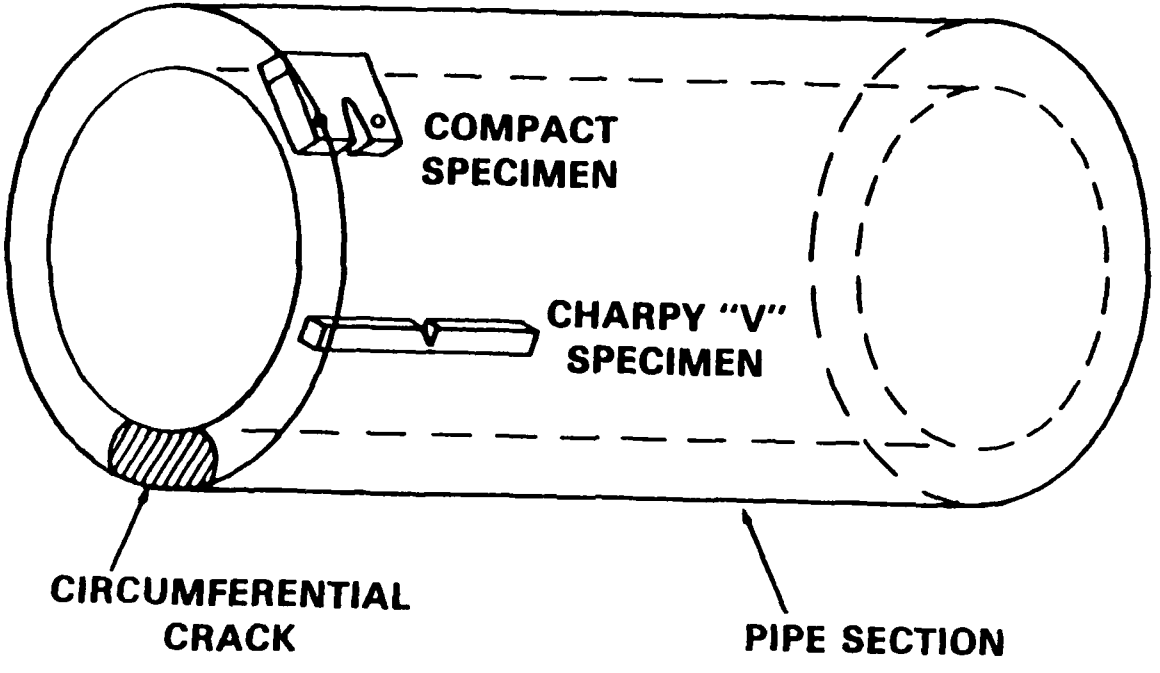

Figure 1 - Schematic Drawing of Pipe Section Showing Test and Mechanical Property Specimen Orientation

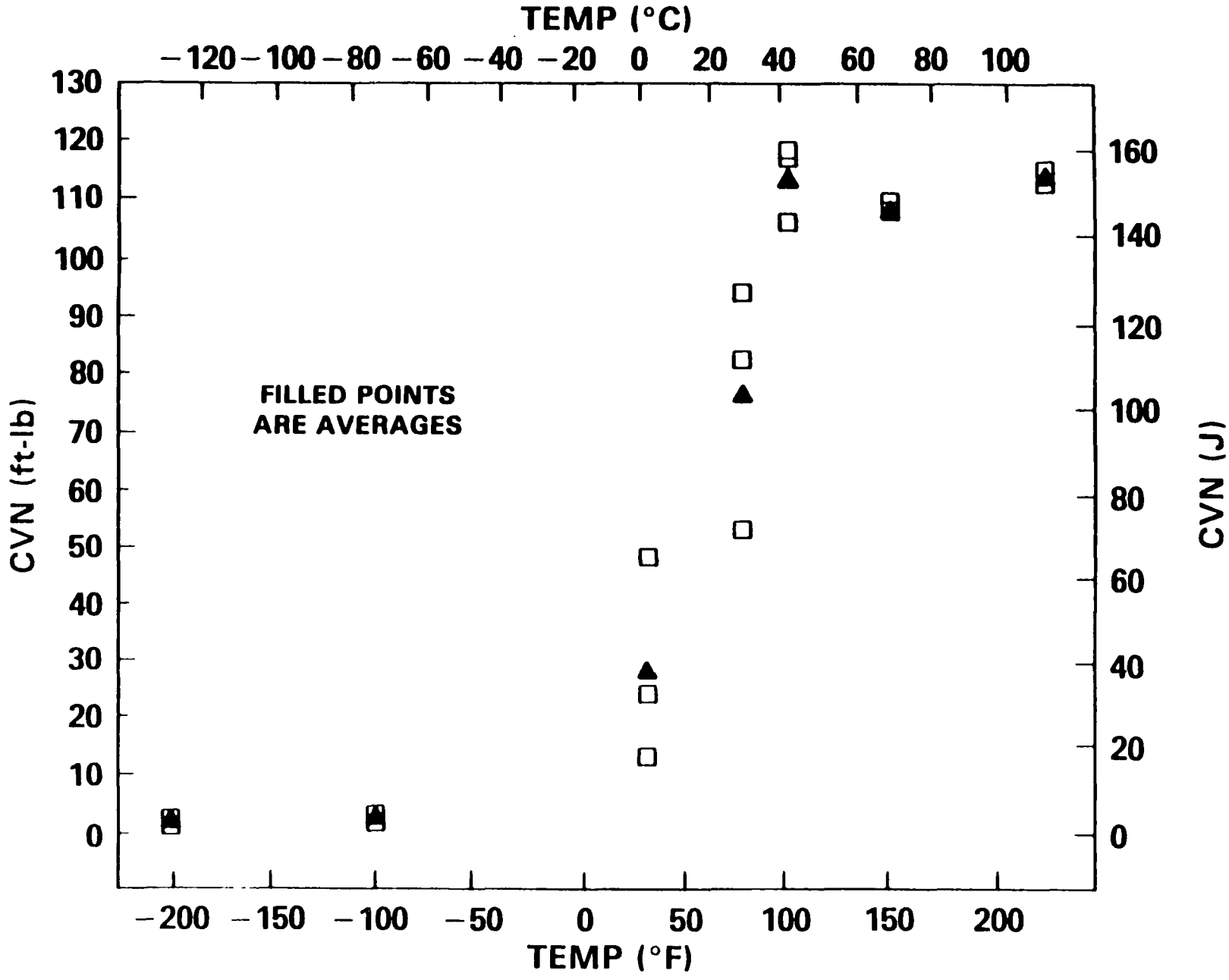

Figure 2 - Plot, Charpy "V" Notch Energy Transition Curve for 8-inch (203 mm) Diameter ASTM A106 Steel Pipe

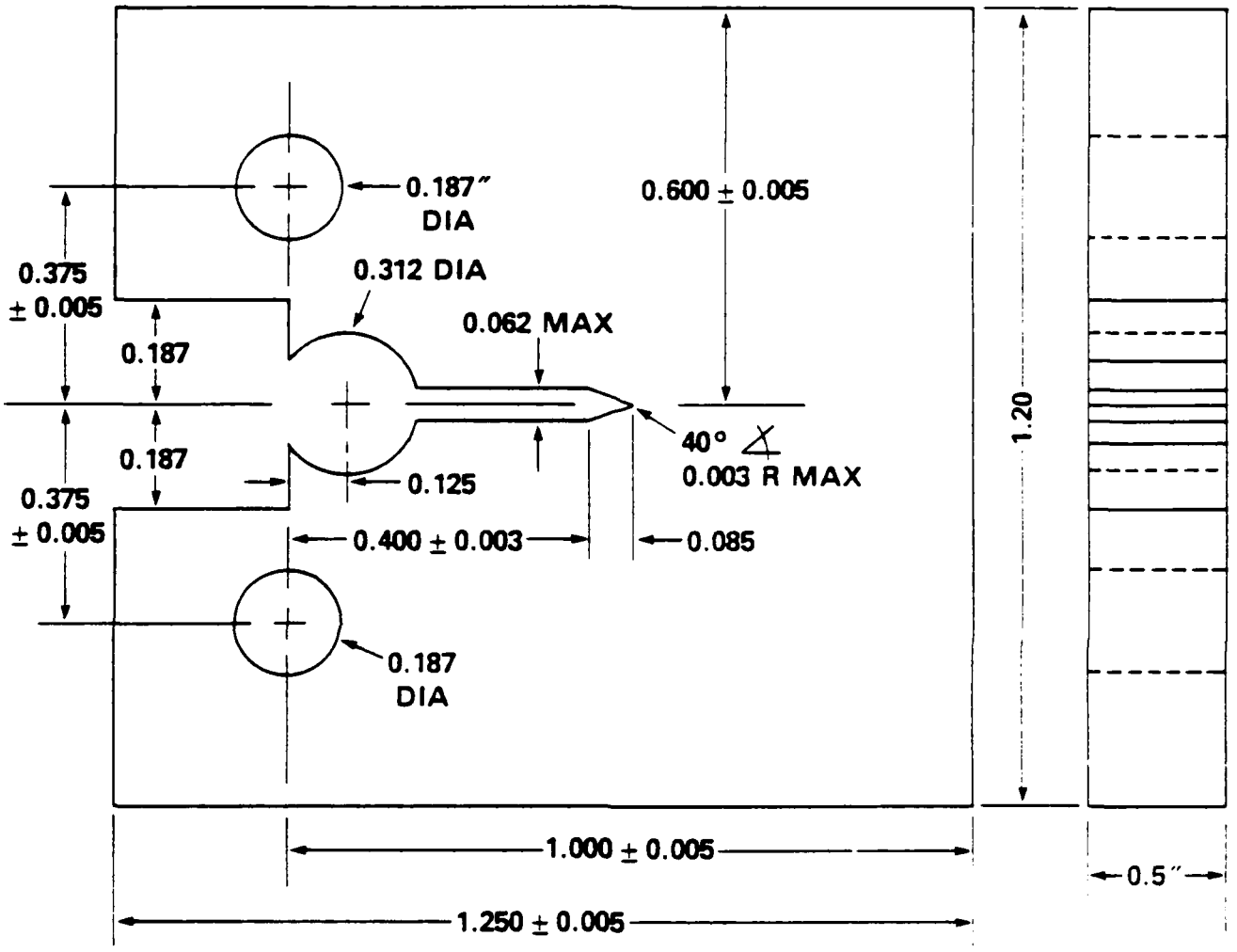

Figure 3 - Drawing, 1/2 T Compact Specimen

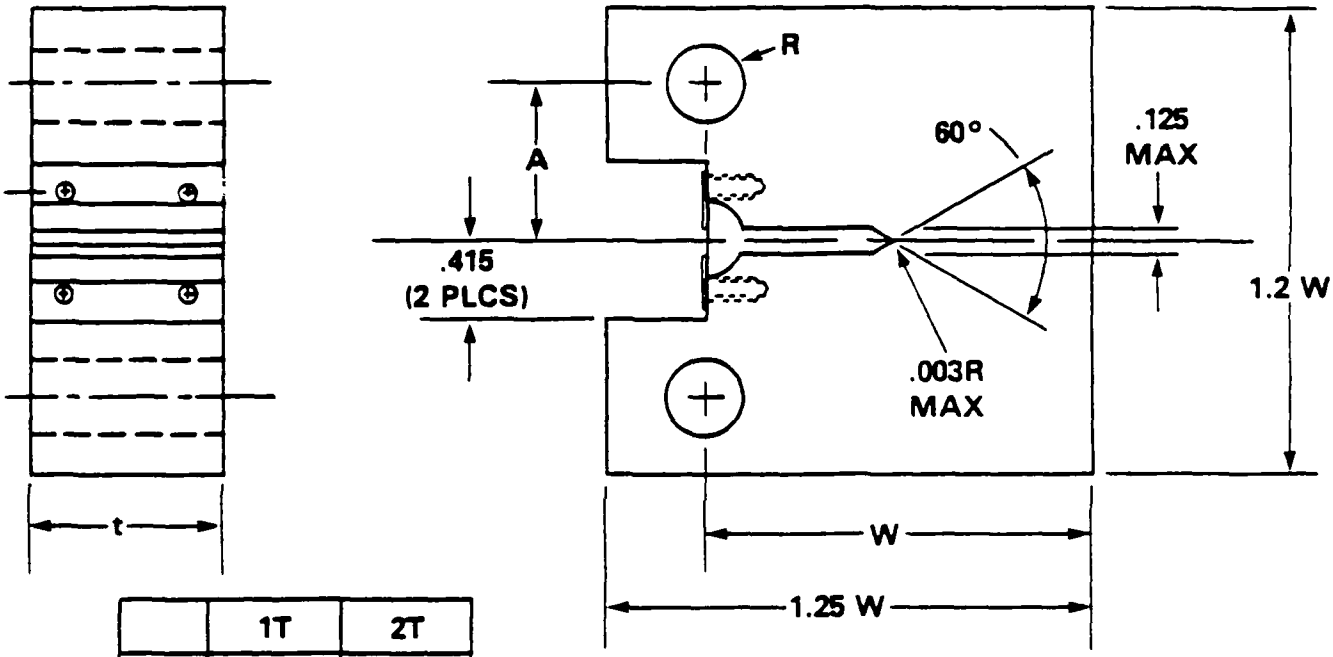

	1T	2T
W	2.00	4.00
A	0.80	1.30
R	0.375	1.00
t	0.475	0.470

Figure 4 - Drawing, 1 and 2 T Plan Compact Specimens

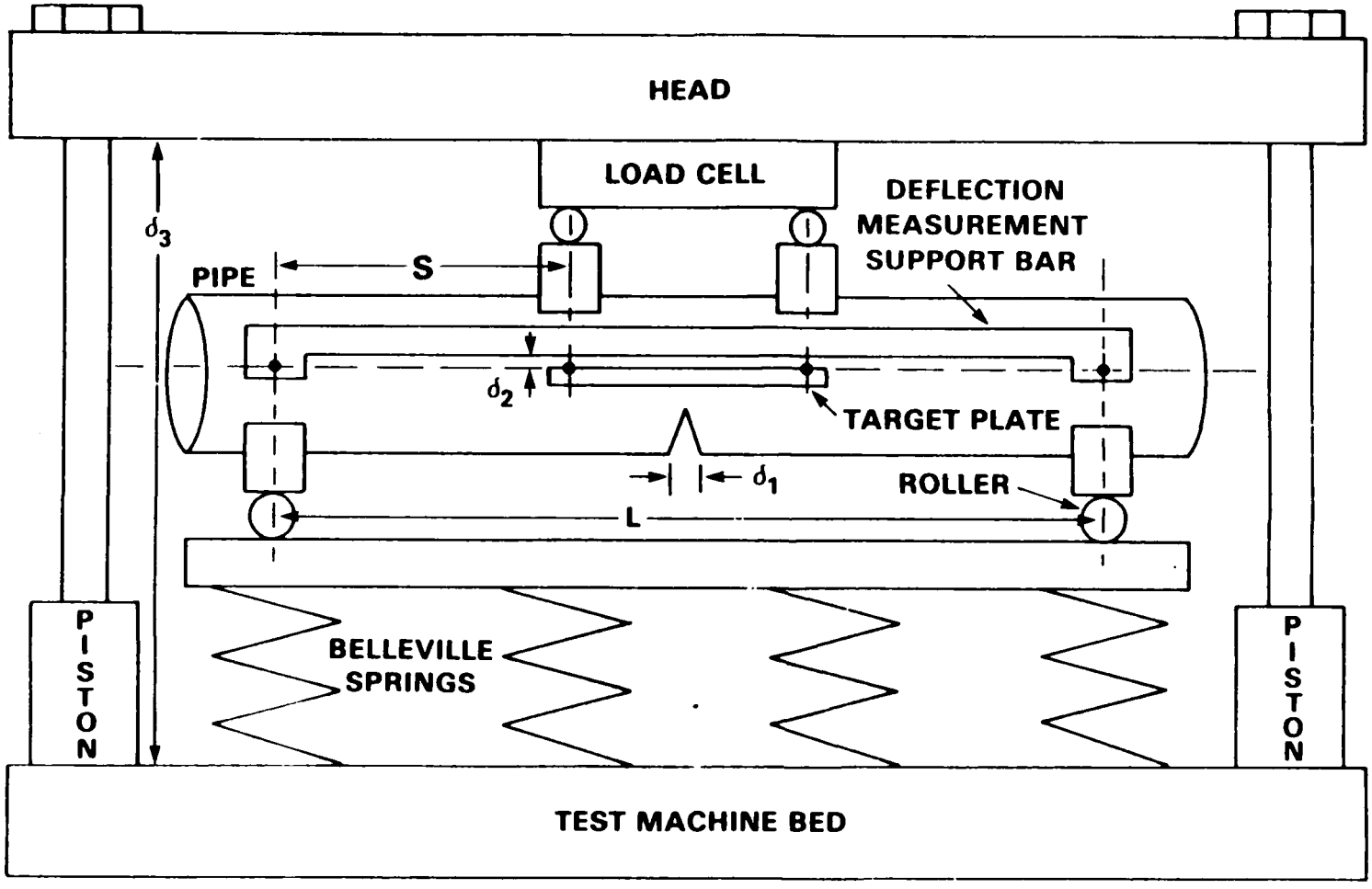

δ_1 = CRACK MOUTH OPENING DISPLACEMENT
δ_2 = PIPE LOAD LINE DEFLECTION
δ_3 = TOTAL DISPLACEMENT OF PIPE, MACHINE AND SPRINGS

Figure 5 - Schematic Drawing of Pipe Test Arrangement

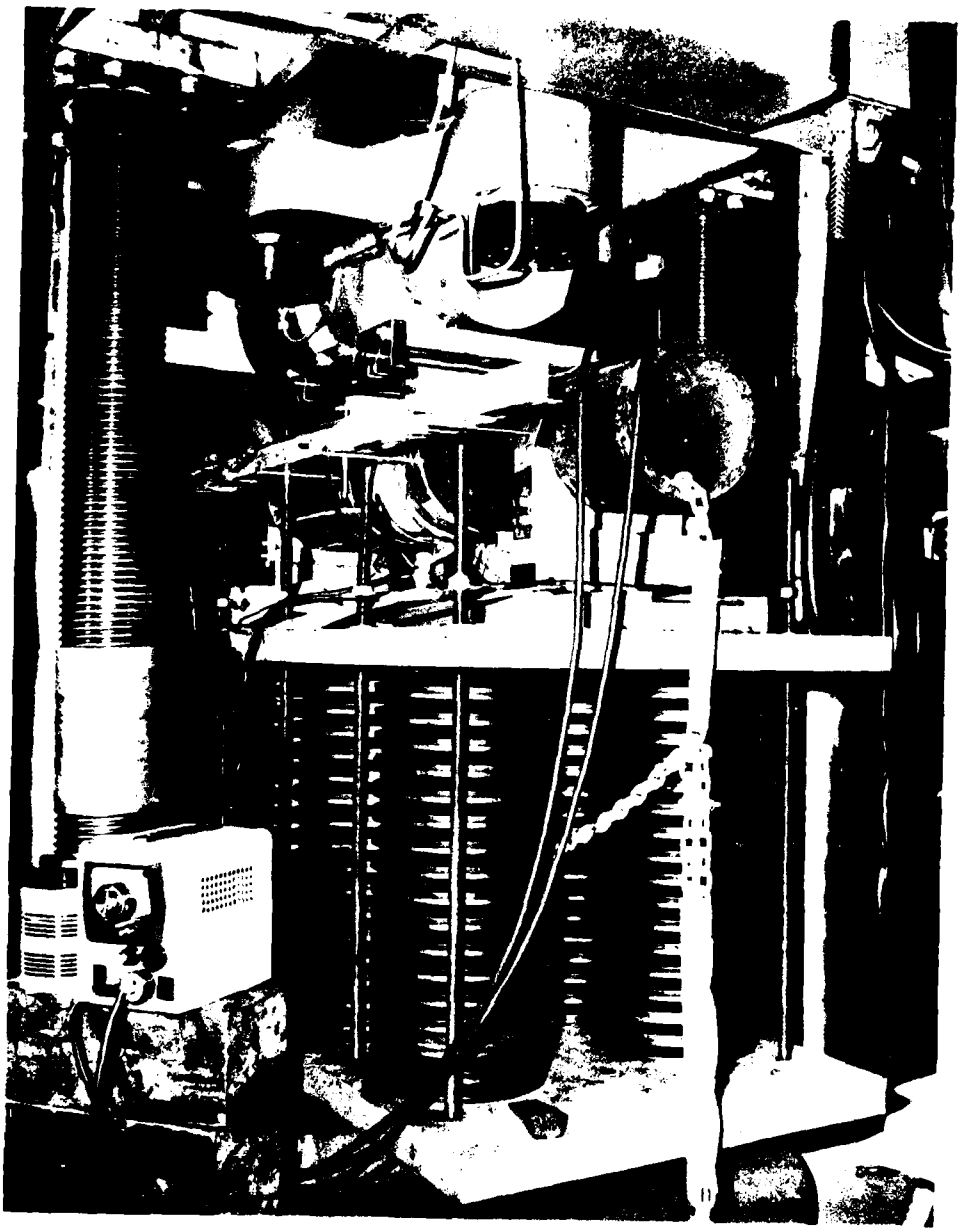

Figure 6 - Photograph, Pipe Test Arrangement

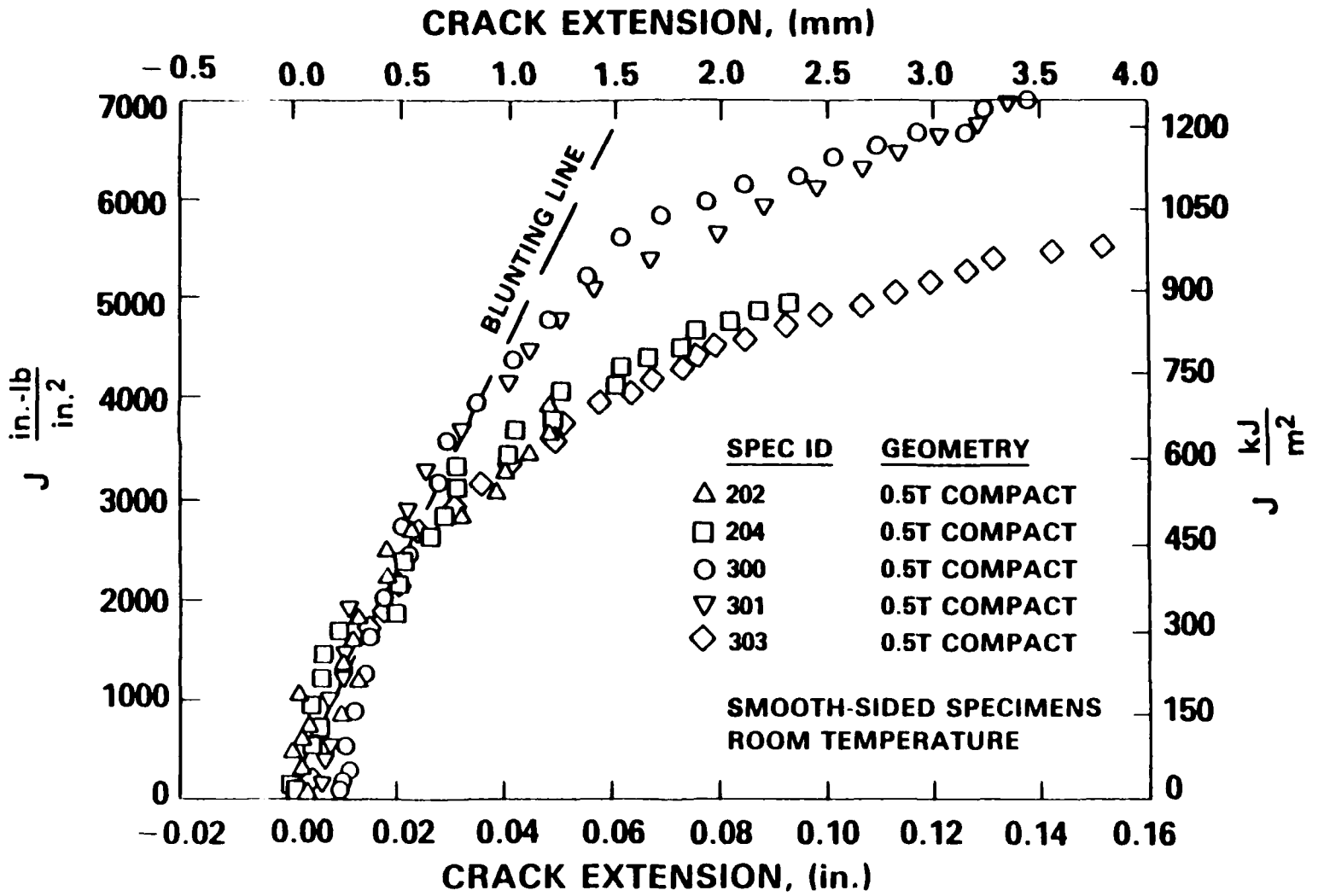

Figure 7 - J_I-R Curves for 1/2 T Compact Specimens of ASTM A106 Steel

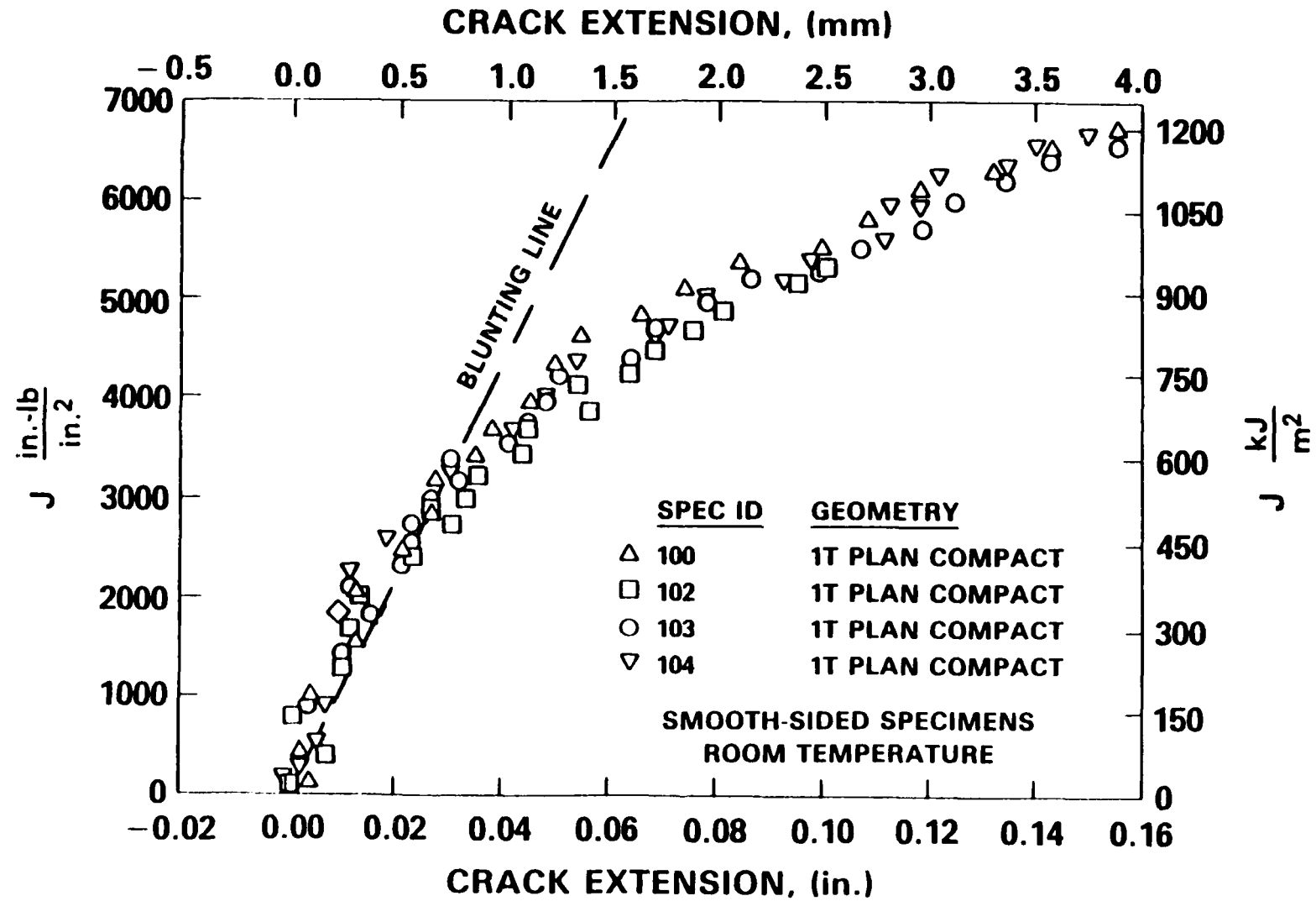

Figure 8 - J_I-R Curves of 1 T Plan Compact Specimens of ASTM A106 Steel

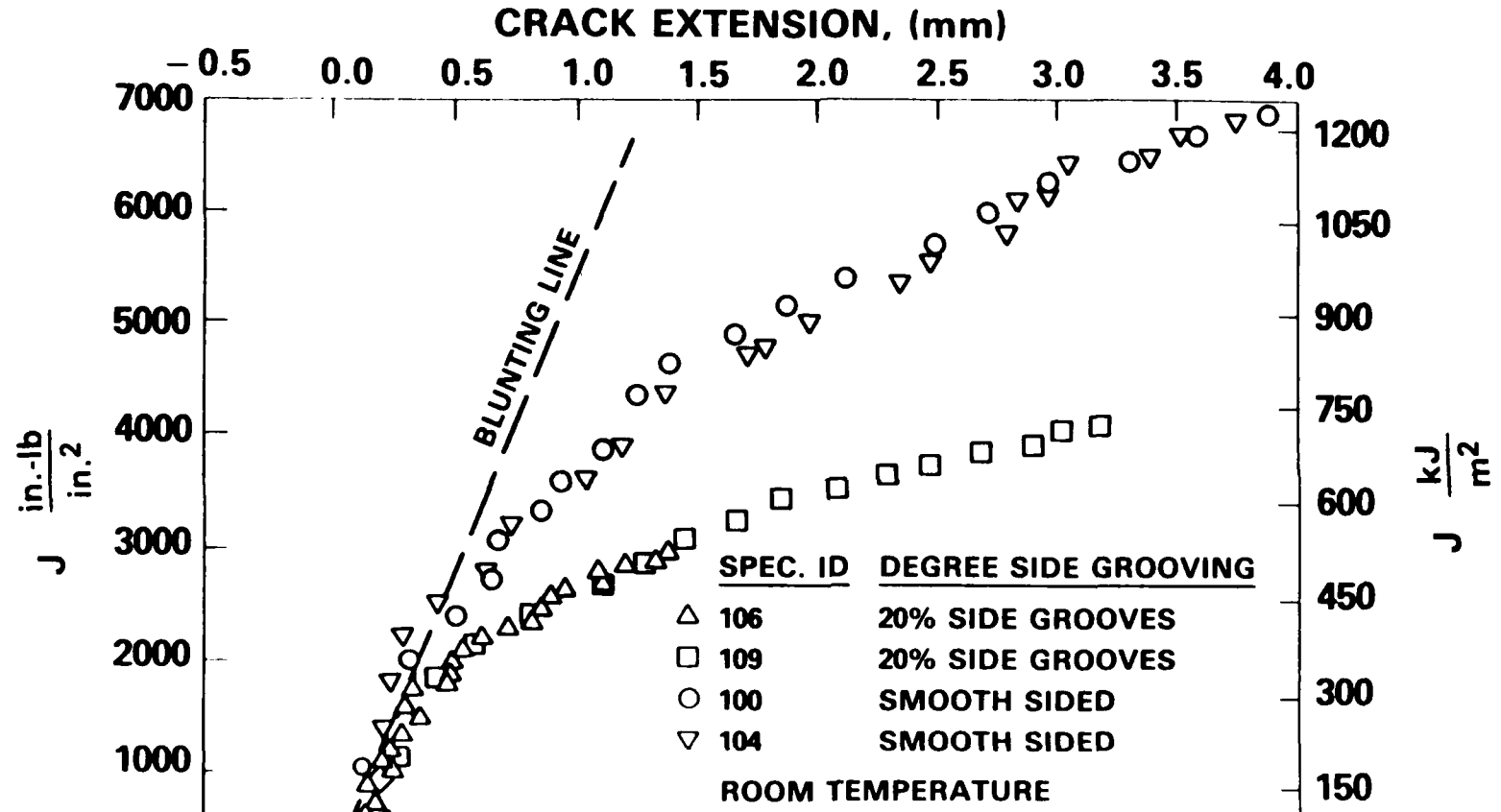

Figure 9 - J_I-R Curves for Smooth Sided and Side Grooved Compact Specimens of ASTM A106 Steel

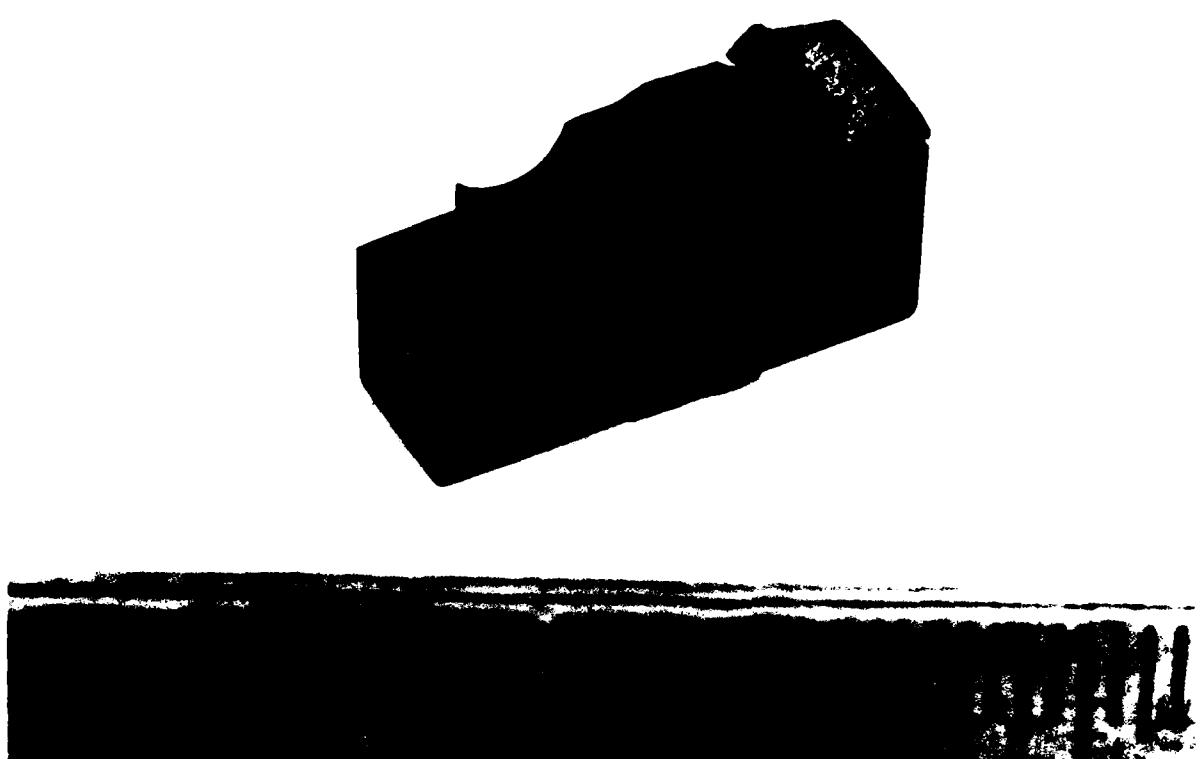

Figure 10 - Photograph, Fractured 1/2 T Compact Specimen of ASTM A106 Steel Pipe

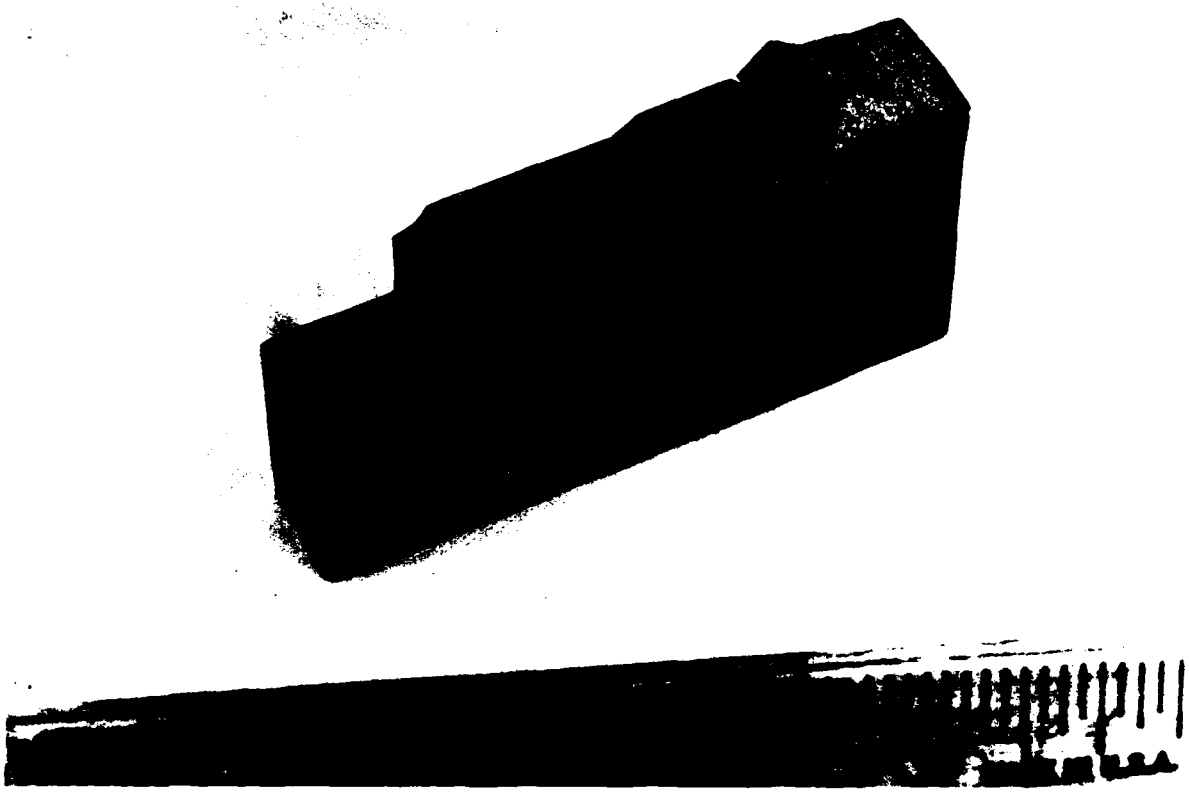

Figure 11 - Photograph, Fractured 1 T Plan Compact Specimen of ASTM A106 Steel Pipe

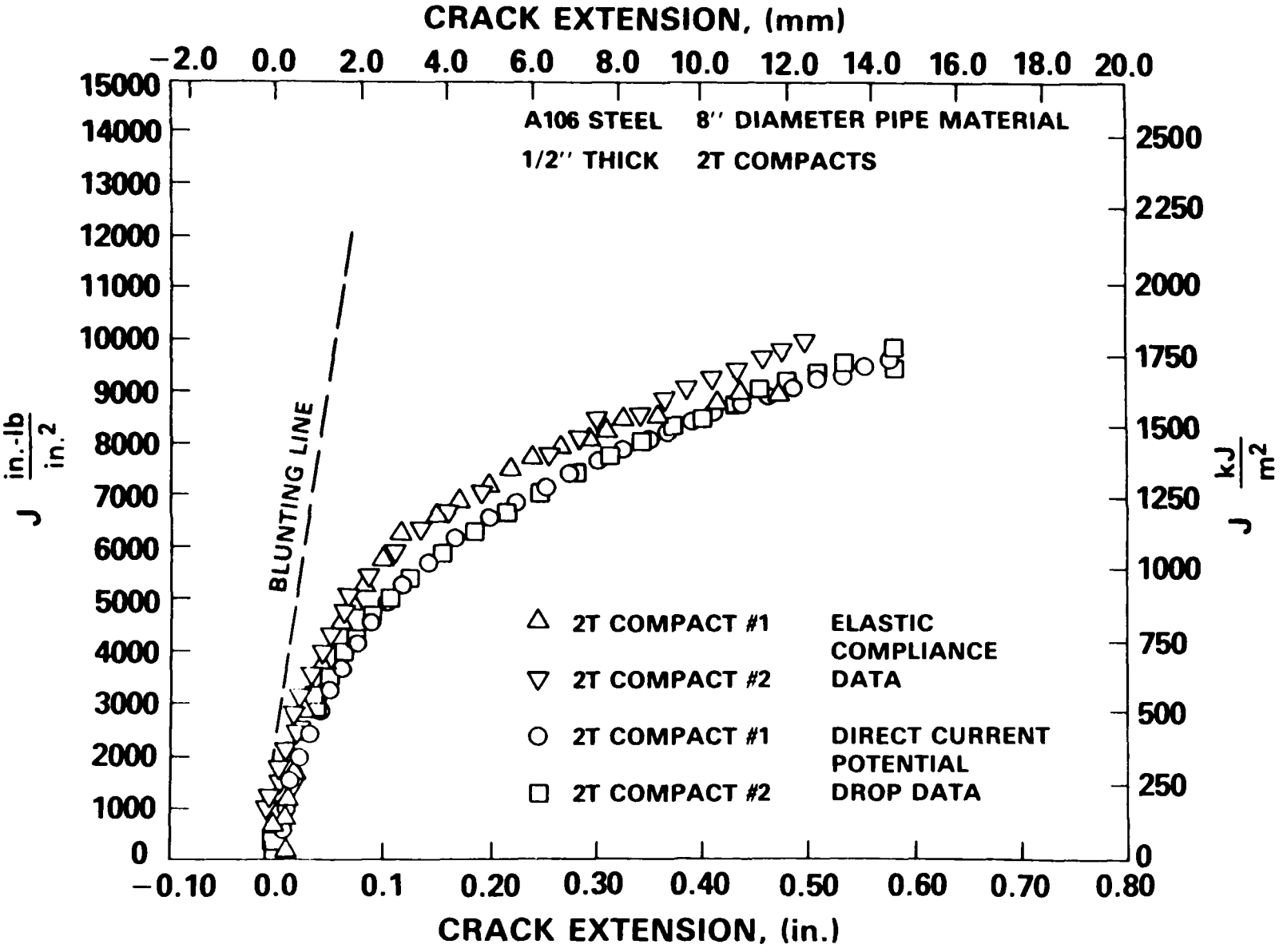

Figure 12 - J_I-R Curves for 2 T Plan Compact Specimens of ASTM A106 Steel Pipe

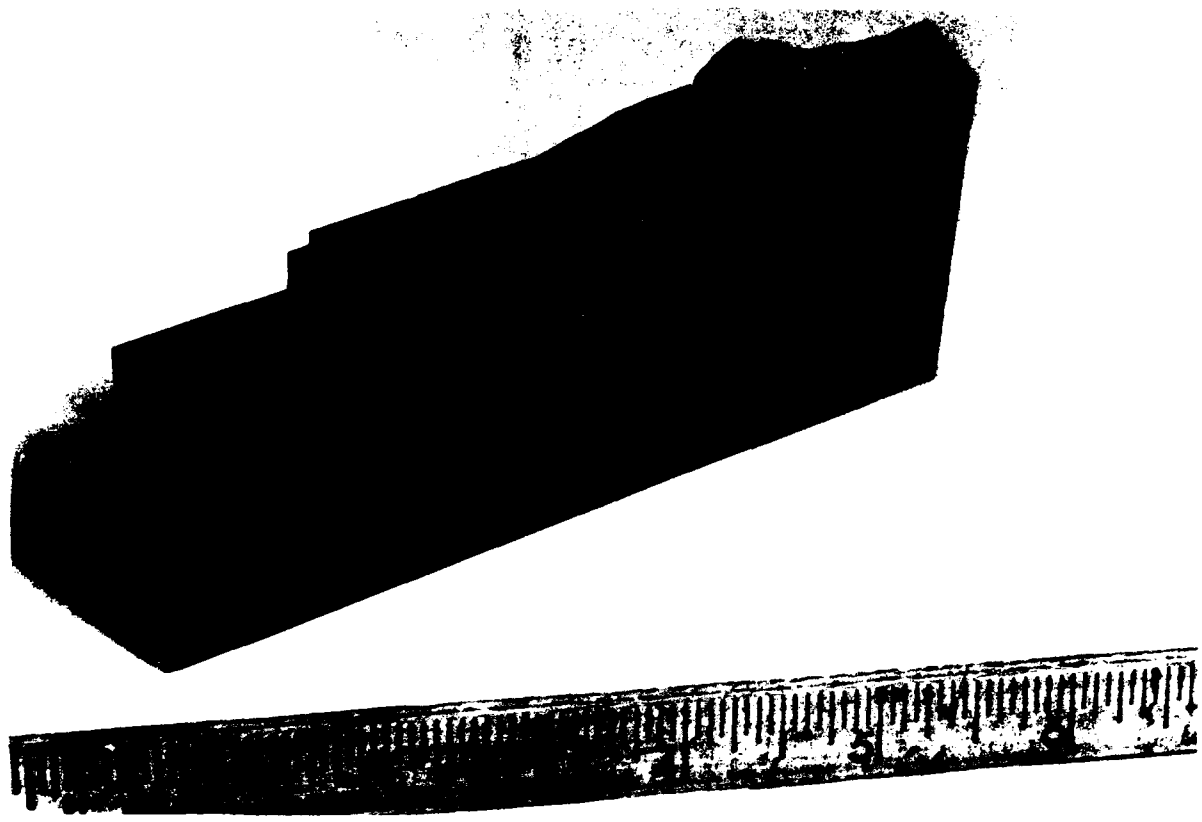

Figure 13 - Photograph, Fractured 2 T Plan Compact Specimen of ASTM A106 Steel Pipe

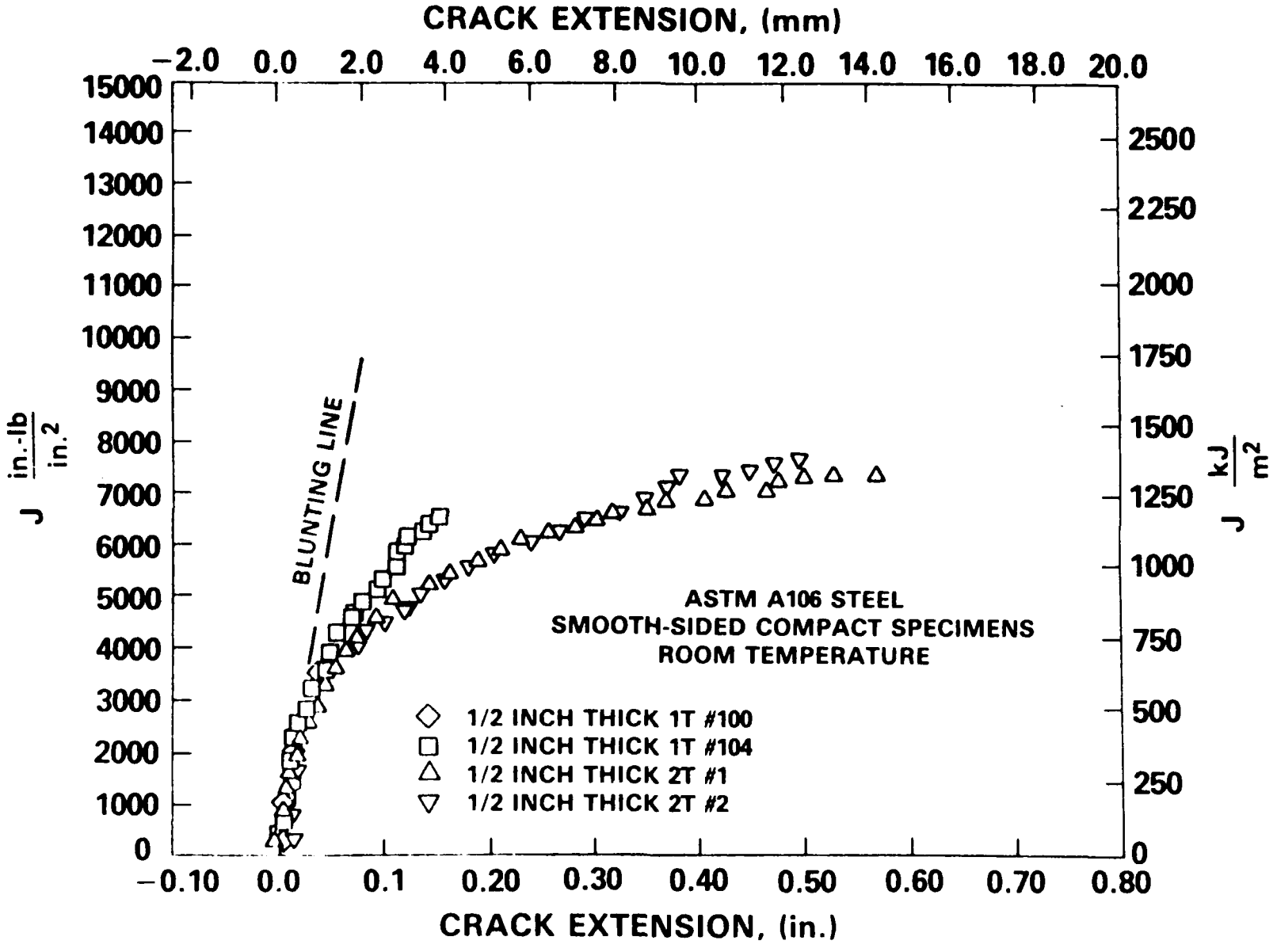

Figure 14 - J_I-R Curves From Elastic Compliance for 1/2-inch Thick 1 T and 2 T Compact Specimens of ASTM A106 Steel Pipe

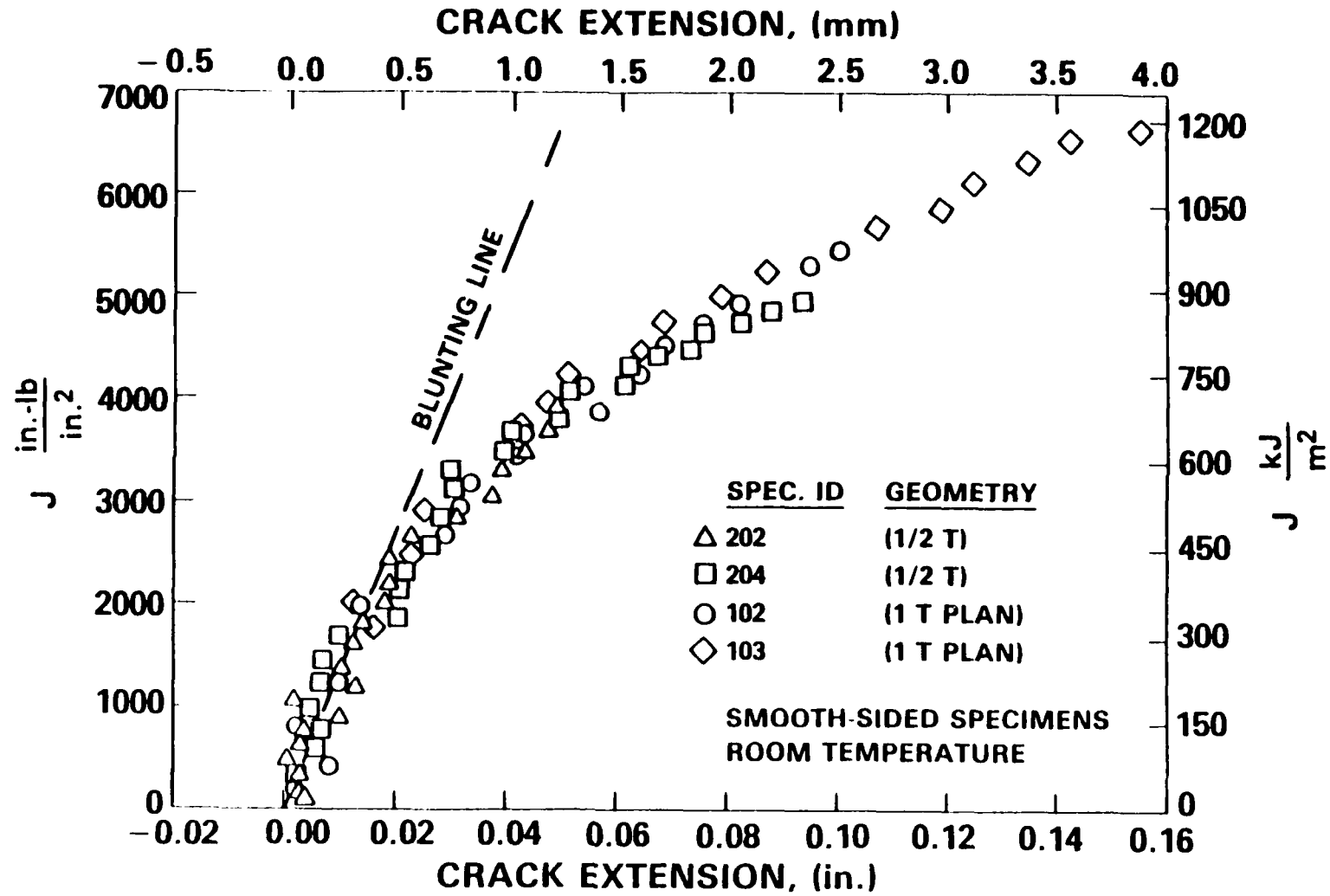

Figure 15 - J_I-R Curves From Elastic Compliance for 1/2 T and 1 T Plan Compact Specimens

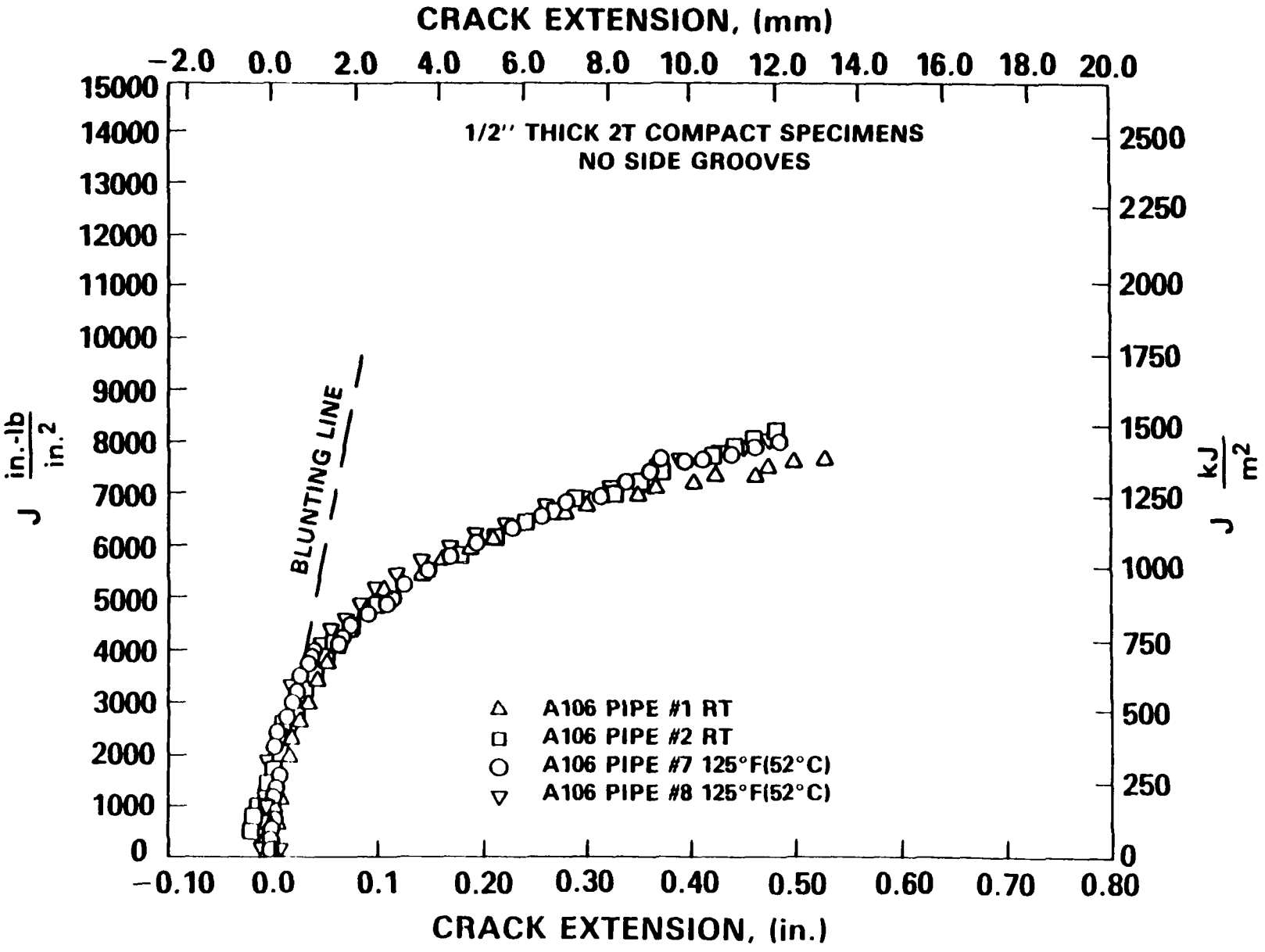

Figure 16 - J_I-R Curves for 2 T Plan Specimens of ASTM A106 Steel Tested at 125°F (52°C) and Room Temperature

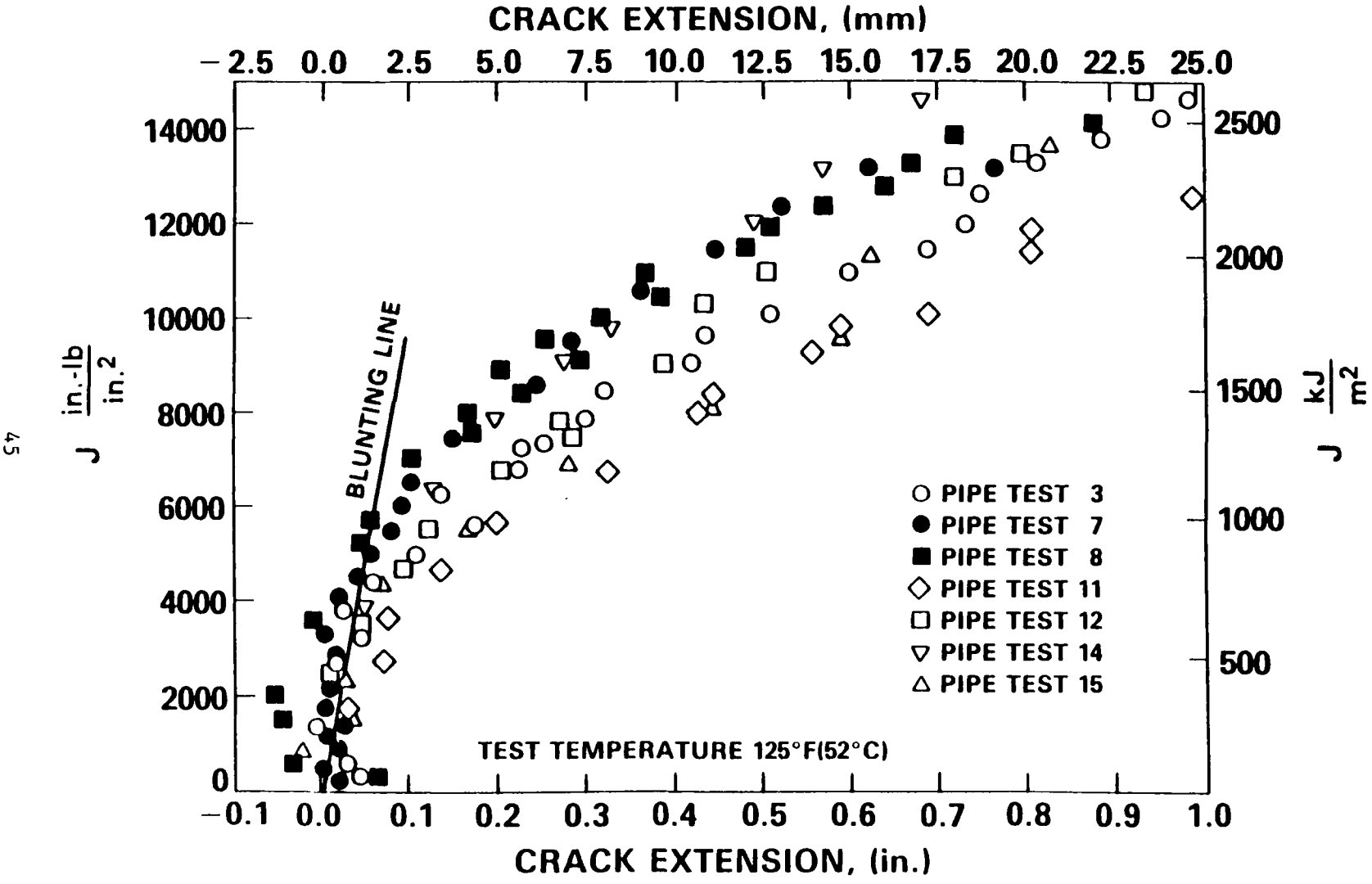

Figure 17 - J_I-R Curves From Elastic Compliance for 4-Point Bend Tests of ASTM A106 Steel Pipe Specimens

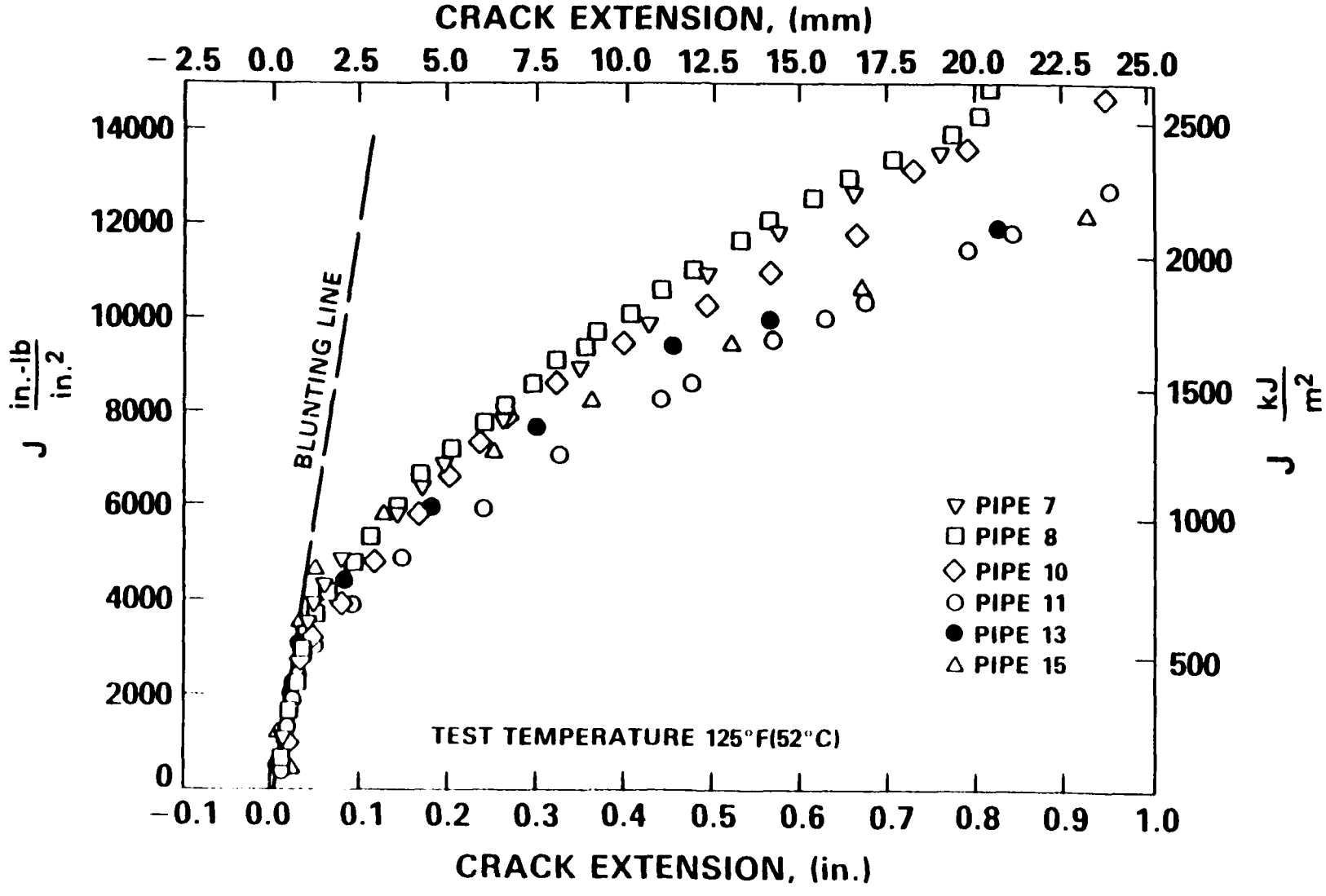

Figure 18 - J_I-R Curves for 4-Point Bend Tests of ASTM A106 Steel Pipe Specimens Using the D.C. Potential Drop Technique

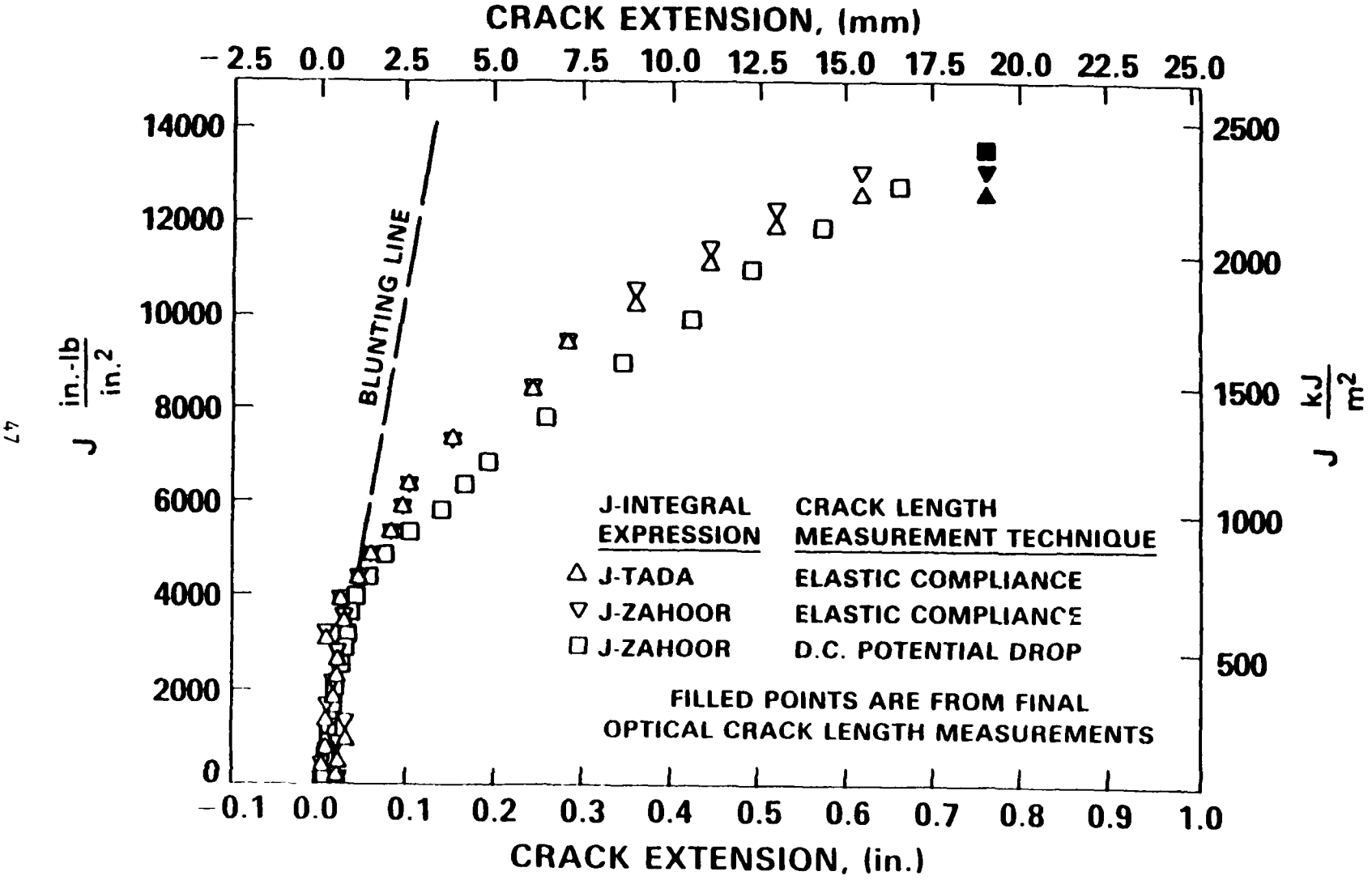

Figure 19 - J_I-R Curves for Pipe Test #7

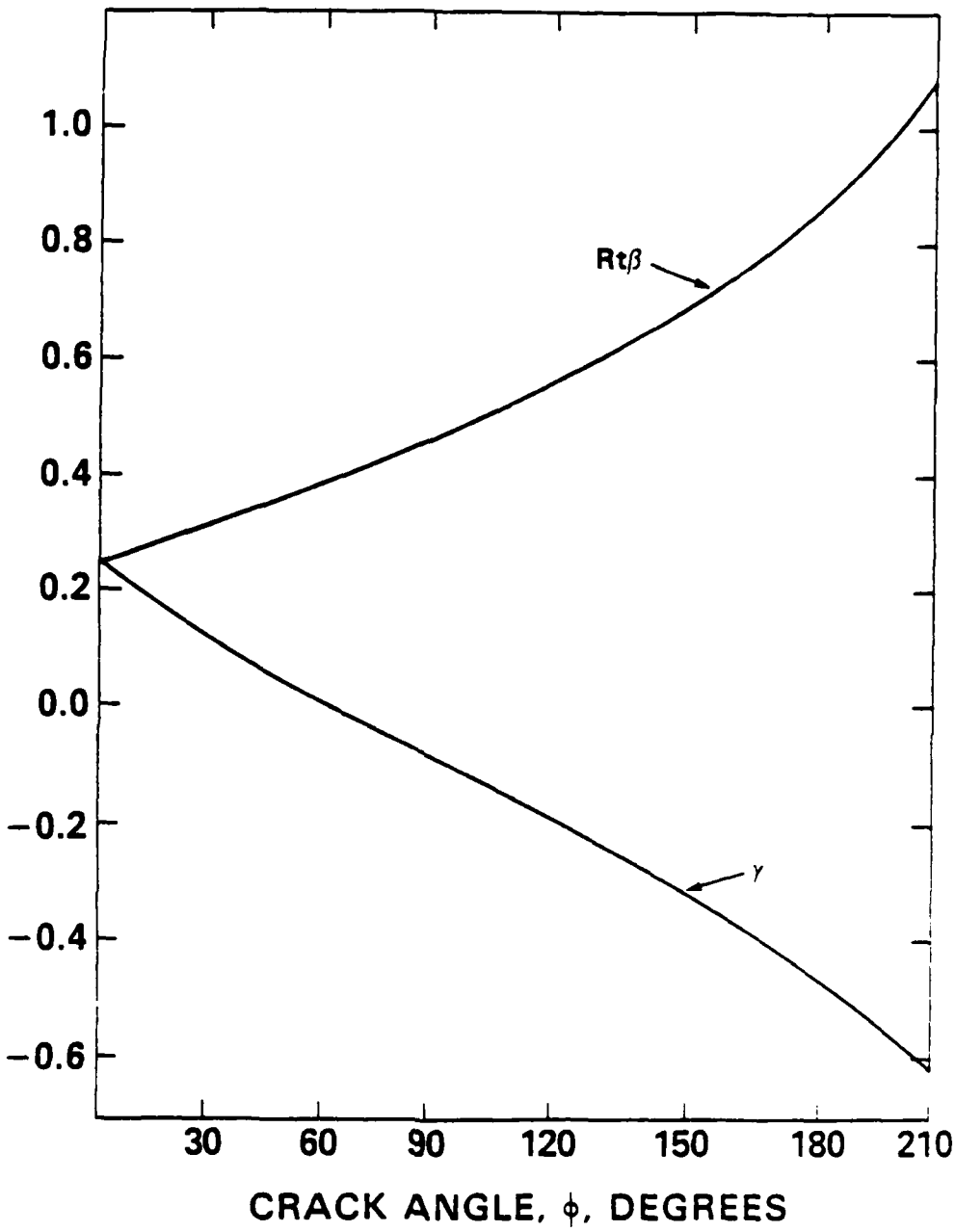

Figure 20 - Variation in Crack Growth Correction Coefficient (γ) With Total Crack Angle (ϕ) (Reference 13)

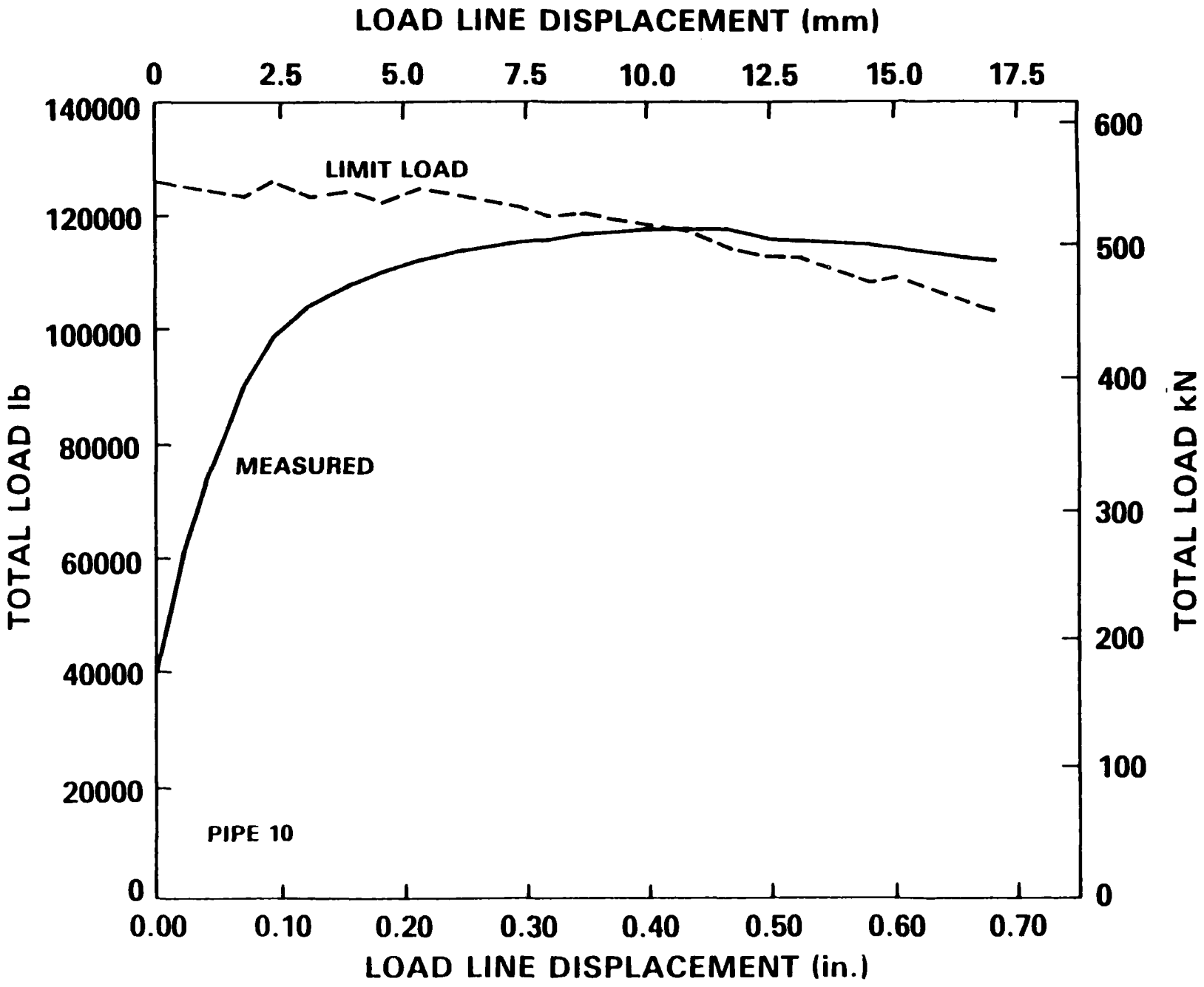

Figure 21 - Limit Load and Measured Loads for Pipe Test #7

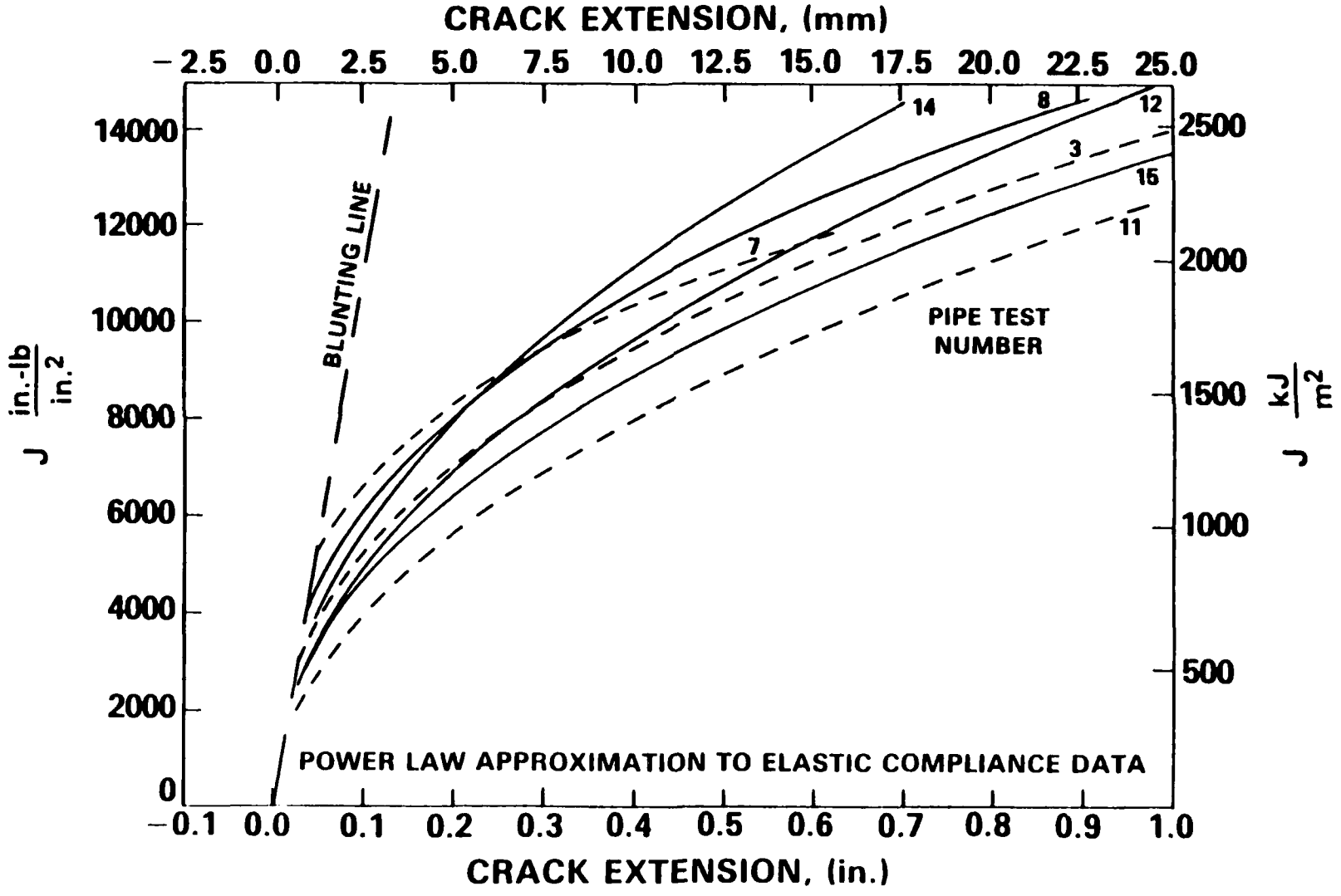

Figure 22 - Power Law Approximation of J_I-R Curve Data for ASTM A106 Steel Pipe Bend Tests Using the Elastic Compliance Technique

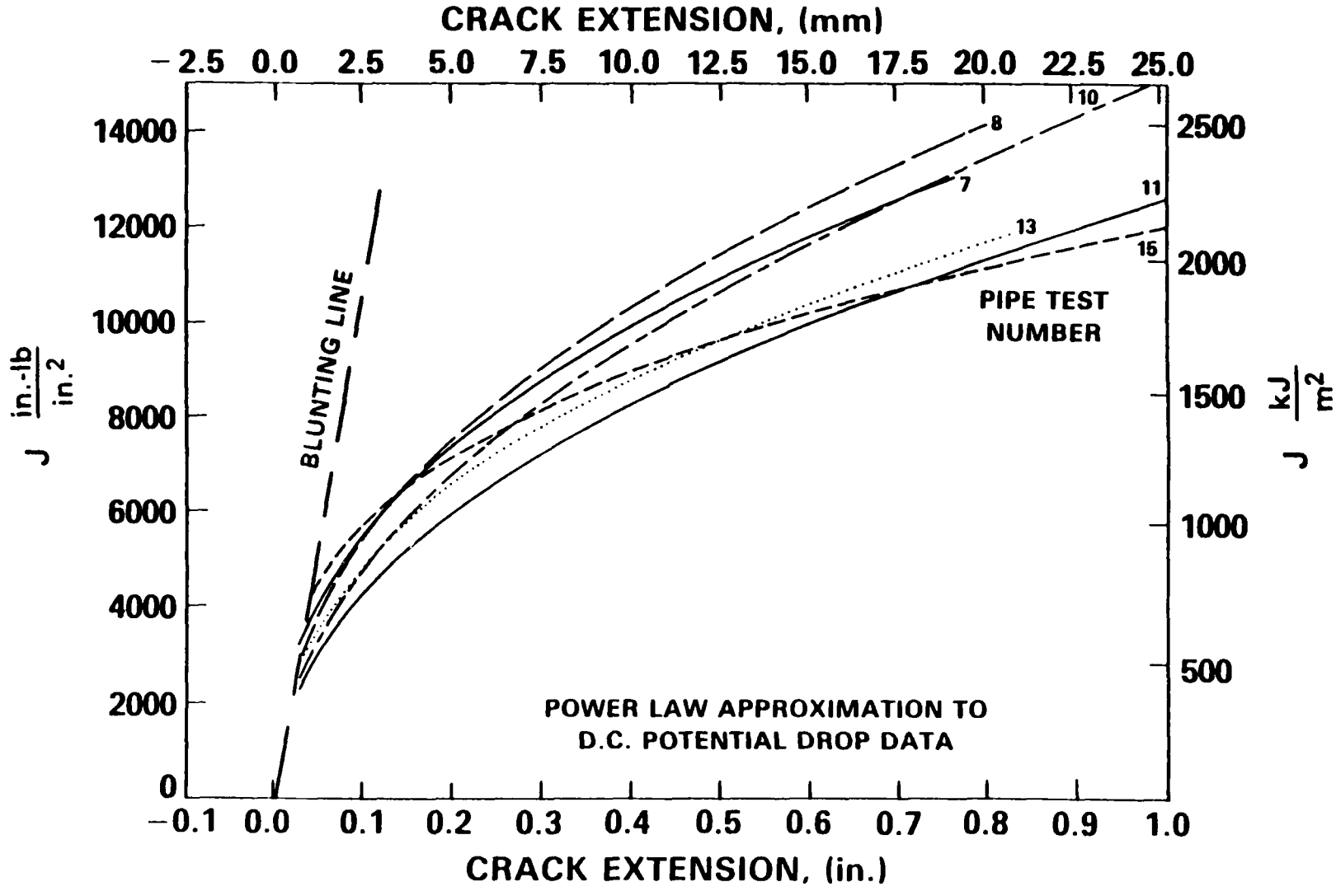

Figure 23 - Power Law Approximation of J_I-R Curve Data for ASTM A106 Steel Pipe Bend Tests Using the D.C. Potential Drop Technique

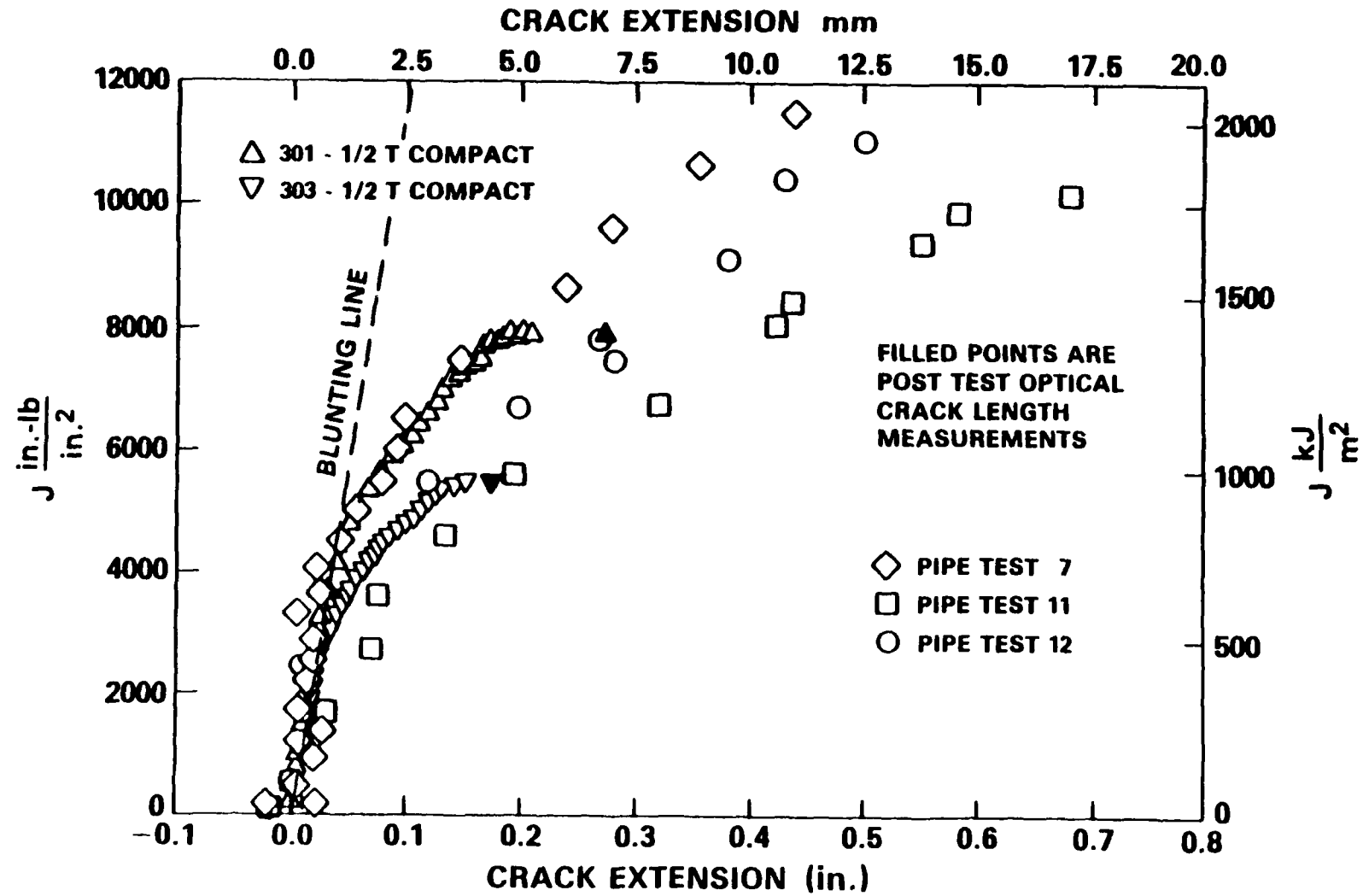

Figure 24 - J_I-R Curves for 1/2 T Compact Specimens and Pipe Bend Specimens of ASTM A106 Steel

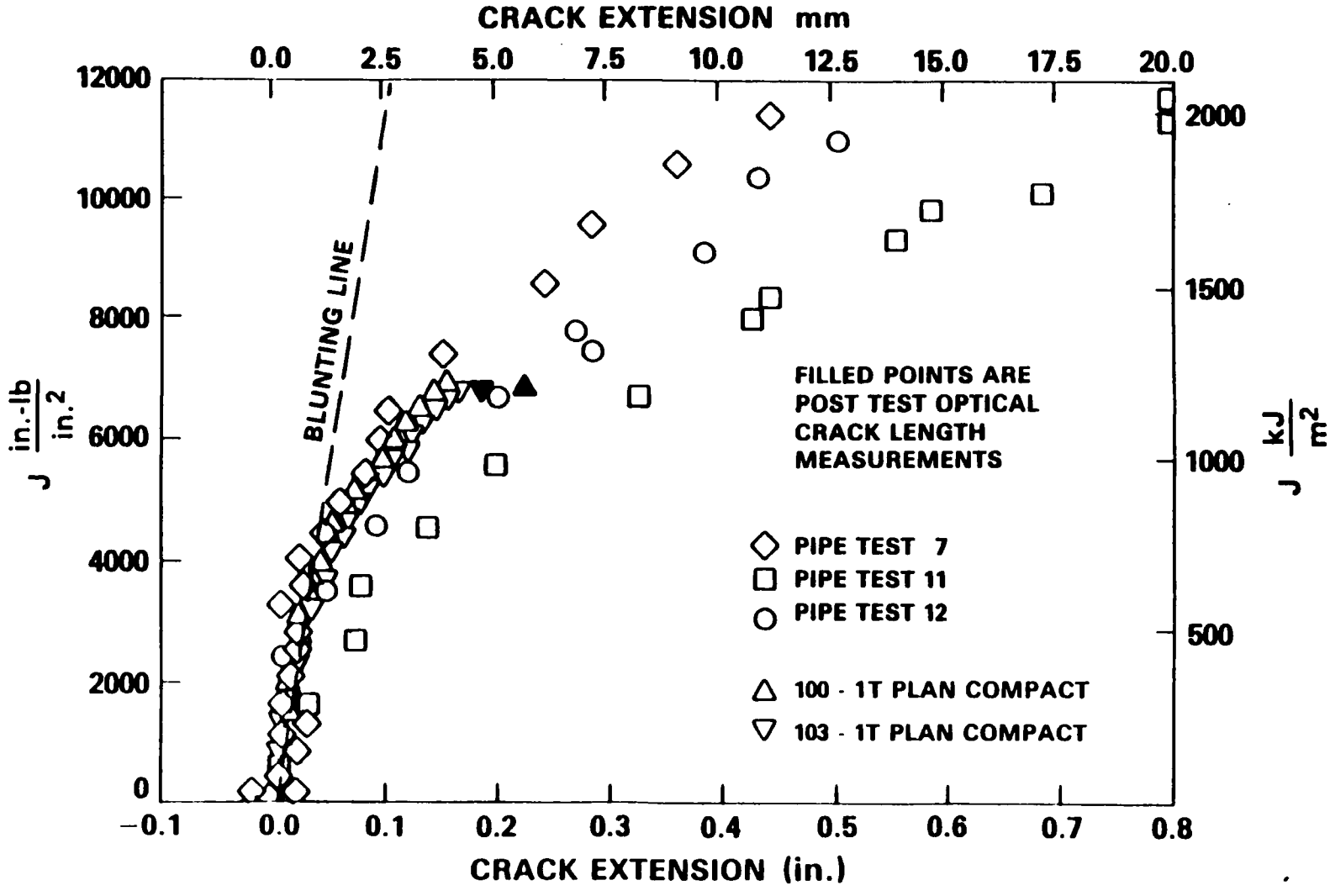

Figure 25 - J_I-R Curves for 1 T Plan Compact Specimens and Pipe Bend Specimens of ASTM A106 Steel

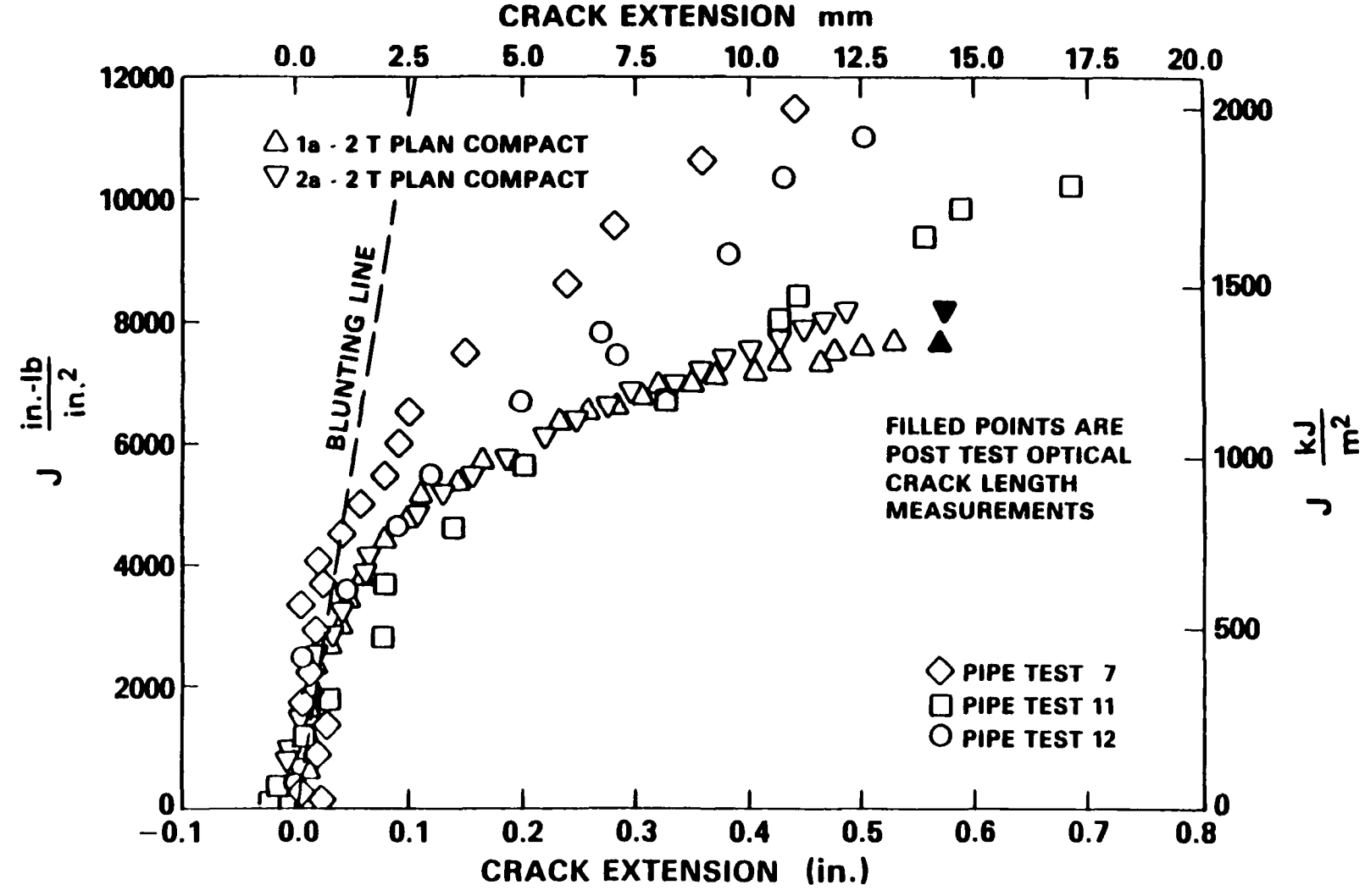

Figure 26 - J_I-R Curves of 2 T Plan Compact Specimens and Pipe Bend Tests of ASTM A106 Steel Using the Elastic Compliance Technique

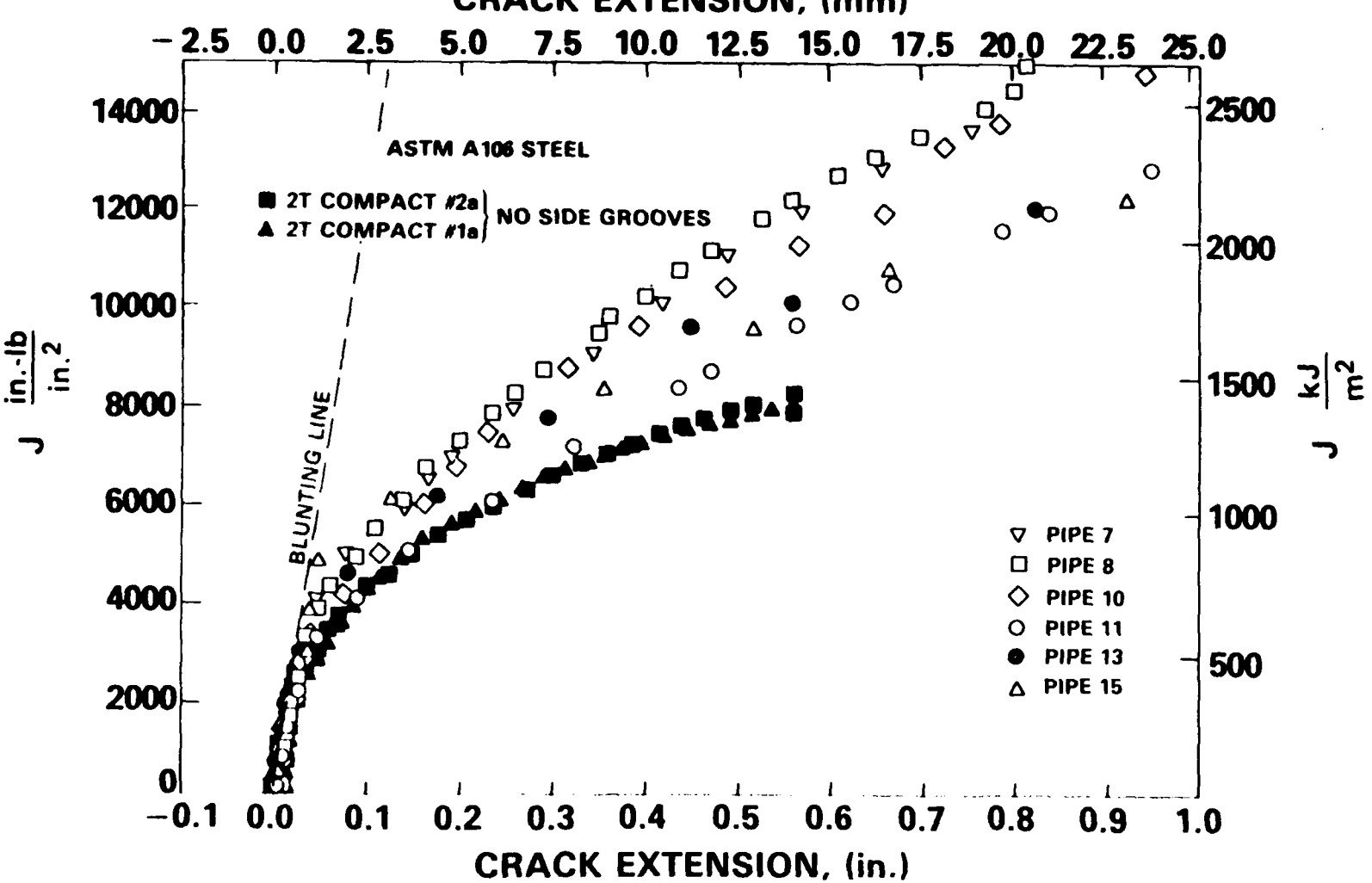

Figure 27 - J_I-R Curves of 2 T Plan Compact Specimens and Pipe Bend Tests of ASTM A106 Steel Using D.C. Potential Drop

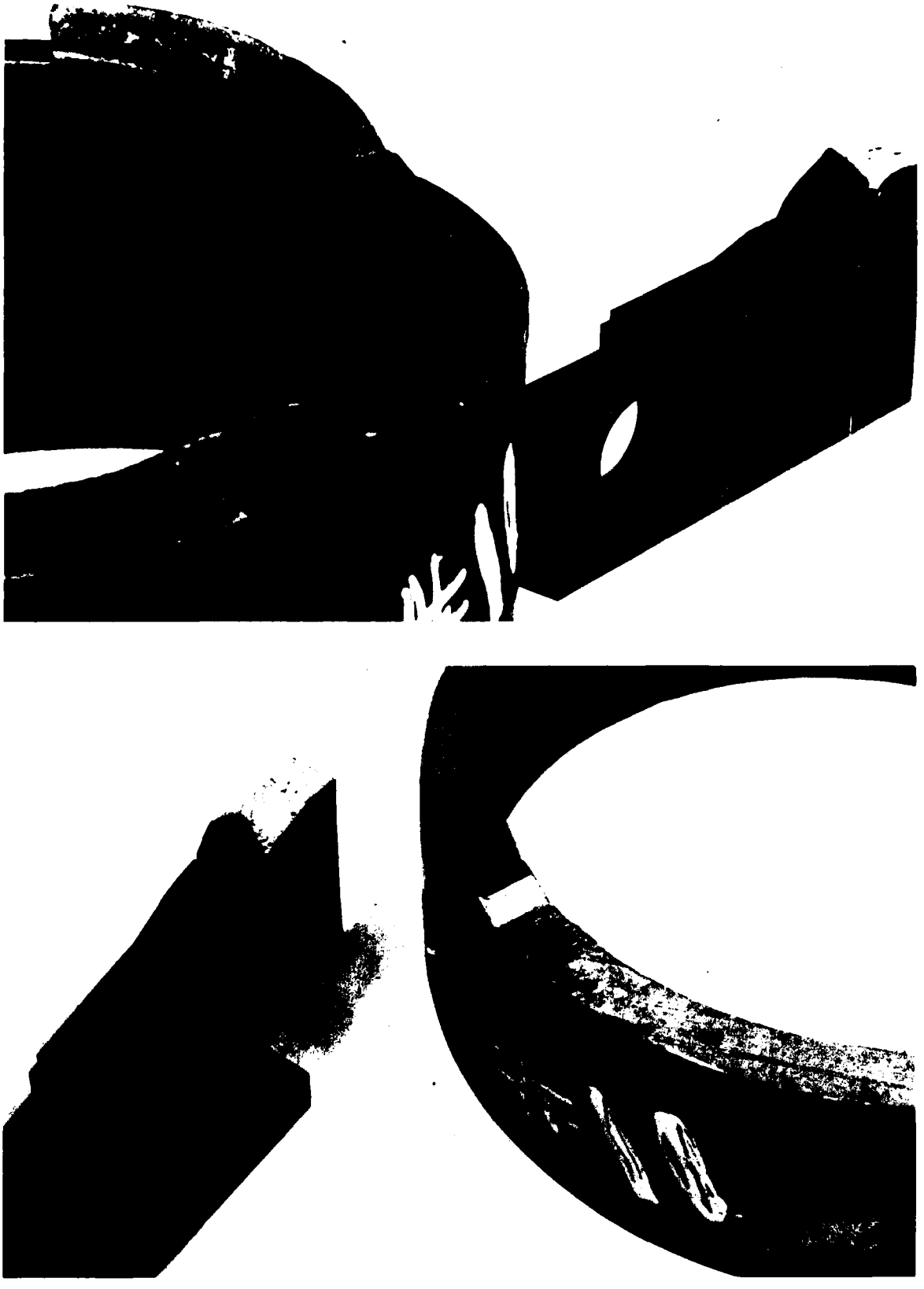

Figure 28 - Photographs Showing Two Views of Fracture Surfaces of 1/2-inch (12 mm) Thick 2 T Plan and Pipe Bend Specimens, ASTM A106 Steel

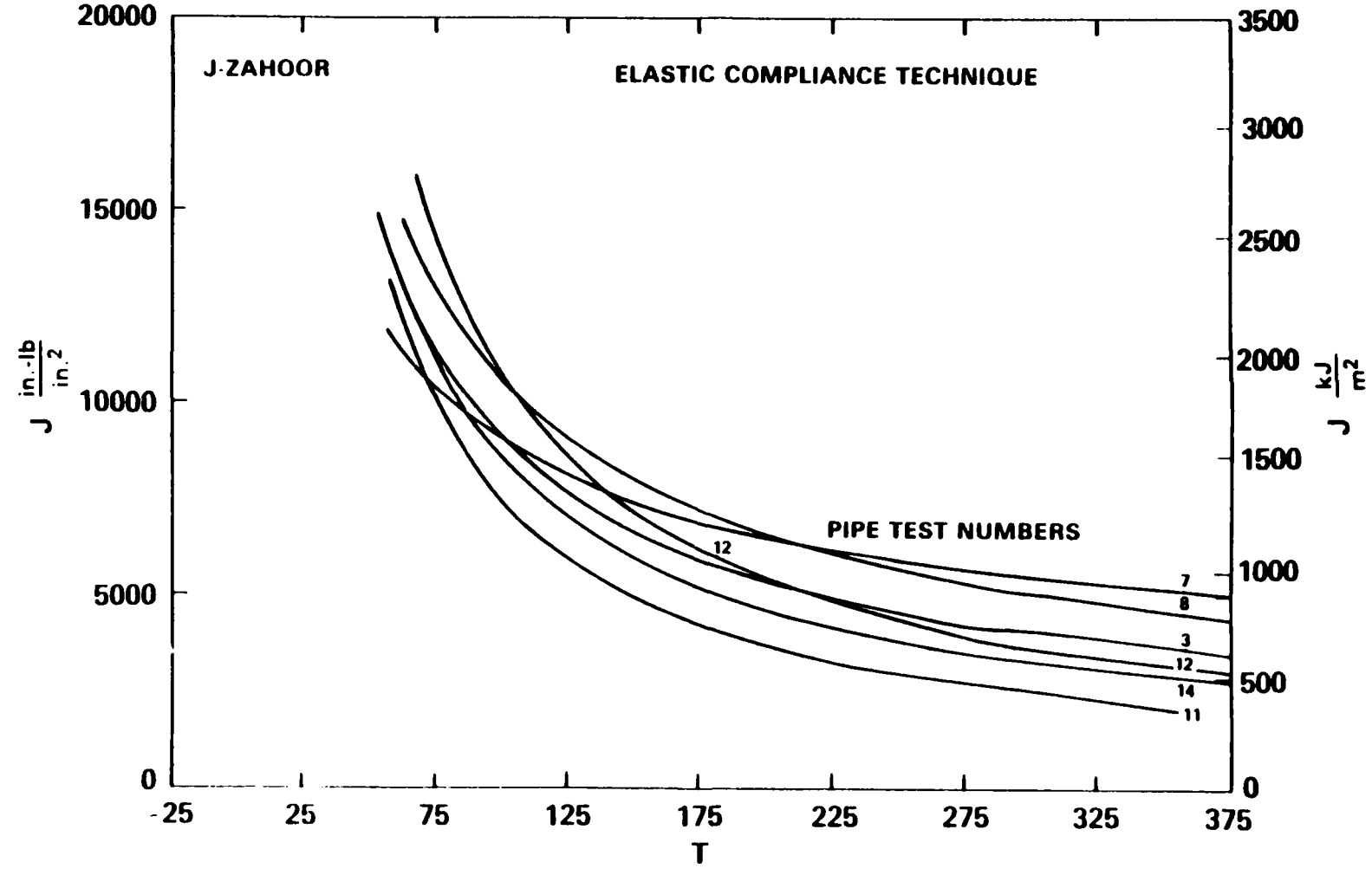

Figure 29 - J/T Plot of Power Law Approximations to J_I-R Curve Data From Pipe Tests Using Elastic Compliance Technique

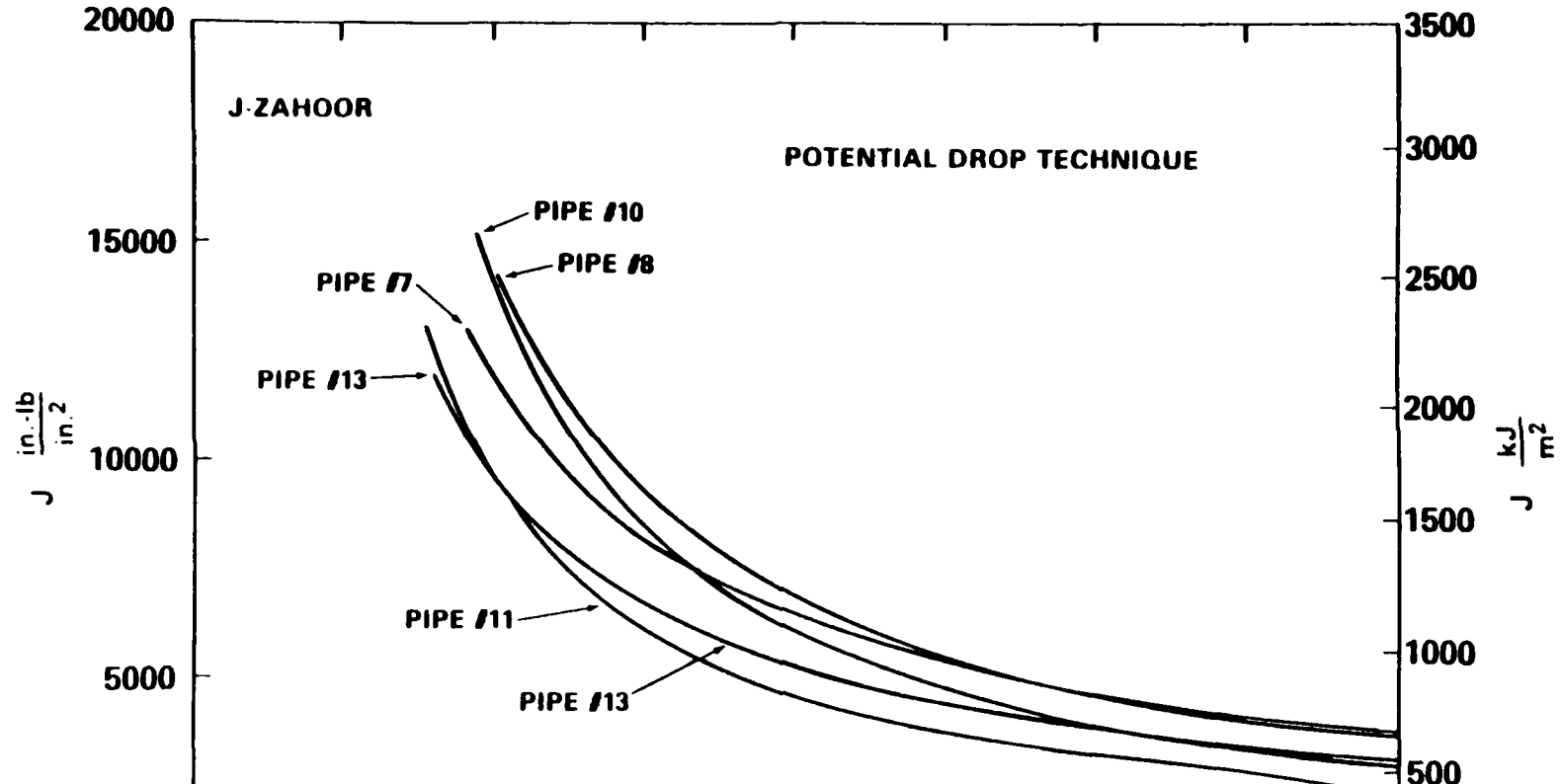

Figure 30 - J/T Plot of Power Law Approximations to J_I-R Curve Data From Pipe Tests Using D.C. Potential Drop Technique

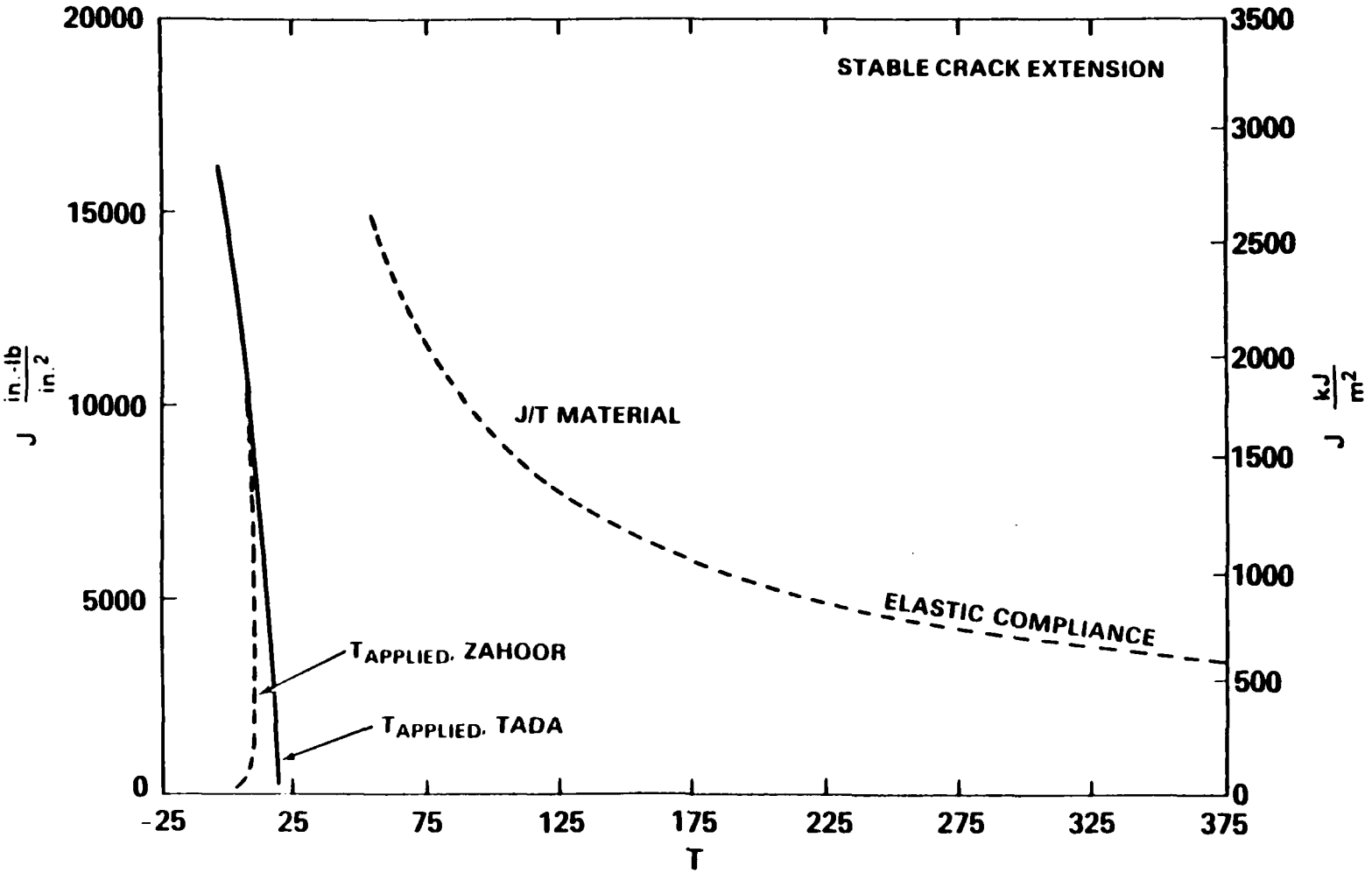

Figure 31 - J/T Plots for $T_{applied}$ and $T_{material}$ Calculated for Pipe Test Number 3 With a Machine Stiffness of 500,000 lb/in. (87,550 N/mm)

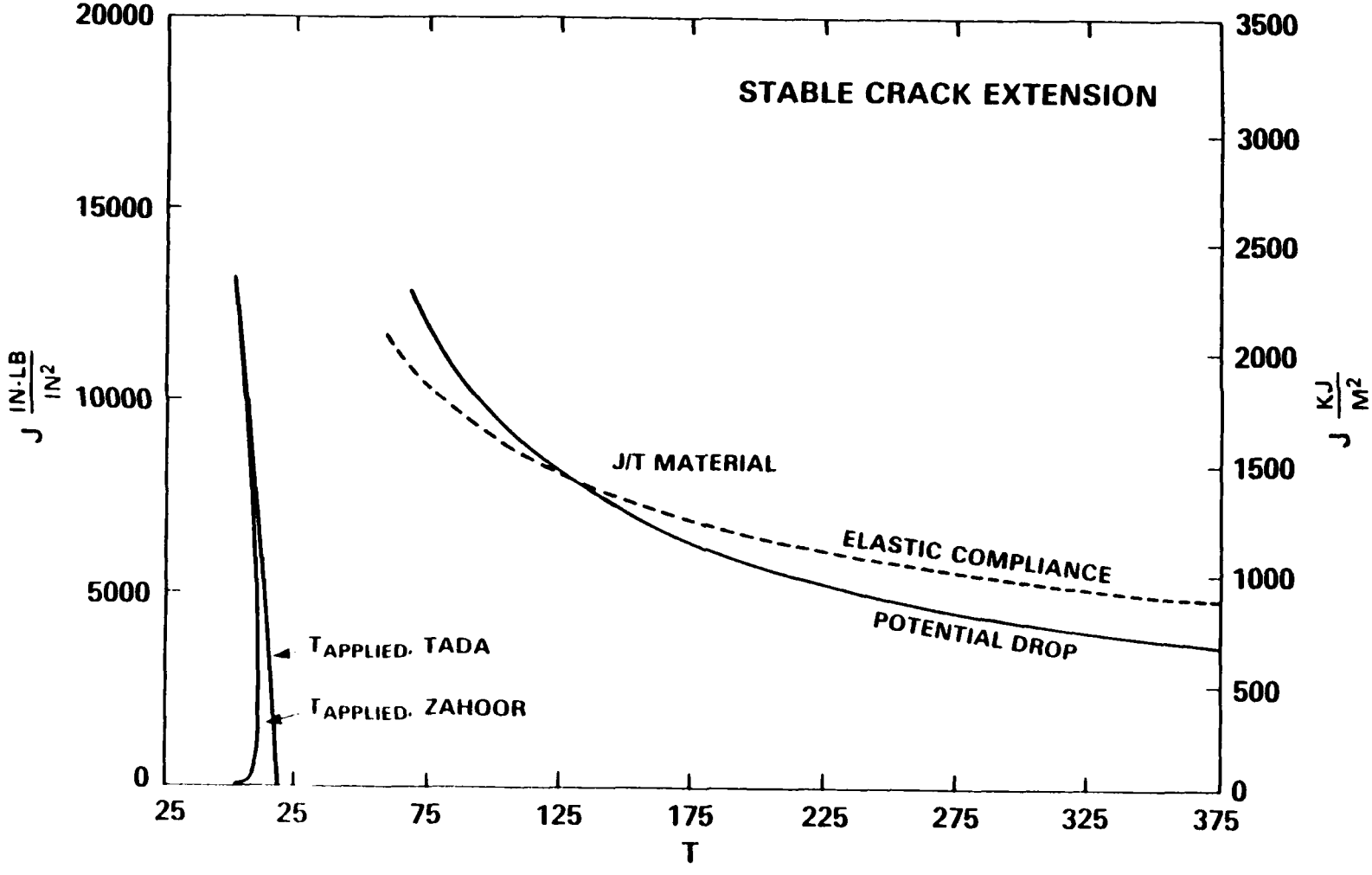

Figure 32 - J/T Plots for $T_{applied}$ and $T_{material}$ Calculated for Pipe Test Number 7 With a Machine Stiffness of 500,000 lb/in. (87,550 N/mm)

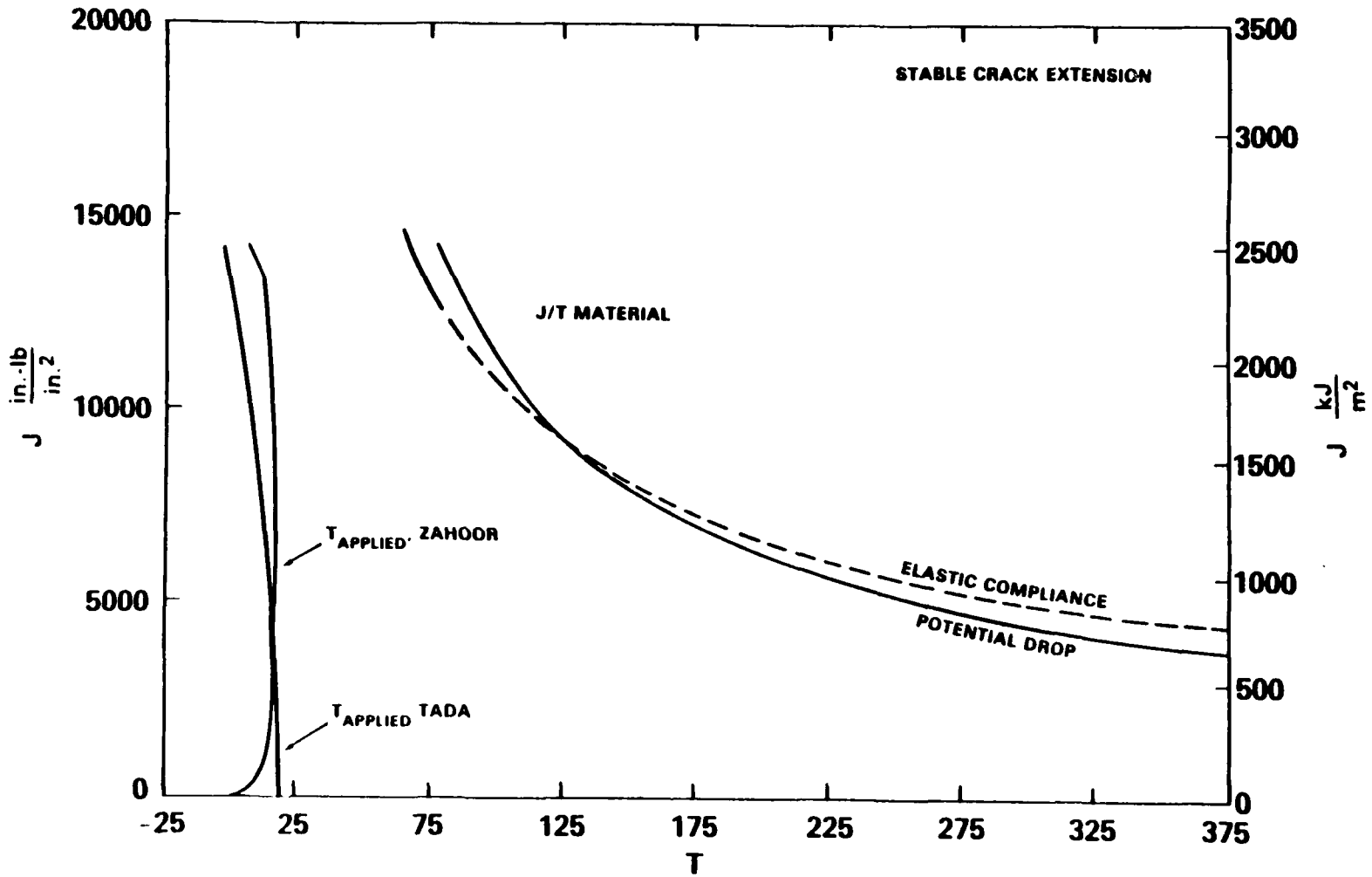

Figure 33 - J/T Plots for $T_{applied}$ and $T_{material}$ Calculated for Pipe Test Number 8 With a Machine Stiffness of 500,000 lb/in. (87,550 N/mm)

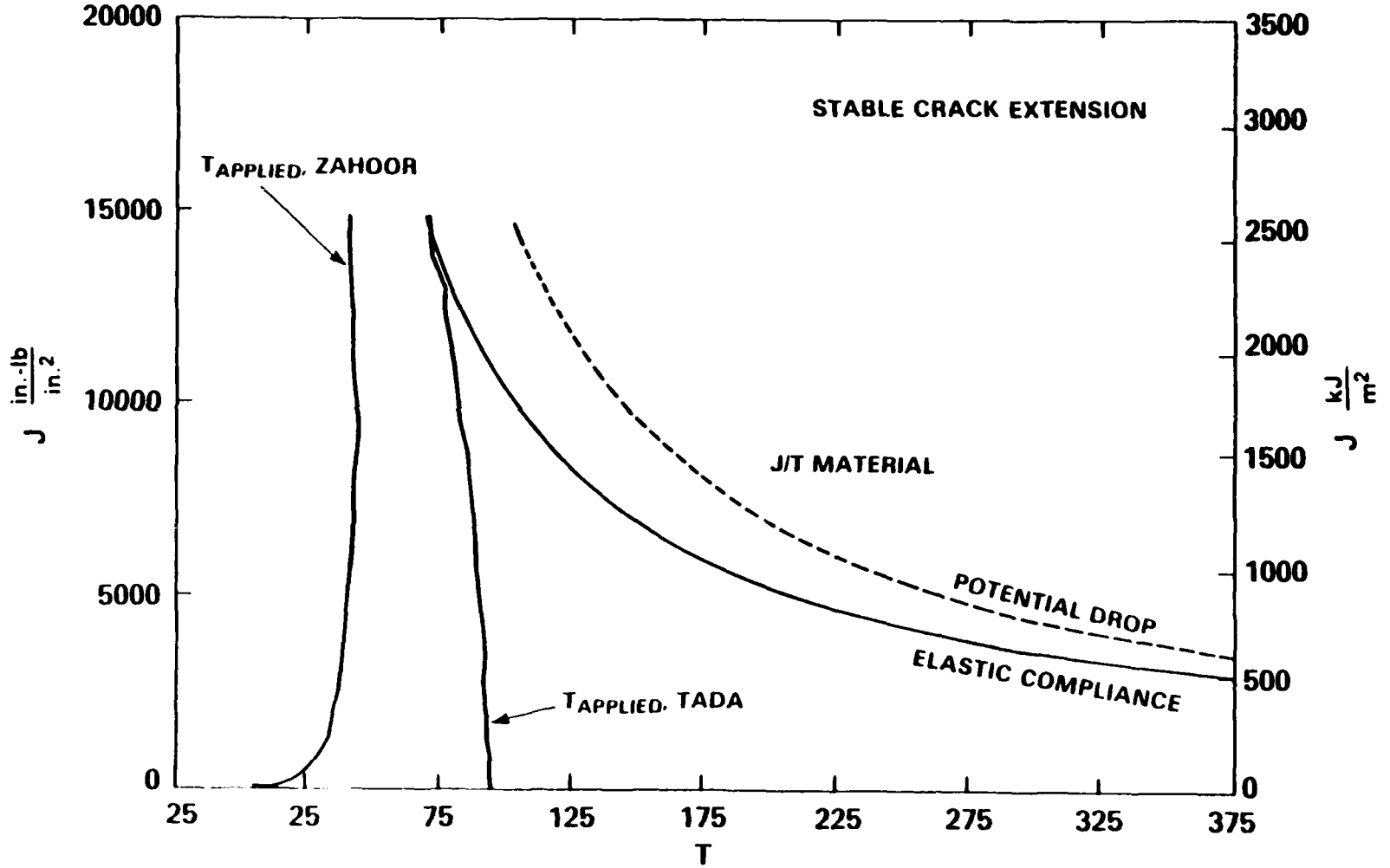

Figure 34 - J/T Plots for $T_{applied}$ and $T_{material}$ Calculated for Pipe Test Number 10 With a Machine Stiffness of 39,000 lb/in. (6,829 N/mm)

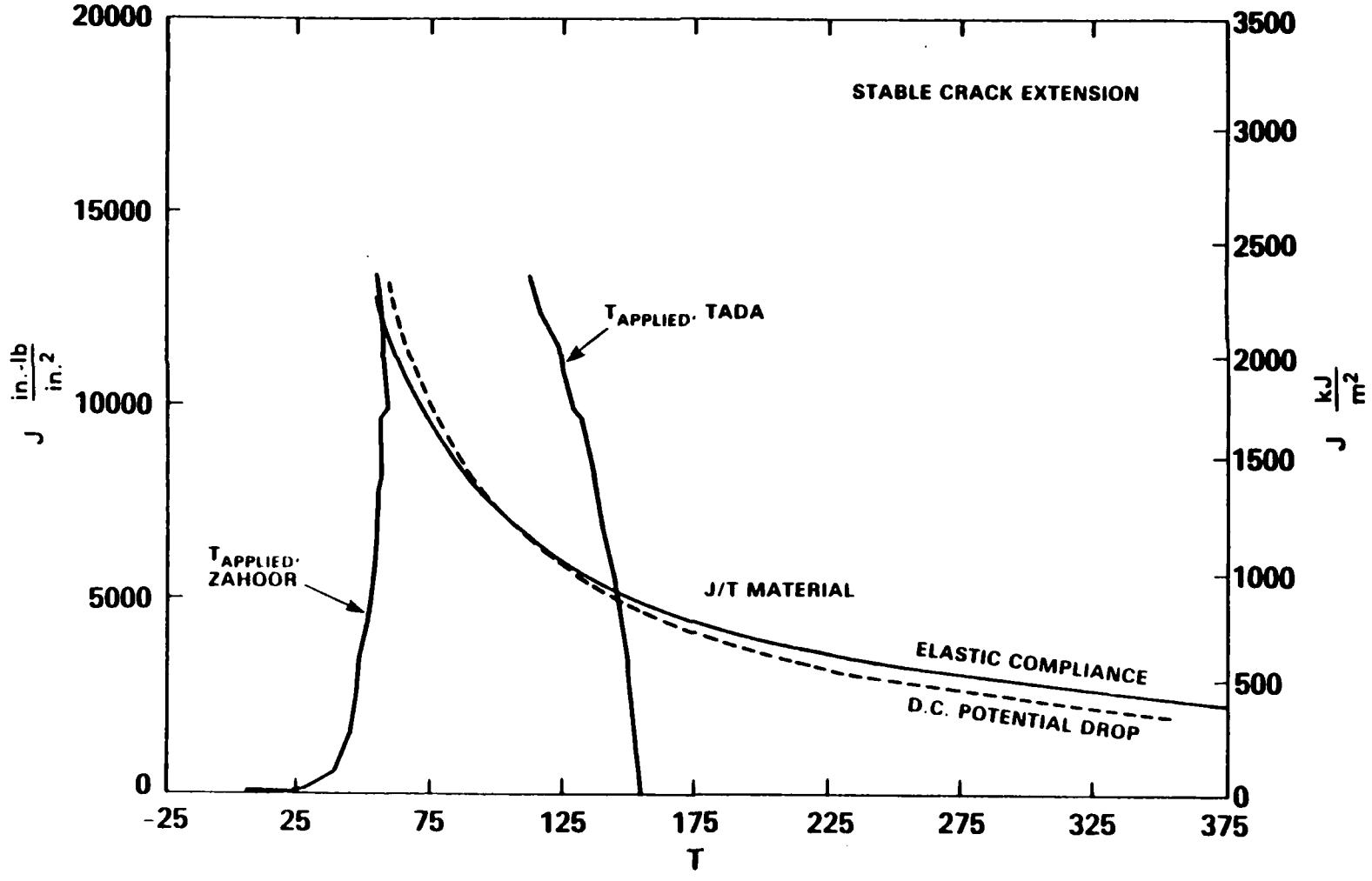

Figure 35 - J/T Plots for $T_{applied}$ and $T_{material}$ Calculated for Pipe Test Number 11 With a Machine Stiffness of 37,000 lb/in. (6,479 N/mm)

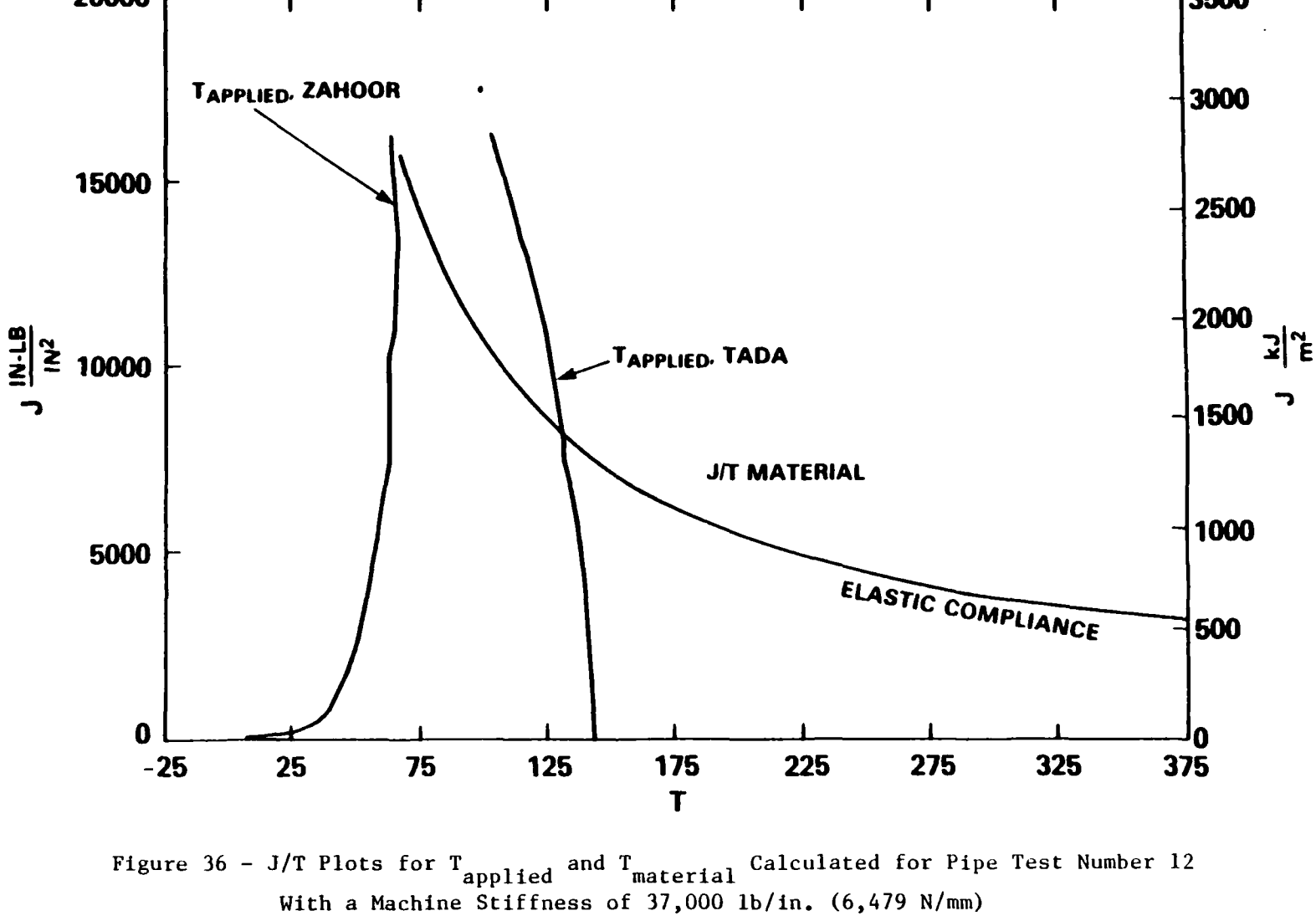

Figure 36 - J/T Plots for $T_{applied}$ and $T_{material}$ Calculated for Pipe Test Number 12 With a Machine Stiffness of 37,000 lb/in. (6,479 N/mm)

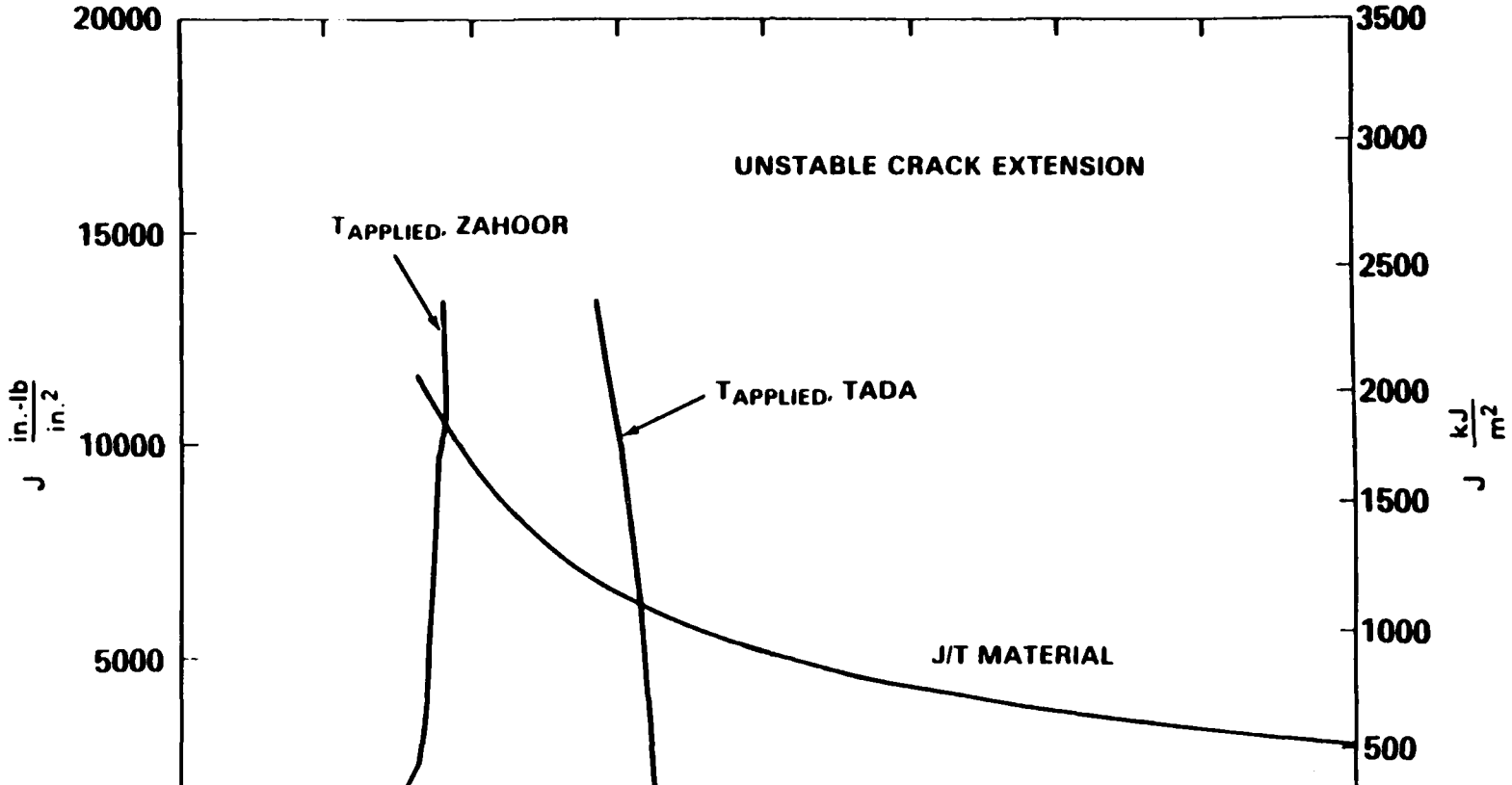

Figure 37 - J/T Plots for $T_{applied}$ and $T_{material}$ Calculated for Pipe Test Number 13 With a Machine Stiffness of 36,200 lb/in. (6,339 N/mm)

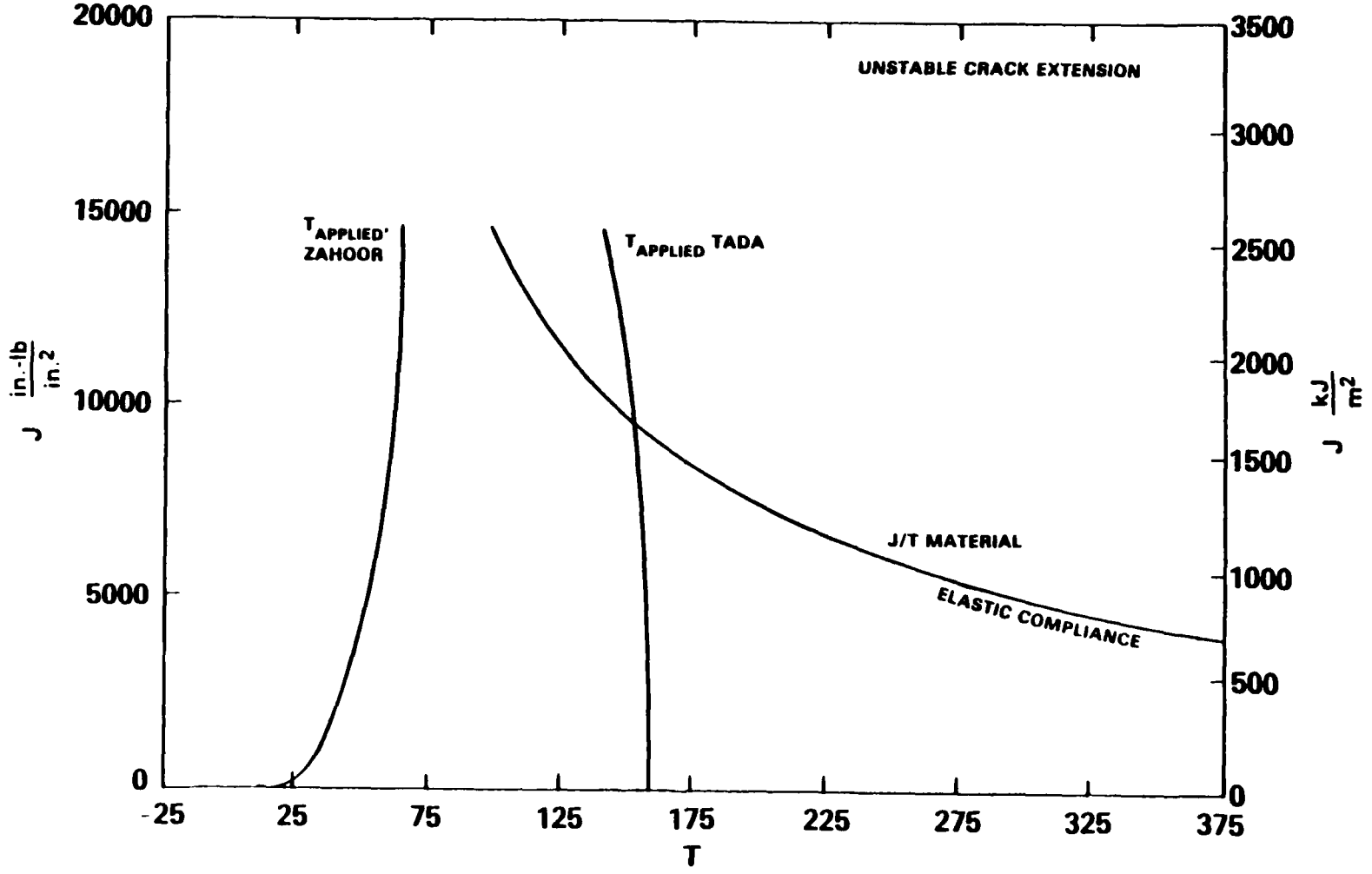

Figure 38 - J/T Plots for $T_{applied}$ and $T_{material}$ Calculated for Pipe Test Number 14 With a Machine Stiffness of 37,000 lb/in. (6,479 N/mm)

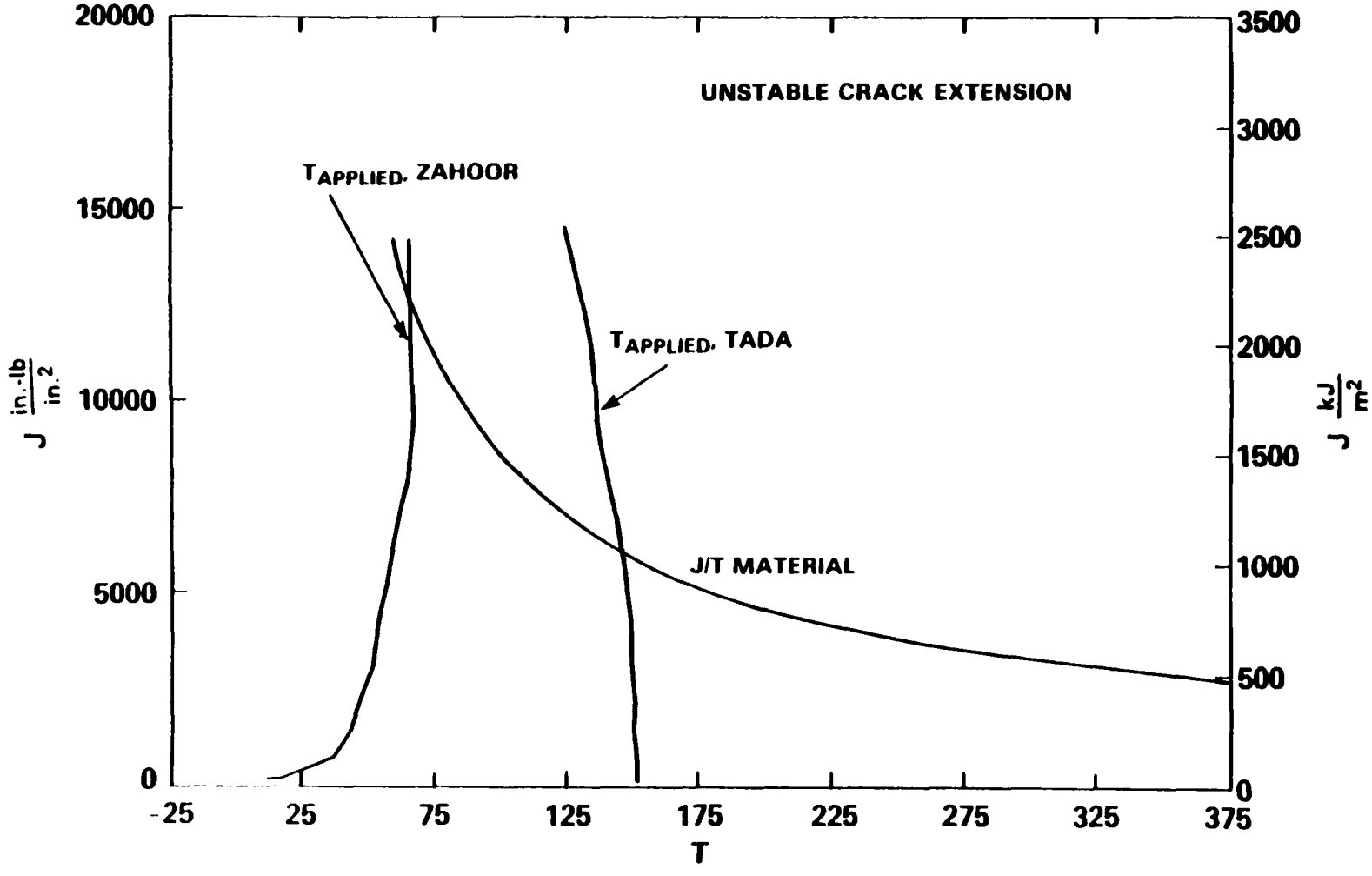

Figure 39 - J/T Plots for $T_{applied}$ and $T_{material}$ Calculated for Pipe Test Number 15 With a Machine Stiffness of 36,800 lb/in. (6,443 N/mm)

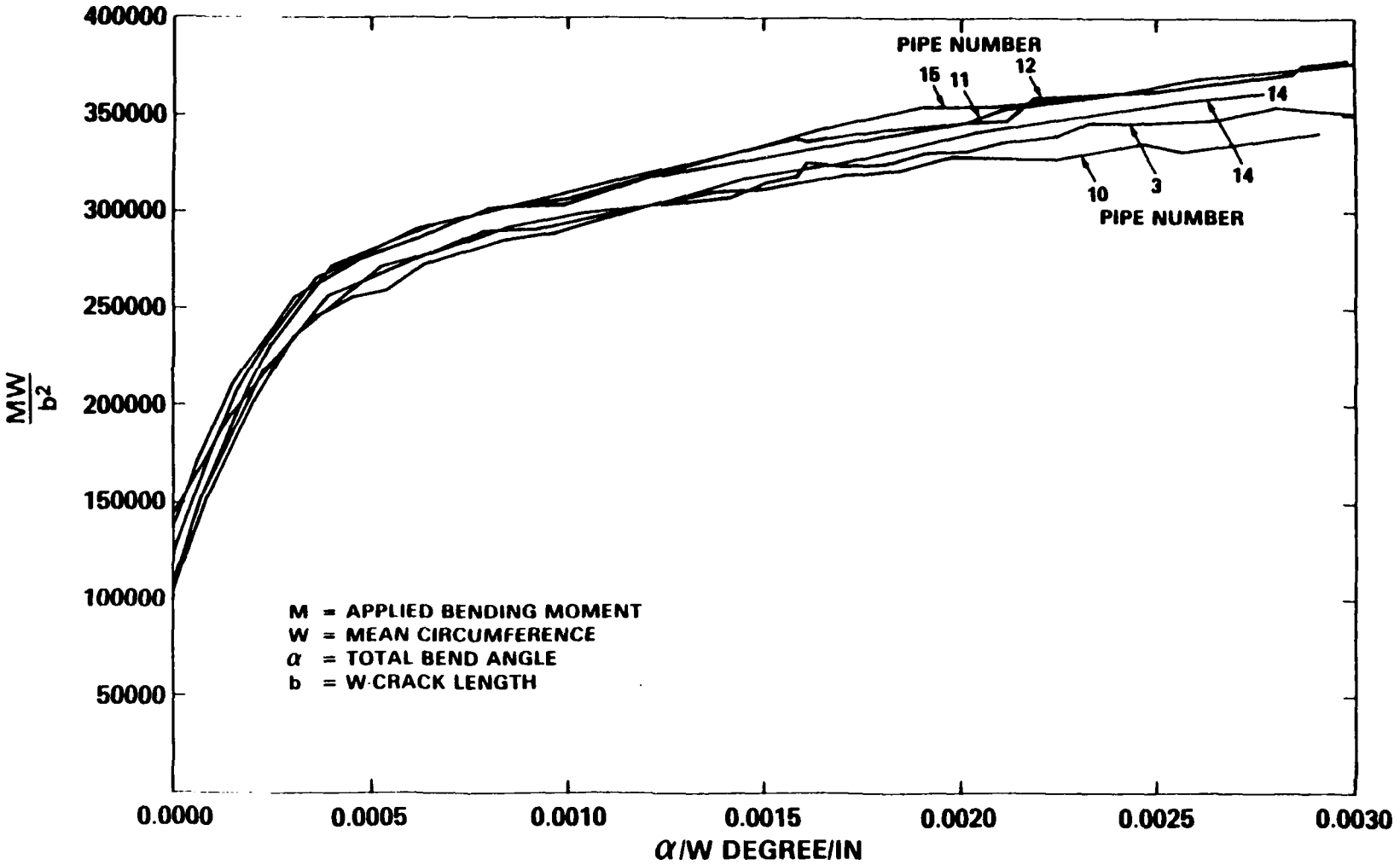

Figure 40 - Normalized Moment Versus Angle of Deflection for ASTM A106 Steel Pipes

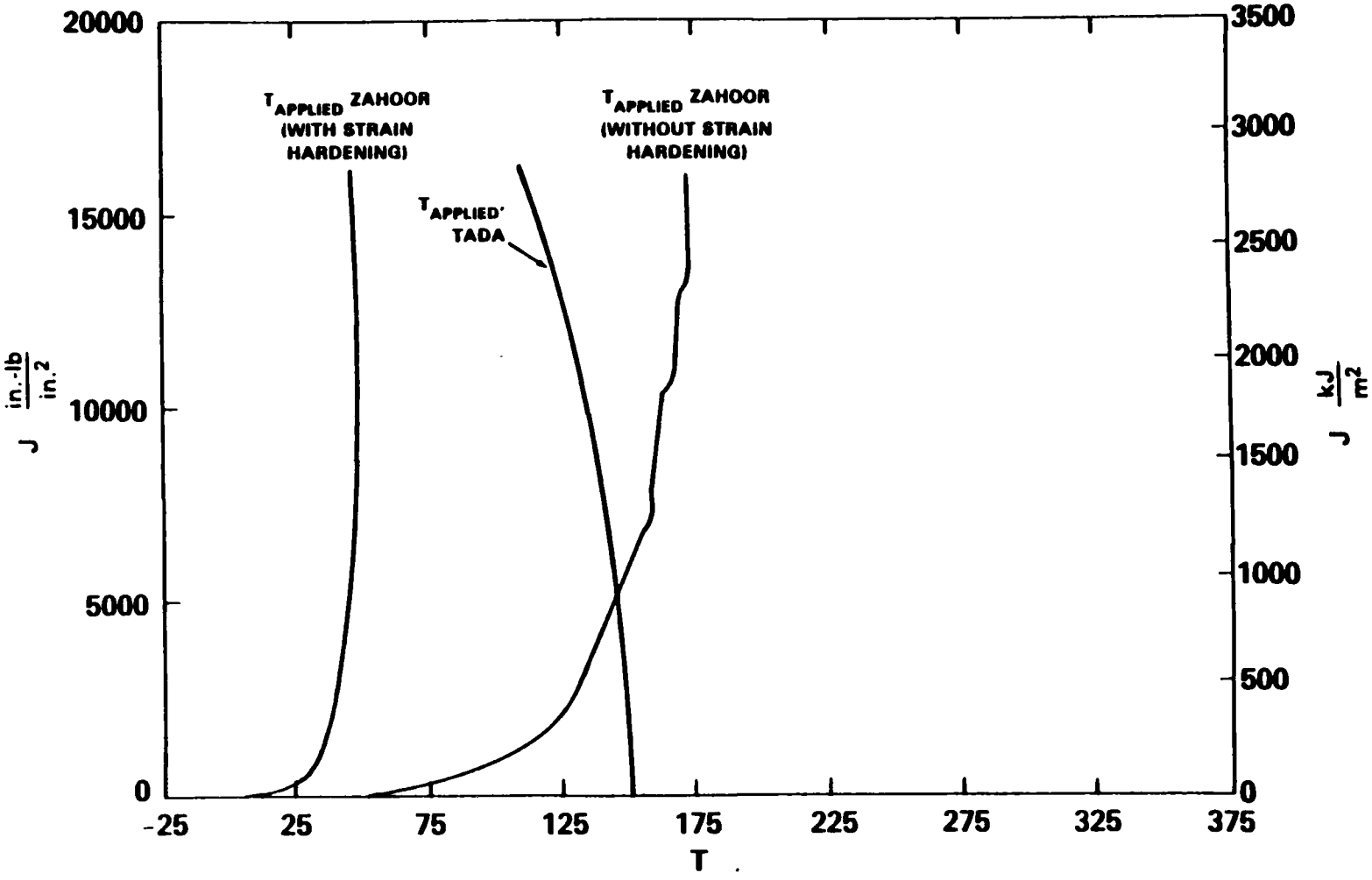

Figure 41 - J/T Plots for $T_{applied}$ Values for Pipe Test Number 12 Calculated With T-Tada, T-Zahoor With Strain Hardening, and T-Zahoor Without Strain Hardening

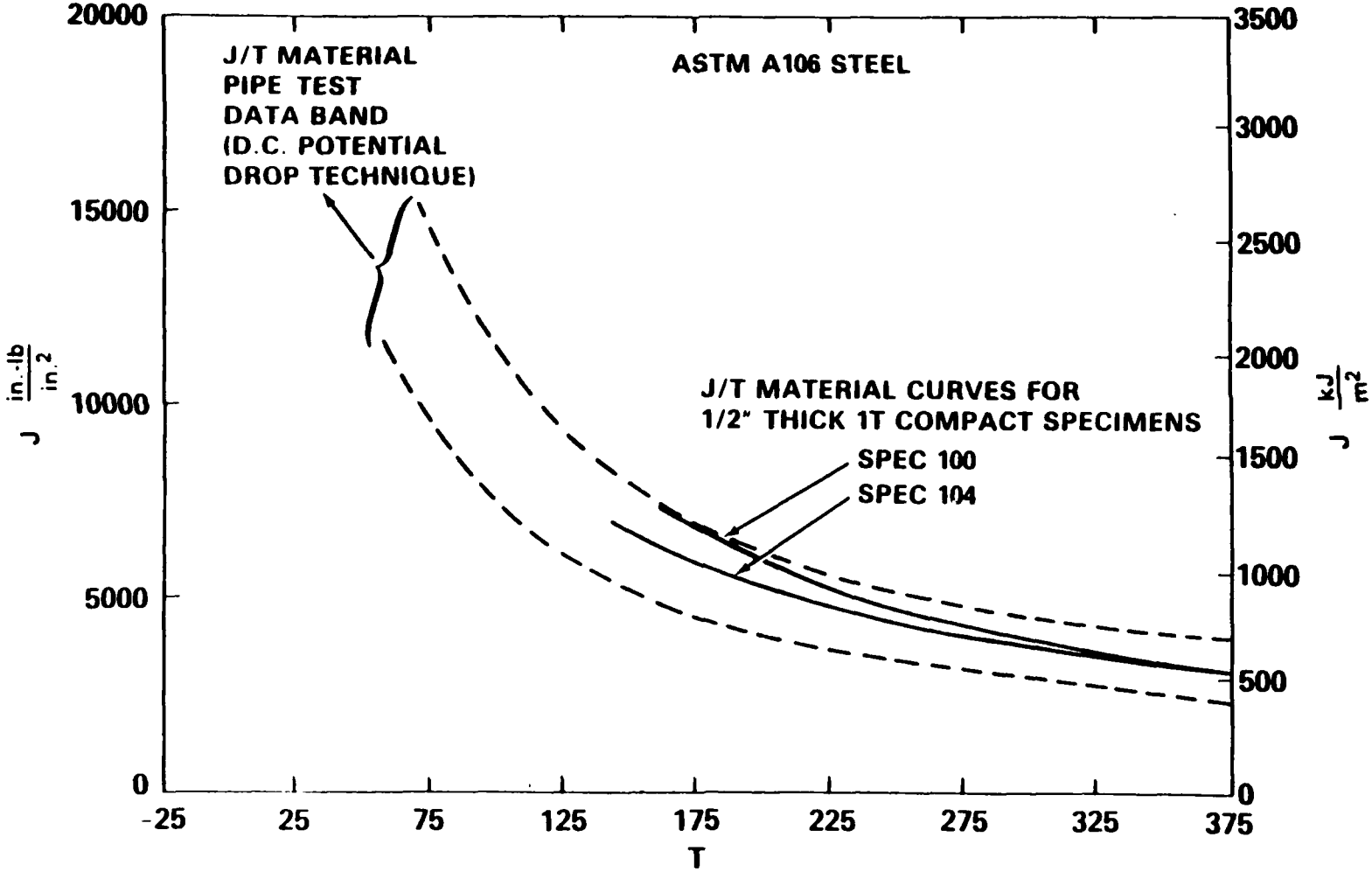

Figure 42 - J/T Plots for Pipe Bend Tests and 1 T Plan Compact Specimen of ASTM A106 Steel

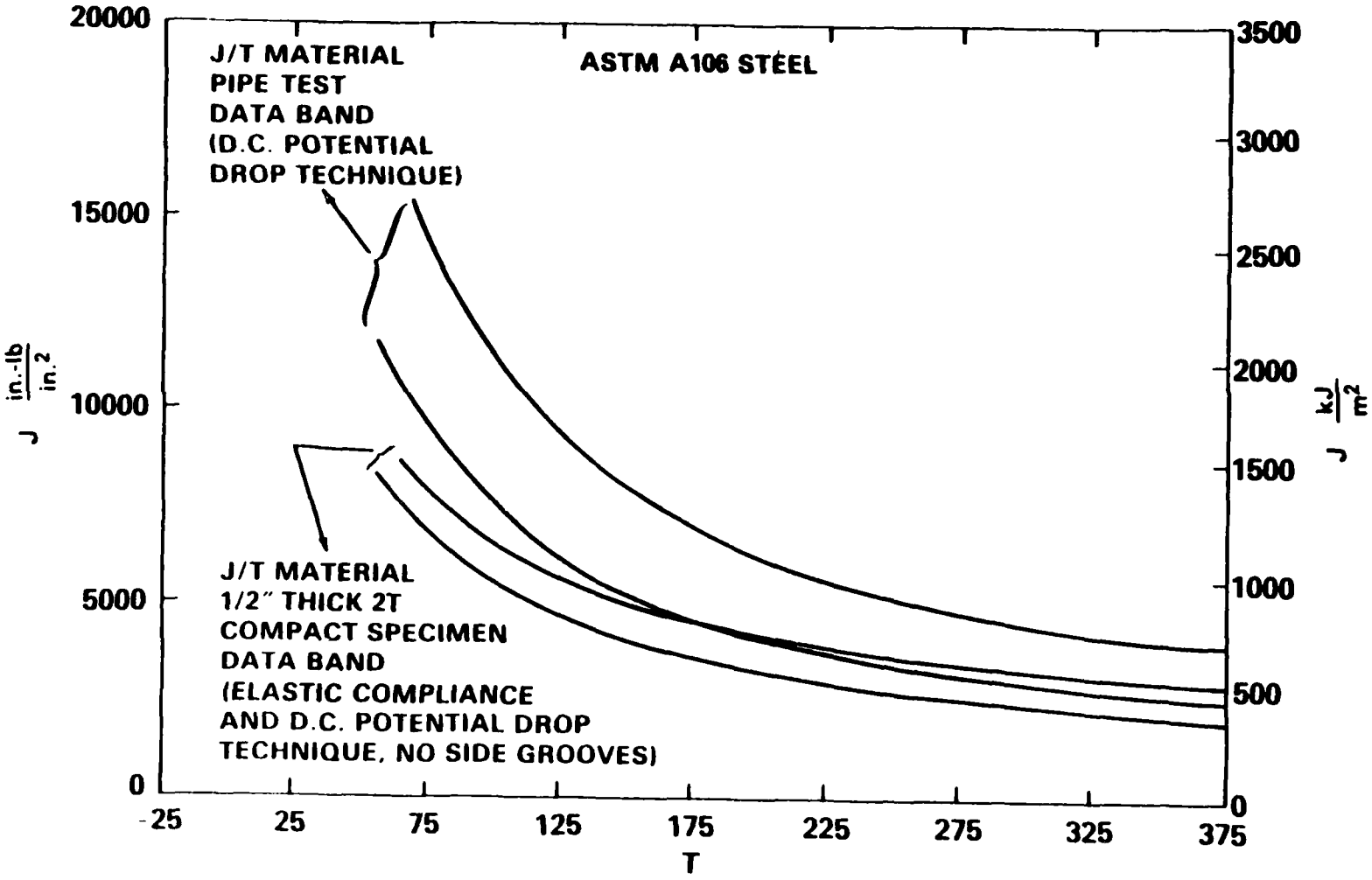

Figure 43 - J/T Plots for Pipe Bend Tests and 2 T Plan Compact Specimen of ASTM A106 Steel

APPENDIX A - TABULATION OF CURVE FIT CRACK EXTENSION DATA AND J(Zahoor), $T_{material}$, and OMEGA CALCULATIONS

POWER LAW CURVE FIT FROM COMPLIANCE DATA FOR PIPE-3

Mean Radius = 4.02 in.
Pipe Length = 48 in.
Span= = 16 in.

Delta a	J(Zahoor)	Tmaterial	Omega*
0.0268	2946.7	440.1	142.3
0.0654	4334.9	265.2	58.0
0.1040	5298.3	203.8	36.3
0.1426	6073.5	170.4	26.4
0.1812	6736.7	148.7	20.7
0.2198	7323.6	133.3	17.0
0.2584	7854.5	121.6	14.4
0.2969	8342.1	112.4	12.4
0.3355	8794.9	104.8	11.0
0.3741	9219.0	98.6	9.8
0.4127	9619.0	93.2	8.8
0.4513	9998.2	88.6	8.0
0.4899	10359.5	84.6	7.4
0.5285	10704.9	81.0	6.8
0.5671	11036.3	77.8	6.3
0.6057	11355.1	75.0	5.9
0.6443	11662.6	72.4	5.5
0.6829	11959.8	70.1	5.2
0.7215	12247.7	67.9	4.9
0.7601	12526.9	65.9	4.6
0.7987	12798.2	64.1	4.4
0.8373	13062.1	62.4	4.1
0.8759	13319.2	60.8	3.9
0.9145	13570.0	59.4	3.7
0.9530	13814.8	58.0	3.6
0.9916	14054.1	56.7	3.4
1.0302	14288.2	55.5	3.3
1.0688	14517.3	54.3	3.1
1.1074	14741.8	53.2	3.0

+ Delta a (in.)
- J (in-lb/in^2)

* $\Omega = \frac{b}{J} \times \frac{dJ}{da}$

POWER LAW CURVE FIT FROM COMPLIANCE DATA FOR PIPE-7

Mean Radius = 4.03 in.
Pipe Length = 48 in.
Span= = 18 in.

Delta a	J(Zahoor)	Tmaterial	Omega *
0.0268	4397.1	480.3	100.2
0.0473	5264.3	325.6	56.6
0.0678	5900.2	254.5	39.4
0.0884	6414.9	212.4	30.2
0.1089	6853.2	184.2	24.4
0.1294	7238.1	163.6	20.5
0.1499	7583.3	148.0	17.6
0.1705	7897.5	135.6	15.5
0.1910	8186.7	125.4	13.8
0.2115	8455.5	117.0	12.4
0.2321	8707.0	109.8	11.3
0.2526	8943.6	103.6	10.3
0.2731	9167.5	98.2	9.5
0.2936	9380.2	93.5	8.9
0.3142	9582.9	89.3	8.3
0.3347	9776.7	85.5	7.7
0.3552	9962.6	82.1	7.3
0.3757	10141.3	79.0	6.9
0.3963	10313.4	76.2	6.5
0.4168	10479.5	73.6	6.1
0.4373	10640.2	71.2	5.8
0.4578	10795.7	69.0	5.6
0.4784	10946.6	67.0	5.3
0.4989	11093.1	65.1	5.1
0.5194	11235.5	63.3	4.9
0.5400	11374.2	61.6	4.7
0.5605	11509.2	60.1	4.5
0.5810	11641.0	58.6	4.3
0.6015	11769.6	57.3	4.2

+ Delta a (in.)
- J (in-lb/in^2)

* $\Omega = \frac{b}{J} \times \frac{dJ}{da}$

POWER LAW CURVE FIT FROM POTENTIAL DROP DATA FOR PIPE-7

Mean Radius = 4.03 in.
Pipe Length = 48 in.
Span= = 18 in.

Delta a	J(Zahoor)	Tmaterial	Omega *
0.0268	3193.6	462.5	132.9
0.0520	4219.4	314.5	68.2
0.0773	4980.9	250.0	45.8
0.1025	5608.0	212.1	34.4
0.1278	6150.5	186.7	27.5
0.1530	6633.7	168.1	22.9
0.1783	7072.6	153.9	19.6
0.2035	7476.6	142.5	17.1
0.2288	7852.5	133.1	15.2
0.2540	8205.0	125.3	13.6
0.2793	8537.7	118.6	12.4
0.3045	8853.4	112.8	11.3
0.3298	9154.2	107.7	10.4
0.3550	9441.9	103.2	9.6
0.3803	9717.9	99.1	9.0
0.4055	9983.5	95.5	8.4
0.4308	10239.7	92.2	7.9
0.4560	10487.3	89.2	7.4
0.4813	10727.0	86.5	7.0
0.5065	10959.6	83.9	6.6
0.5318	11185.5	81.6	6.3
0.5570	11405.3	79.4	6.0
0.5823	11619.4	77.4	5.7
0.6075	11828.1	75.5	5.5
0.6328	12031.9	73.8	5.2
0.6580	12231.0	72.1	5.0
0.6833	12425.7	70.5	4.8
0.7085	12616.2	69.1	4.6
0.7338	12802.9	67.7	4.4

+ Delta a (in.)
- J (in-lb/in^2)

* $\Omega = \frac{b}{J} \times \frac{dJ}{da}$

POWER LAW CURVE FIT FROM COMPLIANCE DATA FOR PIPE-8

Mean Radius = 4.04 in.
Pipe Length = 48 in.
Span= = 18 in.

Delta a	J(Zahoor)	Tmaterial	Omega *
0.0357	3984.5	418.5	100.3
0.0656	5099.5	291.5	54.4
0.0955	5938.5	233.2	37.2
0.1254	6632.2	198.4	28.3
0.1553	7233.2	174.7	22.7
0.1852	7768.6	157.3	19.0
0.2151	8254.9	144.0	16.3
0.2450	8702.4	133.2	14.3
0.2749	9118.5	124.4	12.7
0.3048	9508.5	117.0	11.4
0.3347	9876.4	110.7	10.3
0.3646	10225.2	105.2	9.5
0.3945	10557.4	100.4	8.7
0.4244	10874.9	96.1	8.1
0.4543	11179.4	92.3	7.5
0.4842	11472.2	88.9	7.0
0.5141	11754.5	85.8	6.6
0.5440	12027.1	82.9	6.2
0.5739	12291.0	80.3	5.9
0.6038	12546.9	77.9	5.5
0.6337	12795.3	75.7	5.3
0.6636	13036.8	73.7	5.0
0.6935	13272.0	71.8	4.8
0.7234	13501.2	70.0	4.6
0.7533	13724.8	68.3	4.4
0.7832	13943.3	66.8	4.2
0.8131	14156.8	65.3	4.0
0.8430	14365.7	63.9	3.9
0.8729	14570.2	62.6	3.7

+ Delta a (in.)
- J (in-lb/in^2)

* $\Omega = \frac{b}{J} \times \frac{dJ}{da}$

POWER LAW CURVE FIT FROM POTENTIAL DROP DATA FOR PIPE-8

Mean Radius = 4.04 in.
Pipe Length = 48 in.
Span= = 18 in.

Delta a	J(Zahoor)	Tmaterial	Omega *
0.0268	2939.9	470.4	152.9
0.0535	4052.3	324.4	76.3
0.0803	4889.5	261.0	50.7
0.1070	5586.6	223.7	37.9
0.1338	6195.1	198.5	30.2
0.1605	6741.2	180.0	25.1
0.1873	7240.3	165.7	21.5
0.2140	7702.4	154.2	18.7
0.2408	8134.4	144.8	16.6
0.2675	8541.4	136.8	14.9
0.2943	8927.1	130.0	13.5
0.3210	9294.4	124.1	12.3
0.3478	9645.7	118.9	11.3
0.3745	9982.7	114.2	10.5
0.4013	10307.0	110.1	9.8
0.4280	10619.9	106.3	9.1
0.4548	10922.5	102.9	8.6
0.4815	11215.6	99.8	8.1
0.5083	11500.2	97.0	7.6
0.5350	11776.8	94.3	7.2
0.5618	12046.2	91.9	6.8
0.5885	12308.7	89.6	6.5
0.6153	12564.9	87.5	6.2
0.6420	12815.1	85.5	5.9
0.6688	13059.9	83.7	5.7
0.6955	13299.4	81.9	5.4
0.7223	13534.1	80.3	5.2
0.7490	13764.1	78.8	5.0
0.7758	13989.8	77.3	4.8

+ Delta a (in_s)
- J ($in\text{-}lb/in^2$)

* $\Omega = \frac{b}{J} \times \frac{dJ}{da}$

POWER LAW CURVE FIT FROM COMPLIANCE DATA FOR PIPE-10

Mean Radius = 4.04 in.
Pipe Length = 48 in.
Span= = 18 in.

Delta a	J(Zahoor)	Tmaterial	Omega *
0.0357	3117.0	424.1	137.2
0.0592	4066.3	333.6	82.5
0.0828	4847.4	284.7	58.9
0.1063	5528.3	252.8	45.8
0.1298	6140.7	229.9	37.4
0.1533	6702.3	212.5	31.6
0.1768	7224.4	198.5	27.3
0.2003	7714.3	187.1	24.0
0.2239	8177.7	177.5	21.5
0.2474	8618.4	169.3	19.4
0.2709	9039.7	162.2	17.6
0.2944	9444.0	155.9	16.2
0.3179	9833.2	150.3	15.0
0.3415	10209.0	145.3	13.9
0.3650	10572.6	140.8	13.0
0.3885	10925.4	136.7	12.1
0.4120	11268.1	132.9	11.4
0.4355	11601.6	129.4	10.8
0.4590	11926.7	126.3	10.2
0.4826	12244.0	123.3	9.7
0.5061	12554.1	120.5	9.2
0.5296	12857.4	118.0	8.8
0.5531	13154.3	115.6	8.4
0.5766	13445.3	113.3	8.0
0.6002	13730.8	111.2	7.7
0.6237	14010.9	109.2	7.4
0.6472	14286.1	107.3	7.1
0.6707	14556.6	105.5	6.8
0.6942	14822.7	103.8	6.6

+ Delta a (in.)
- J (in-lb/in^2)

* $\Omega = \frac{b}{J} \times \frac{dJ}{da}$

POWER LAW CURVE FIT FROM POTENTIAL DROP DATA FOR PIPE-10

Mean Radius = 4.04 in.
Pipe Length = 48 in.
Span= = 18 in.

Delta a	J(Zahoor)	Tmaterial	Omega *
0.0268	2530.0	431.0	172.0
0.0607	3788.0	284.9	75.6
0.0946	4715.4	227.5	48.4
0.1285	5484.9	194.8	35.5
0.1624	6156.8	173.0	28.0
0.1963	6760.7	157.2	23.0
0.2302	7313.7	145.0	19.6
0.2641	7826.8	135.3	17.0
0.2980	8307.4	127.2	15.0
0.3319	8761.1	120.5	13.4
0.3658	9191.8	114.7	12.1
0.3997	9602.8	109.6	11.1
0.4336	9996.5	105.2	10.2
0.4675	10374.8	101.3	9.4
0.5014	10739.5	97.8	8.7
0.5353	11091.9	94.6	8.1
0.5692	11433.2	91.7	7.6
0.6031	11764.3	89.0	7.2
0.6370	12086.1	86.6	6.8
0.6709	12399.4	84.3	6.4
0.7048	12704.7	82.3	6.1
0.7387	13002.7	80.3	5.8
0.7726	13293.9	78.5	5.5
0.8065	13578.6	76.8	5.2
0.8404	13857.3	75.3	5.0
0.8743	14130.4	73.8	4.8
0.9082	14398.2	72.4	4.6
0.9421	14661.0	71.0	4.4
0.9760	14919.0	69.8	4.2

+ Delta a (in.)
- J (in-lb/in^2)

* $\Omega = \frac{b}{J} \times \frac{dJ}{da}$

POWER LAW CURVE FIT FROM COMPLIANCE DATA FOR PIPE-11

Mean Radius = 4.03 in.
Pipe Length = 42 in.
Span= = 15 in.

Delta a	J(Zahoor)	Tmaterial	Omega*
0.0268	2041.8	355.8	178.8
0.0633	3151.6	232.4	75.4
0.0998	3966.1	185.5	47.6
0.1363	4642.0	159.0	34.7
0.1728	5232.7	141.3	27.3
0.2093	5764.3	128.5	22.4
0.2458	6251.6	118.7	19.0
0.2824	6704.1	110.8	16.5
0.3189	7128.6	104.4	14.6
0.3554	7529.5	98.9	13.0
0.3919	7910.5	94.2	11.7
0.4284	8274.3	90.2	10.7
0.4649	8623.1	86.6	9.8
0.5014	8958.5	83.4	9.1
0.5379	9282.1	80.5	8.4
0.5744	9594.9	78.0	7.9
0.6109	9898.0	75.6	7.4
0.6474	10192.3	73.5	6.9
0.6840	10478.5	71.5	6.5
0.7205	10757.2	69.7	6.2
0.7570	11029.0	68.0	5.8
0.7935	11294.4	66.4	5.5
0.8300	11553.8	65.0	5.3
0.8665	11807.6	63.6	5.0
0.9030	12056.2	62.3	4.8
0.9395	12299.8	61.1	4.6
0.9760	12538.8	60.0	4.4
1.0125	12773.4	58.9	4.2
1.0490	13003.9	57.9	4.1

+ Delta a (in.)
- J (in-lb/in^2)

* $\Omega = \frac{b}{J} \times \frac{dJ}{da}$

POWER LAW CURVE FIT FROM POTENTIAL DROP DATA FOR PIPE-11

Mean Radius = 4.03 in.
Pipe Length = 42 in.
Span= = 15 in.

Delta a	J(Zahoor)	Tmaterial	Omega*
0.0268	2348.5	376.4	164.4
0.0628	3488.5	238.4	69.8
0.0989	4305.6	187.0	44.2
0.1349	4973.8	158.3	32.3
0.1709	5551.6	139.4	25.4
0.2070	6067.1	125.8	20.9
0.2430	6536.4	115.5	17.7
0.2790	6969.7	107.2	15.4
0.3151	7373.9	100.5	13.6
0.3511	7754.1	94.8	12.1
0.3871	8113.8	90.0	10.9
0.4232	8456.1	85.8	10.0
0.4592	8783.0	82.1	9.2
0.4952	9096.5	78.8	8.5
0.5313	9397.9	75.9	7.8
0.5673	9688.6	73.3	7.3
0.6033	9969.6	70.9	6.9
0.6394	10241.7	68.8	6.4
0.6754	10505.7	66.8	6.1
0.7114	10762.2	64.9	5.7
0.7475	11011.9	63.2	5.4
0.7835	11255.2	61.7	5.2
0.8195	11492.6	60.2	4.9
0.8556	11724.5	58.8	4.7
0.8916	11951.1	57.5	4.5
0.9276	12173.0	56.3	4.3
0.9637	12390.2	55.2	4.1
0.9997	12603.2	54.1	4.0
1.0357	12812.0	53.1	3.8

+ Delta a ($in.$)
- J ($in\text{-}lb/in^2$)

* $\Omega = \frac{b}{J} \times \frac{dJ}{da}$

POWER LAW CURVE FIT FROM COMPLIANCE DATA FOR PIPE-12

Mean Radius = 4.03 in.
Pipe Length = 42 in.
Span= = 15 in.

Delta a	J(Zahoor)	Tmaterial	Omega *
0.0268	2550.2	434.2	178.6
0.0637	3909.4	279.9	74.8
0.1006	4898.0	222.0	47.2
0.1375	5714.2	189.5	34.4
0.1744	6425.1	168.0	27.0
0.2114	7063.0	152.4	22.2
0.2483	7646.6	140.5	18.8
0.2852	8187.6	130.9	16.3
0.3221	8694.1	123.1	14.4
0.3590	9172.0	116.5	12.9
0.3959	9625.6	110.9	11.6
0.4329	10058.2	106.0	10.6
0.4698	10472.4	101.7	9.7
0.5067	10870.5	97.8	9.0
0.5436	11254.1	94.4	8.3
0.5805	11624.7	91.3	7.8
0.6174	11983.6	88.5	7.3
0.6543	12331.7	85.9	6.8
0.6913	12670.1	83.6	6.4
0.7282	12999.4	81.4	6.1
0.7651	13320.3	79.4	5.8
0.8020	13633.4	77.5	5.5
0.8389	13939.4	75.8	5.2
0.8758	14238.6	74.1	5.0
0.9127	14531.5	72.6	4.8
0.9497	14818.4	71.2	4.6
0.9866	15099.7	69.8	4.4
1.0235	15375.7	68.5	4.2
1.0604	15646.8	67.3	4.0

+ Delta a (in.)
- J (in-lb/in^2)

* $\Omega = \frac{b}{J} \times \frac{dJ}{da}$

POWER LAW CURVE FIT FROM POTENTIAL DROP DATA FOR PIPE-13

Mean Radius = 4.04 in.
Pipe Length = 42 in.
Span= = 15 in.

Delta a	J(Zahoor)	Tmaterial	Omega*
0.0268	2873.3	411.1	195.9
0.0543	3850.0	271.9	96.5
0.0818	4562.6	213.9	63.9
0.1092	5144.9	180.5	47.7
0.1367	5646.4	158.3	38.1
0.1642	6091.7	142.2	31.6
0.1917	6495.2	129.9	27.0
0.2192	6866.1	120.1	23.6
0.2467	7210.7	112.0	20.9
0.2741	7533.4	105.3	18.8
0.3016	7837.7	99.6	17.0
0.3291	8126.1	94.6	15.6
0.3566	8400.8	90.3	14.3
0.3841	8663.3	86.4	13.3
0.4116	8915.0	83.0	12.4
0.4390	9157.1	79.9	11.6
0.4665	9390.5	77.1	10.9
0.4940	9615.9	74.6	10.2
0.5215	9834.1	72.3	9.7
0.5490	10045.7	70.1	9.2
0.5765	10251.1	68.2	8.7
0.6039	10450.9	66.3	8.3
0.6314	10645.5	64.6	7.9
0.6589	10835.1	63.0	7.6
0.6864	11020.2	61.5	7.2
0.7139	11201.0	60.1	7.0
0.7414	11377.7	58.8	6.7
0.7688	11550.6	57.6	6.4
0.7963	11720.0	56.4	6.2

+ Delta a (in.)
- J (in-lb/in^2)

* $\Omega = \frac{b}{J} \times \frac{dJ}{da}$

POWER LAW CURVE FIT FROM COMPLIANCE DATA FOR PIPE-14

Mean Radius = 4.06 in.
Pipe Length = 42 in.
Span= = 15 in.

Delta a	J(Zahoor)	Tmaterial	Omega*
0.0357	5039.0	421.6	92.9
0.0582	5901.0	302.9	56.9
0.0807	6558.0	242.8	40.9
0.1032	7101.0	205.5	31.9
0.1257	7568.0	179.9	26.2
0.1482	7981.0	160.9	22.1
0.1707	8354.0	146.2	19.2
0.1932	8695.0	134.5	16.9
0.2157	9010.0	124.8	15.1
0.2382	9304.0	116.7	13.7
0.2607	9579.0	109.8	12.5
0.2832	9839.0	103.8	11.4
0.3058	10085.0	98.6	10.6
0.3283	10319.0	93.9	9.8
0.3508	10542.0	89.8	9.2
0.3733	10756.0	86.1	8.6
0.3958	10962.0	82.8	8.1
0.4183	11159.0	79.7	7.6
0.4408	11350.0	76.9	7.2
0.4633	11534.0	74.4	6.9
0.4858	11712.0	72.0	6.5
0.5083	11885.0	69.9	6.2
0.5308	12052.0	67.9	6.0
0.5533	12215.0	66.0	5.7
0.5758	12374.0	64.2	5.5
0.5983	12528.0	62.6	5.2
0.6208	12678.0	61.0	5.0
0.6433	12825.0	59.6	4.9

+ Delta a (in.)
- J (in-lb/in^2)

* $\Omega = \frac{b}{J} \times \frac{dJ}{da}$

POWER LAW CURVE FIT FROM COMPLIANCE DATA FOR PIPE-15

Mean Radius = 4.03 in.
Pipe Length = 42 in.
Span= = 15 in.

Delta a	J(Zahoor)	Tmaterial	Omega *
0.0268	2495.6	404.2	174.7
0.0614	3681.6	260.3	76.0
0.0959	4540.2	205.3	48.4
0.1305	5245.3	174.4	35.5
0.1651	5856.6	153.9	28.0
0.1996	6403.1	139.1	23.0
0.2342	6901.2	127.8	19.6
0.2688	7361.6	118.8	17.0
0.3034	7791.5	111.4	15.0
0.3379	8196.1	105.2	13.4
0.3725	8579.3	99.9	12.1
0.4071	8944.0	95.3	11.1
0.4417	9292.6	91.3	10.2
0.4762	9627.0	87.7	9.4
0.5108	9948.7	84.5	8.7
0.5454	10259.1	81.6	8.1
0.5800	10559.2	79.0	7.6
0.6145	10849.9	76.6	7.2
0.6491	11132.1	74.4	6.8
0.6837	11406.4	72.4	6.4
0.7182	11673.5	70.5	6.1
0.7528	11933.8	68.8	5.8
0.7874	12187.8	67.1	5.5
0.8220	12435.9	65.6	5.2
0.8565	12678.6	64.2	5.0
0.8911	12916.2	62.9	4.8
0.9257	13148.9	61.6	4.6
0.9603	13377.0	60.4	4.4
0.9948	13600.8	59.3	4.2

+ Delta a (in.)
- J (in-lb/in^2)

* $\Omega = \frac{b}{J} \times \frac{dJ}{da}$

REFERENCES

1. Paris, P.C., et al, "The Theory of Instability of the Tearing Mode of Elastic-Plastic Crack Growth," Elastic-Plastic Fracture, ASTM STP 668, pp. 5-36 (1979).

2. Hutchinson, J.W. and P.C. Paris, "The Theory of Stability Analysis of J-Controlled Crack Growth," Elastic-Plastic Fracture, ASTM STP 668, pp 37-64 (1979).

3. Paris, P.C., et al, "An Initial Experimental Investigation of the Tearing Instability Theory," Elastic-Plastic Fracture, ASTM STP 668, pp. 251-265 (1979).

4. Joyce, J.A., and M.G. Vassilaros, "An Experimental Evaluation of Tearing Instability Using the Compact Specimen," Fracture Mechanics, ASTM STP 743, pp 525-542 (1981).

5. Vassilaros, M.G., J.P. Gudas and J.A. Joyce "Experimental Investigation of Tearing Instability Phenomena for Structural Materials" U.S. Nuclear Regulatory Commission, NUREG/CR-2570 Rev 1 (August 1982).

6. Wilkowski, G.M., A. Zahoor, and M.F. Kanninen, "A Plastic Fracture Mechanics Prediction of Fracture Instability in a Circumferentially Cracked Pipe in Bending-part II. Experimental Verification on a Type 304 Stainless Steel Pipe", ASME J. of Pressure Vessel Technology, Vol. 103, Number 4, Nov. 1981.

7. Joyce, J.A. and Gudas, J.P., "Elastic-Plastic Fracture," ASTM STP 668, J.D. Landes, J.A. Begley, and G.A. Clarke, Eds., American Society for Testing and Materials, 1979, pp. 251-265.

8. Vassilaros, M.G. and E.M. Hackett, "J-Integral R-Curve Testing of High Strength Steel Utilizing the D.C. Potential Drop Method," Presented at the Fifteenth National Symposium on Fracture Mechanics" July 7-9, 1982, University of Maryland, College Park, MD to be published.

9. Ernst, H.A., Paris, P.C. and J.D. Landes, "Estimations on J-Integral and Tearing Modulus T from a Single Specimen Test Record," Presented at the 13th National Symposium on Fracture Mechanics (June 1980). To be published.

10. Joyce, J.A., "Instability Tests of Compact and Pipe Specimens Utilizing a Test System Made Compliant by Computer Control", U.S. Nuclear Regulatory Commission Report, NUREG CR-2257, March 1982.

11. Wilkowski, G.M. and W.A. Maxey, "Applications of the Electric Potential Method for Measuring Crack Growth in Specimens, Flawed Pipes and Pressure Vessels", Presented at the Fourteenth National Symposium on Fracture Mechanics, Los Angeles, California, June 30-July 2, 1981, to be published.

12. Tada, H., P. Paris, and R. Gamble, "Stability Analysis of Circumferential Cracks in Reactor Piping Systems", U.S. Nuclear Regulatory Commission Report, NUREG CR-0838, June 1979.

13. Zahoor, A. and M.F. Kanninen, "A Plastic Fracture Mechanics Prediction of Fracture Instability in a Circumferentially Cracked Pipe in Bending - Part I: J-Integral Analysis", ASME, J. of Pressure Vessel Technology, Vol. 103, Number 4, Nov. 1981.

14. Green, G., R. F. Smith and J. F. Knott, "Mechanics and Mechanisms of Crack Growth," BSC Conference, Cambridge, Great Britian, April 1973 (ed M. J. May) p. 58.

15. Clayton, J. O. and J. F. Knott: "Materials Science," 1976, Vol 10, No. 63.

16. Johnson, R., "Resolution of the Task A-11 Reactor Vessel Materials Toughness Safety Issue," U. S. Nuclear Regulartory Commission Report NUREG-0744, Appendix B (P. Paris), October 1982.

AD-A142 589 J-INTEGRAL TEARING INSTABILITY ANALYSIS FO 8-INCH DIAMETER ASTM A106 STE..(U) DAVID W TAYLOR NAVAL SHIP RESEARCH AND DEVELOPMENT CENTER ANN..

2/2

UNCLASSIFIED M G VASSILAROS ET AL. MAY 84 F/G 11/6 NL

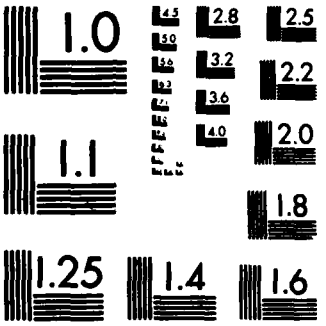

INITIAL DISTRIBUTION

Copies	
1	ONR Code 471
1	NAVMAT 034
4	NRL
	1 Code 6000
	1 Code 6320
	1 Code 6380
	1 Code 6396
12	NAVSEA
	1 SEA 05D
	2 SEA 05R
	1 SEA 08
	1 SEA 092
	2 SEA 323
	1 PMS 393
	1 PMS 395
	1 PMS 396
	2 SEA 99612
1	NISC Code 369
12	DTIC

CENTER DISTRIBUTION

Copies	Code	
1	17	W. Murray
1	172	M. Krenzke
1	173	A.B. Stavovy
1	1720.1	T. Kiernan
1	28	J. Belt
1	2802	I. Kramer
1	2803	V. Schaper
1	2809	A. Malec
5	281	G. Wacker
2	2811	J. Cavallaro
21	2814	J. Gudas
1	282	J. Crisci
1	522.2	Unclass Library
2	5231	Office Services

DTNSRDC ISSUES THREE TYPES OF REPORTS

1. DTNSRDC REPORTS, A FORMAL SERIES, CONTAIN INFORMATION OF PERMANENT TECHNICAL VALUE. THEY CARRY A CONSECUTIVE NUMERICAL IDENTIFICATION REGARDLESS OF THEIR CLASSIFICATION OR THE ORIGINATING DEPARTMENT

2. DEPARTMENTAL REPORTS, A SEMIFORMAL SERIES, CONTAIN INFORMATION OF A PRELIMINARY, TEMPORARY, OR PROPRIETARY NATURE OR OF LIMITED INTEREST OR SIGNIFICANCE THEY CARRY A DEPARTMENTAL ALPHANUMERICAL IDENTIFICATION.

3. TECHNICAL MEMORANDA, AN INFORMAL SERIES, CONTAIN TECHNICAL DOCUMENTATION OF LIMITED USE AND INTEREST. THEY ARE PRIMARILY WORKING PAPERS INTENDED FOR INTERNAL USE. THEY CARRY AN IDENTIFYING NUMBER WHICH INDICATES THEIR TYPE AND THE NUMERICAL CODE OF THE ORIGINATING DEPARTMENT. ANY DISTRIBUTION OUTSIDE DTNSRDC MUST BE APPROVED BY THE HEAD OF THE ORIGINATING DEPARTMENT ON A CASE-BY-CASE BASIS.